APPENDIX A

Storm Surge Atlas for the Narragansett Bay, Rhode Island and Buzzards Bay, Massachusetts Area

A STORM SURGE ATLAS FOR THE NARRAGANSETT BAY, RHODE ISLAND AND BUZZARDS BAY, MASSACHUSETTS AREA

Storm Surge Group
National Hurricane Center
National Oceanic and Atmospheric Administration
Coral Gables, Florida 33146

TABLE OF CONTENTS

		Page
1.	INTRODUCTION	1
2.	THE GRID FOR THE SLOSH MODEL OF THE NARRAGANSETT AND BUZZARDS BAYS AREAS	1
3.	SLOSH MODEL	4
	A. Hurricane Model and Input	4
	B. Storm Surge Model	5
4.	OUTPUT AND INTERPRETATION OF THE MODEL RESULTS	5
	A. Output from the SLOSH Model	5
	B. Interpretation of Results	6
5.	HURRICANE CLIMATOLOGY	7
	A. Tracks	7
	B. Intensities	9
6.	MAPS OF MAXIMUM ENVELOPE OF WATER ("MEOW") FROM SLOSH RUNS USING DATA FOR HYPOTHETICAL HURRICANES	10
	A. Hypothetical Storm Tracks and Populations	10
	B. Intensities and Radii of Maximum Winds of Hypothetical Storms	12
	C. Initial Water Height	15
	D. The "MEOW" Figures	15
7.	REFERENCES	16
8.	APPENDIX: MAXIMUM ENVELOPES OF WATER (MEOW) SERIES "A"	18
9.	FIGURE CAPTIONS	20

1. INTRODUCTION

Storm surge is the abnormal rise in water level caused by wind and pressure forces of a hurricane. Storm surge produces most of the flood damage and drownings associated with tropical storms that make landfall or that closely approach a coastline (Anthes, 1982).

A numerical storm surge model developed by Jelesnianski (1967, 1972), Jelesnianski and Taylor (1973) and Jelesnianski et al. (1984) has been applied to the Narragansett Bay, RI and Buzzards Bay, MA region. The model, which calculates sea, lake and overland surges from hurricanes, and has the acronym "SLOSH," is a pairing of a model of a hurricane coupled to a model for storm surge. Crawford (1979) discussed some preliminary results using this model in the southeast Louisiana region.

The purpose of this atlas is to provide maps of SLOSH-modeled heights of storm surge and extent of flood inundation, for various combinations of hurricane strength, forward speed of storm and direction of storm motion. Strength is modeled by use of the central pressure and storm eye size using four of the five categories of storm intensity (Table 1), developed by Saffir and Simpson (Simpson and Riehl, 1981). Six storm-track headings were selected as being representative of storm behavior in this region on the basis of observations by forecasters at NOAA's National Hurricane Center.

The maps in this atlas summarize surge calculations made using the SLOSH model, when initialized with observed values (depths of water and heights of terrain and barriers) in the region centered on Narragansett Bay, RI and Buzzards Bay, MA.

2. THE GRID FOR THE SLOSH MODEL OF THE NARRAGANSETT AND BUZZARDS BAYS AREAS

Figure 1 illustrates the area covered by the grid for the Narragansett and Buzzards Bays SLOSH model. The area covered by the grid is called a

Table 1. Saffir/Simpson hurricane intensity categories.

	Central Pressure		Wind Speed		
Category	Millibars	Inches (Hg)	Miles per Hr.	Knots	Damage
1	≥ 980	≥ 28.9	74 - 95	64 - 83	Minimal
2	965 - 979	28.5 - 28.9	96 - 110	84 - 96	Moderate
3	945 - 964	27.9 - 28.5	111 - 130	97 - 113	Extensive
4	920 - 944	27.2 - 27.9	131 - 155	114 - 135	Extreme
5	< 920	< 27.2	> 155	> 135	Catastrophic

"basin"--the "Narragansett and Buzzards Bays Basin." The grid is a telescoping polar coordinate system with 80 arc lengths ($1 \leq I \leq 80$) and 82 radials ($1 \leq J \leq 82$). Unlike a true polar coordinate grid, which would have radial increment (ΔR) that was invariant with radius, this grid uses a ΔR that increases with increasing distance from the grid's pole. The result is that in each grid of the mesh, the increment of arc length (ΔS) of the side of a grid "square" is approximately equal to the radial increment of the "square," or $\Delta S \approx \Delta R$.

The telescoping grid is a compromise between conflicting needs. What is desired is that the model domain include a large geographical area, but also that small, detailed topography be included in the model. In a Cartesian coordinate system, this combination of big area, but spatially-small grid increment, requires that a computational mesh with many grid squares be used. A large mesh requires a computer with a large central processing unit (CPU) as well as more time to perform calculations in the more numerous grid squares. The telescoping grid, by comparison, permits a resolution of these conflicting needs: it has an acceptably small spatial resolution of 1 to 10 mi^2 per grid square over land, which is the area of greatest interest. Thus, topographic details, such as highway and railroad embankments, and dikes in harbors of cities are included in the model. However, the range increment contained in each grid square becomes progressively larger with increasing distance from the pole. As a result, a large geographic area is included in the model, so that the effects of the model's boundaries on the dynamics of the storm are diminished and the storm's physics are better emulated.

The grid is tangent to the earth at the basin center, Quicksand Point on the Rhode Island-Massachusetts border at 41°27'N and 71°24'W. There, the grid increment is 1.25 statute miles. The pole (or origin) of the grid is located at 42°N and 71°01'W.

The telescoping grid has some disadvantages. Primarily, these stem from the distortion that occurs when the basin is remapped onto a display that has constant-sized increments in the vertical and horizontal, as happens when the basin is printed out by a conventional (computer) line printer. This distortion from remapping produces some difficulties in "reading" the results by the uninitiated. For example, neither latitude nor longitude lines remain uncurved and "parallels" become non-parallel. However, the projection is conformal. The projection scheme results in each grid square at I = 1, closest to the pole, representing an area of about 0.35 square mile. By contrast, at maximum distance from the pole, at I = 80, each grid square contains about 33.5 square miles. Thus, the distortions require that aids be provided to "read" and interpret the results.

3. SLOSH MODEL

A. Hurricane Model and Input

The hurricane model which drives the storm surge model was developed by Jelesnianski and Taylor (1973). It is a trajectory model of a stationary vortex and it balances the forces from pressure gradient, centrifugal, Coriolis and surface frictional effects. Adjustments are made to the computed vector wind to incorporate the hurricane's forward motion. The model's input includes the radius of maximum wind (RMW) and the difference (ΔP) in sea-level pressure between the ambient value and the minimum value in the storm's center. Directly measured wind vectors are not used. The model also requires input of the coordinates of the storm's center. Thus, input data include thirteen sets of latitude, longitude, ΔP and RMW, at six hour increments, beginning 48 hours before storm landfall and ending 24 hours after landfall. These 13 sets are then linearly interpolated into values/positions at hourly (or smaller) time increments. The model then generates the meteorological

forces--surface stress and the gradient of atmospheric pressure-that drive the underlying ocean.

B. Storm Surge Model

Storm surge is the response by the ocean to meteorological forces. The model's governing equations are those given by Jelesnianski (1967), except now for the inclusion of the finite amplitude effect. Coefficients for surface drag, eddy viscosity and bottom slip are the same as those used in an earlier model (Jelesnianski, 1972). There is no calibration or tuning to force agreement between observed and computed surges; coefficients are fixed, and do not vary from one geographical region to another.

Special techniques are incorporated to model two-dimensional inland inundation, routing of surges inland when barriers are overtopped, the effect of trees, the movement of the surge up rivers, and flow through channels, cuts and over submerged sills. Besides surge, other processes affect water height (section 4B), but are not incorporated in the model.

Not surprisingly, the accuracy of modeled surge values increases as the accuracy of the input terrain and storm data improves.

4. OUTPUT AND INTERPRETATION OF THE MODEL RESULTS

A. Output from the SLOSH Model

The output for the Narragansett and Buzzards Bays "SLOSH" model consists of maps of water heights. At each grid point, the water height is the maximum value that was computed at that point during the 72 (maximum) hours of model time. Thus, the map displays the highest water levels and does not display events at any particular instant in time. The analyzed envelopes of high water show shaded areas that represent dry land which has been inundated and contours of high water relative to mean sea level (MSL). Height of water

above terrain was not calculated because terrain height varies within a grid square. For example, the altitude of a grid square may be assigned a value of 6-ft MSL, but this value represents an average of land heights that may include values ranging from 3 ft to 9 ft MSL. Thus, a surge value of 8 ft in this square, implying 2 ft average depth of water over the grid's terrain, would include some terrain without inundation and other parts with as much as 5 ft of overlying water. Therefore, the depth of surge flooding above terrain at a specific site in the grid square is deduced by subtracting the actual terrain height from the model-generated storm surge height in that square. Also supplied are printout lists of values of surge height, wind speed and wind direction for each of 80 sites. The values are ten-minute averages, every 30 minutes. These are useful for determining the time of onset of gale force winds and surge heights, for evacuation planning.

B. Interpretation of Results

Even if the model is supplied accurate data on storm positions, intensities and sizes, the computed surges may contain errors of +/- 20% of observed water levels. These primarily stem from:

1) Maps that are outdated: The maps which supplied heights of terrain and depths of water sometimes did not include changes, often man-made, that had been made to the heights and positions of barriers (e.g., highway and railway embankments) and depths and locations of channels. Inaccuracies of topography or bathymetry will contribute directly to errors in the modeling of all storm surges.

2) Anomalous water heights: Sea level can be at an altitude different from "mean sea level," days or even weeks before a storm is actually affecting a basin. The value of the actual, local sea level -- the "local datums" for pre-storm anomaly in the Atlantic Ocean -- must be supplied to the model, before calculations are initiated.

3) Local processes, such as waves, astronomical tides, rainfall and flooding from overflowing rivers: These processes are usually included in "observations" of storm surge height, but are not surge and are not calculated by the SLOSH model.

Factors such as the foregoing must be considered when comparisons are made between modeled and observed values of storm surge.

5. HURRICANE CLIMATOLOGY

A. Tracks

Between 1886 and 1987, 21 tropical cyclones of hurricane intensity passed within 105 statute miles of Quicksand Point, RI/MA (Neumann et al., 1985), for an average of one hurricane within the 105-mile circle every 4.8 years (see Table 2).

Figures 2-4 show the tracks of these 21 storms with hurricane force winds. Figure 2 depicts the tracks for northwestbound and northbound storms, Figure 3 shows tracks for storms heading north-northeastward, and Figure 4 displays the tracks of storms heading northeastward or east-northeastward. In Figures 2-4, the tracks are labeled at 6-h intervals with month/day/hour (GMT).

The tracks represent "best estimates" and are based on a variety of data sources. Historically, storm strength, location and motion were only inferred, from analyses of wind, pressure and cloud observations made at ships and land stations being influenced by the storm. In 1943, aircraft reconnaissance of hurricanes began. Not until 1959 were there land-based weather radars, as now at Atlantic City, New York City and Chatham, Massachusetts which could be used to observe and record structure, development and motion of precipitation fields, and help infer center location and radius of maximum winds. The 1960's saw the advent of photography of tropical storms from weather satellites. Observations by aircraft, radar and satellite have shown

Table 2. Hurricanes passing within 105 statute mile circle of Quicksand Point, RI/MA (41.45°N, 71.4°W), during 1886-1987.

			>>> At Closest Point of Approach: (@CPA) <<<		
Index (1)	Date (@CPA) (2)	Storm Name (3)	Range/Bearing (miles/degrees) (to CPA) (4) / (5)	Wind (in circle) (mph) (6)	Storm Motion (@CPA) (dir / mph) (7) (8)
1	1888 Nov 27	Unnamed	91 / 120	98	NNE / 11
2	1891 Oct 14	Unnamed	77 / 132	98	NE / 15
3	1896 Sep 20	Unnamed	89 / 087	108	N / 10
4	1904 Sep 15	Unnamed	1 / 036	75	NE / 53
5	1916 Jul 21	Unnamed	20 / 124	91	NNE / 18
6	1924 Aug 26	Unnamed	73 / 112	106	NE / 43
7	1927 Aug 24	Unnamed	75 / 130	105	NE / 48
8	1933 Sep 17	Unnamed	99 / 136	81	NE / 29
9	1936 Sep 19	Unnamed	40 / 140	92	ENE / 32
10	1938 Sep 21	Unnamed	102 / 259	90	N / 51
11	1940 Sep 2	Unnamed	98 / 123	81	NE / 26
12	1944 Sep 15	Unnamed	40 / 296	83	NE / 29
13	1953 Aug 15	Barbara	84 / 154	86	ENE / 23
14	1954 Aug 31	Carol	64 / 279	96	NNE / 35
15	1954 Sep 11	Edna	26 / 143	96	NNE / 46
16	1958 Aug 29	Daisy	98 / 144	119	NE / 28
17	1960 Sep 12	Donna	54 / 274	98	NNE / 39
18	1961 Sep 21	Esther	46 / 160	127	NE / 6
19	1962 Aug 29	Alma	90 / 127	98	NE / 13
20	1969 Sep 9	Gerda	105 / 122	124	NNE / 48
21	1985 Sep 27	Gloria	92 / 288	86	NNE / 45

Notes:

(1) Storm number for this list.

(2) Year, month and date that storm had maximum winds exceeding 74 mph and was closest to Quicksand Point, RI/MA.

(3) Storms were not formally named before 1950.

(4)-(5) Distance (statute miles) and direction (degrees) from Quicksand Point to storm when it passed abeam.

(6) Maximum sustained wind speed near storm center while center was within 105 statute miles of Quicksand Point. This is not necessarily the wind recorded at a given site.

(7)-(8) Storm heading and forward speed (mph) at hour of closest point of approach.

that the tracks of centers of hurricanes contain wobbles, gyrations and cycloidal motions (Lawrence and Mayfield, 1977) and that there often are rapid developments in size and intensity of rain bands, contractions of eyewall diameters and formation of concentric ("double") eyewalls. These factors, poorly documented even today, indicate asymmetries in the storm's dynamical structure and can affect the storm's surge. But they usually are smoothed out of analyses, as in Figures 2-4.

B. Intensities

Hurricane intensity is usually defined by measurements at sea level of the maximum sustained wind speed and/or by minimum barometric pressure. Neither of these is easily obtained. Accurate estimates of these parameters at sea level were acquired only when a ship or land station was traversed by the storm's "eye." Minimum central pressure was gotten only when a barometer was in the precise path of the storm's center. Because the area covered by the strongest winds is much larger than that covered by the pressure minimum, strength of many older storms was deduced from measurements of wind speed. However, with the advent of aircraft reconnaissance, measurements made at flight level of meteorological parameters allow the calculation of barometric pressure at sea level. By comparison, winds at sea level are not so readily deduced from flight level data. For all the storm tracks in Figures 2-4, an estimate was made of the maximum wind speed at intervals of 6 hours. For some, only very indirect evidence exists of actual speeds. From the hourly values of the maximum wind speed inside the 105 mile circle, the largest value was selected. This maximum sustained wind speed for the hurricane is listed in Table 2 under the heading of "wind (in circle)." Storm heading and forward speed at hour of closest point of approach are listed in the last two columns.

The values listed in column 6 sometimes are poor estimates of the maximum wind speed; the following must be considered:

1) Actual wind speeds and directions exhibit gustiness.
2) The "average wind speed" has been calculated with a variety of time intervals over the years; thus, one can find historical wind records that have used time periods such as 1 hour, or 10 or 5 minutes or 1 minute as the "standard" period of measurement. Given the same record from a recording anemometer, the use of each of these measurement periods would likely yield a different average wind speed, with shorter periods probably giving higher average speeds.
3) The platforms for measuring maximum surface wind speed have changed over the years; data from ship and land stations now are supplemented by remotely-sensed data from aircraft, satellites and radar. However, the remote platforms, especially the last two, observe the motions of clouds or precipitation echoes, and these motions are not wind speed, nor are they at sea level.

Because of these limitations in determination of maximum wind speed, the SLOSH model uses storm-center sea-level pressure as a measure of storm intensity in modeling the Narragansett and Buzzards Bays basin.

6. MAPS OF MAXIMUM ENVELOPE OF WATER ("MEOW") FROM SLOSH RUNS USING DATA FOR HYPOTHETICAL HURRICANES

A. Hypothetical Storm Tracks and Populations

The skill of the SLOSH model was evaluated by Jarvinen and Lawrence (1985), who compared modeled and observed surges at 523 sites during 10 hurricanes. They found that the mean absolute error in surge height calculated by SLOSH was 1.4 ft. Although the error range was from -7.1 ft to

+8.8 ft, the standard deviation was only 2.0 ft and 79% of the errors lay within one standard deviation of the mean error, -0.3 ft. (On the average, modeled values were slightly less than those observed.)

Because of this skill in calculating storm surge, the SLOSH model was used to create maps of surge flooding in the Narragansett and Buzzards Bays basin for use in evacuation planning. The model was supplied with data from hypothetical storms and the resulting surge calculations were composited to produce maps of the maximum envelope of water. This section details why these calculations were made and how the compositing was done.

Storm surge height partly depends on distance between the location of a particular site and the storm's center. For a single storm, the model would produce a map of surge height for the modeled period of time (usually 72 hours), with values valid for only that particular storm track. If there were two storms, identical in every respect except that one followed a track parallel to, but separated from the other by 50 miles,[1] and if the model was run with first one and then the other set of storm parameters, and a comparison made of surge values, then very likely there would be geographical sites with surge values from one storm that differed markedly from those modeled for the other storm. This dependency of surge height on storm track can be troublesome, when preparing plans for emergency evacuation. Maps are needed for basin-wide surge flooding potential—maps showing surge height for only one intensity (using the categories defined by Saffir and Simpson), one

---

[1]A difference ("error") of 50 miles in storm track is not very large when compared to the vagaries of tracks of real hurricanes. The average error of 12-hour forecast landfall position, for U.S. Atlantic coast tropical cyclones, during 1970-1979, was about 59 statute miles, while for 24-hour forecasts, landfall position error was about 125 statute miles (Neumann and Pelissier, 1981). Thus, if a storm were forecast to make (eye) landfall at Quicksand Point, in 24 hours, and if, in fact, it made landfall anywhere between Rockaway Beach, Long Island and Rye Beach, New Hampshire, the error in forecast landfall position would be no worse than average.

storm speed and direction. We created such maps for this basin by making surge calculations for each of an ensemble of 3 to 12 storms all having the same intensity and speed and on parallel headings, separated by 15 miles. Then, at each grid square, the maximum surge value that was calculated from any storm in the ensemble was extracted and saved. After this procedure was performed for all grid squares, the result was a basin map depicting the "maximum envelope of water," or MEOW, for the specified storm category, direction and speed. For the Narragansett and Buzzards Bays basin, the hypothetical storms were specified to move in one of six directions, at one of three constant speeds, as summarized in Table 3. There were 8 tracks for the west-northwestward (WNW) moving storms (Figure 5), 10 tracks for the northwest-bound (NW) storms (Figure 6), 12 tracks for the north-northwest (NNW) storm headings (Figure 7), 12 tracks for the northward (N) moving storms (Figure 8), 11 tracks for the north-northeastward (NNE) storm headings (Figure 9), and up to 7 tracks for storms heading northeastward (NE), in Figure 10. In total, 536 hypothetical storms were run, using the SLOSH model, to create the results to be presented below. The selection of directions and speeds was based on advice of hurricane specialists at NOAA's National Hurricane Center.

B. Intensities and Radii of Maximum Winds of Hypothetical Storms

Most hurricanes weaken after making landfall because the central pressure increases (the storm "fills") and the RMW tends to increase. Table 4 summarizes pressure filling and RMW increases with time for the hypothetical storm runs. These rates of change were based partly on the work of Schwerdt et al. (1979). Storms heading northeastward were modeled to not undergo filling or to change RMW.

Table 3. Narragansett/Buzzards Bays Basin's hypothetical storms: Directions, speeds, (Saffir/Simpson) intensities, number of tracks and the number of runs.

Direction	Speed (mph)	Intensities	Tracks	Runs
WNW	20	1 through 4	8	32
NW	20	1 through 4	10	40
NNW	20, 40, 60	1 through 4	12	144
N	20, 40, 60	1 through 4	12	144
NNE	20, 40, 60	1 through 4	11	132
NE*	20, 40	1, 2, 3, 4	7, 7, 5, 3	44
				Total = 536

*Several NE moving hurricanes near or over land cannot maintain all intensity levels.

Table 4. Time change of pressure difference and radius of maximum wind for hypothetical hurricanes having headings towards the west-northwest, northwest, north-northwest, north or north-northeast in Narragansett and Buzzards Bays Basin.

Values of pressure difference (ΔP, millibars) and radius of maximum wind (RMW, statute miles), beginning at time of landfall (LF) of center of storm and every six hours after LF.

	Landfall		LF + 6		LF + 12		LF + 18		LF + 24	
Category	ΔP	RMW	ΔP	RMW	ΔP	RMW	ΔP	RMW	ΔP	RMW
1	20	30	14	30	10	30	10	35	10	40
2	40	30	31	30	22	30	13	35	10	40
3	60	30	48	30	36	30	24	35	12	40
4	80	30	65	30	50	30	35	35	20	40

C. Initial Water Height

Based on observations from tide gages in the area of this basin, tidal anomalies of about +1 ft MSL before arrival of a hurricane are not uncommon. Thus, all SLOSH runs of hypothetical hurricanes were supplied with initial datums of +1 ft MSL. In an actual hurricane, if tide gage data in this basin indicate that there is no tide anomaly, then subtract 1 ft from the modeled values found in the maps (below).

D. The "MEOW" Figures

There are 52 MEOWS and they use the distorted geography mentioned in Section 2. They are presented in the Appendix. The MEOW figures are grouped by direction: MEOWS for west-northwestbound storms are in Figures A1-A4, northwestbound storms' MEOWS are in Figures A5-A8, MEOWS for north-northwestbound storms are in Figures A9-A20, northbound storms' MEOWS are in Figures A21-A32, north-northeastbound storms' MEOWS are in Figures A33-A44, and northeast-moving storms' MEOWS are in Figures A45-A52. In the figures, the contours represent the height of water above mean sea level, in 1-ft increments, while the shaded areas indicate land areas that were modeled to have been inundated.

7. REFERENCES

Anthes, R. A. (1982): Tropical cyclones — their evolution, structure and effects. Amer. Meteor. Soc., Meteor. Monogr., 19, 208 pp.

Crawford, K. C. (1979): Hurricane surge potentials over southeast Louisiana as revealed by a storm-surge forecast model: a preliminary study. Bull. Amer. Meteor. Soc., 60, 422-429.

Jarvinen, B. R., and M. B. Lawrence (1985): An evaluation of the SLOSH storm-surge model. Bull. Amer. Meteor. Soc., 66, 1408-1411.

Jelesnianski, C. P. (1967): Numerical computations of storm surges with bottom stress. Mon. Wea. Rev., 95, 740-756.

_____, (1972): "SPLASH" (Special Program to List Amplitudes of Surges from Hurricanes): I. Landfall storms. U.S. Dept. of Commerce, National Oceanic and Atmospheric Administration, Tech. Memo. NWS TDL-46, Washington, D.C., 52 pp.

_____, and A. D. Taylor (1973): A preliminary view of storm surges before and after storm modifications. U.S. Dept. of Commerce, National Oceanic and Atmospheric Administration, Tech. Memo ERL WMPO-3, Washington, D.C., 33 pp.

_____, J. Chen, W. A. Shaffer, and A. J. Gilad (1984): SLOSH - A hurricane storm surge forecast model. Preprints, Oceans '84, Washington, D.C., Marine Technology Society and IEEE/Oceanic Engineering Society, 314-317.

Lawrence, M. B., and B. M. Mayfield (1977): Satellite observations of trochoidal motion during Hurricane Belle, 1976. Mon. Wea. Rev., 105, 1458-1461.

Neumann, C. J., and J. M. Pelissier (1981): An analysis of Atlantic tropical cyclone forecast errors, 1970-1979. Mon. Wea. Rev., 109, 1248-1266.

_____, G. W. Cry, E. L. Caso, and B. R. Jarvinen (1985): Tropical cyclones of the North Atlantic Ocean, 1871-1980, with storm track maps updated through 1984. U.S. Dept. of Commerce, National Oceanic and Atmospheric Administration, National Climatic Center, Asheville, North Carolina, 174 pp.

Schwerdt, R. W., F. P. Ho, and R. R. Watkins (1979): Meteorological criteria for standard project hurricane and probable maximum hurricane wind fields, Gulf and east coasts of the United States. NOAA Tech. Rept. NWS 23, U.S. Dept. of Commerce, National Oceanic and Atmospheric Administration, National Weather Service, Washington, D.C., 317 pp.

Simpson, R. H., and H. Riehl (1981): The Hurricane and Its Impact. Louisiana State University Press, Baton Rouge, LA, 398 pp.

8. APPENDIX: MAXIMUM ENVELOPES OF WATER (MEOW) SERIES "A"

Figure	MEOW
A- 1	West-northwestbound, 20 mph, category 1 hurricane.
A- 2	West-northwestbound, 20 mph, category 2 hurricane.
A- 3	West-northwestbound, 20 mph, category 3 hurricane.
A- 4	West-northwestbound, 20 mph, category 4 hurricane.
A- 5	Northwestbound, 20 mph, category 1 hurricane.
A- 6	Northwestbound, 20 mph, category 2 hurricane.
A- 7	Northwestbound, 20 mph, category 3 hurricane.
A- 8	Northwestbound, 20 mph, category 4 hurricane.
A- 9	North-northwestbound, 20 mph, category 1 hurricane.
A-10	North-northwestbound, 20 mph, category 2 hurricane.
A-11	North-northwestbound, 20 mph, category 3 hurricane.
A-12	North-northwestbound, 20 mph, category 4 hurricane.
A-13	North-northwestbound, 40 mph, category 1 hurricane.
A-14	North-northwestbound, 40 mph, category 2 hurricane.
A-15	North-northwestbound, 40 mph, category 3 hurricane.
A-16	North-northwestbound, 40 mph, category 4 hurricane.
A-17	North-northwestbound, 60 mph, category 1 hurricane.
A-18	North-northwestbound, 60 mph, category 2 hurricane.
A-19	North-northwestbound, 60 mph, category 3 hurricane.
A-20	North-northwestbound, 60 mph, category 4 hurricane.
A-21	Northbound, 20 mph, category 1 hurricane.
A-22	Northbound, 20 mph, category 2 hurricane.
A-23	Northbound, 20 mph, category 3 hurricane.
A-24	Northbound, 20 mph, category 4 hurricane.

A-25 Northbound, 40 mph, category 1 hurricane.

A-26 Northbound, 40 mph, category 2 hurricane.

A-27 Northbound, 40 mph, category 3 hurricane.

A-28 Northbound, 40 mph, category 4 hurricane.

A-29 Northbound, 60 mph, category 1 hurricane.

A-30 Northbound, 60 mph, category 2 hurricane.

A-31 Northbound, 60 mph, category 3 hurricane.

A-32 Northbound, 60 mph, category 4 hurricane.

A-33 North-northeastbound, 20 mph, category 1 hurricane.

A-34 North-northeastbound, 20 mph, category 2 hurricane.

A-35 North-northeastbound, 20 mph, category 3 hurricane.

A-36 North-northeastbound, 20 mph, category 4 hurricane.

A-37 North-northeastbound, 40 mph, category 1 hurricane.

A-38 North-northeastbound, 40 mph, category 2 hurricane.

A-39 North-northeastbound, 40 mph, category 3 hurricane.

A-40 North-northeastbound, 40 mph, category 4 hurricane.

A-41 North-northeastbound, 60 mph, category 1 hurricane.

A-42 North-northeastbound, 60 mph, category 2 hurricane.

A-43 North-northeastbound, 60 mph, category 3 hurricane.

A-44 North-northeastbound, 60 mph, category 4 hurricane.

A-45 Northeastbound, 20 mph, category 1 hurricane.

A-46 Northeastbound, 20 mph, category 2 hurricane.

A-47 Northeastbound, 20 mph, category 3 hurricane.

A-48 Northeastbound, 20 mph, category 4 hurricane.

A-49 Northeastbound, 40 mph, category 1 hurricane.

A-50 Northeastbound, 40 mph, category 2 hurricane.

A-51 Northeastbound, 40 mph, category 3 hurricane.

A-52 Northeastbound, 40 mph, category 4 hurricane.

9. FIGURE CAPTIONS

Figure 1. Grid mesh for SLOSH model for Narragansett/Buzzards Bays basin.

Figure 2. Tracks of hurricanes (1886-1986) passing within 105 miles of Quicksand Point, Rhode Island/Massachusetts: northbound storms only.

Figure 3. Same as Figure 2, but only storms heading north-northeastward.

Figure 4. Same as Figure 2, but only northeastward and east-northeastward moving storms.

Figure 5. Tracks of the hypothetical hurricanes that were used for calculating the maximum envelope of water (MEOW). Hurricane symbol is at point of landfall of eye of storm, and dots are eye positions at 6 hour increments (20 mph). Tracks are identified by the distance in miles of their landfall point to the left side (LS) or right side (RS) of Quicksand Point, Rhode Island/Massachusetts. Storms heading west-northwestward (WNW) only.

Figure 6. Same as Figure 5, but only for northwestbound (NW) storms.

Figure 7. Same as Figure 5, but only for north-northwestbound (NNW) storms.

Figure 8. Same as Figure 5, except for northbound (N) storms only.

Figure 9. Same as Figure 5, except for north-northeastward (NNE) moving storms only.

Figure 10. Same as Figure 5, except for northeastbound (NE) storms only. "Landfall points" lie on a perpendicular through Quicksand Point.

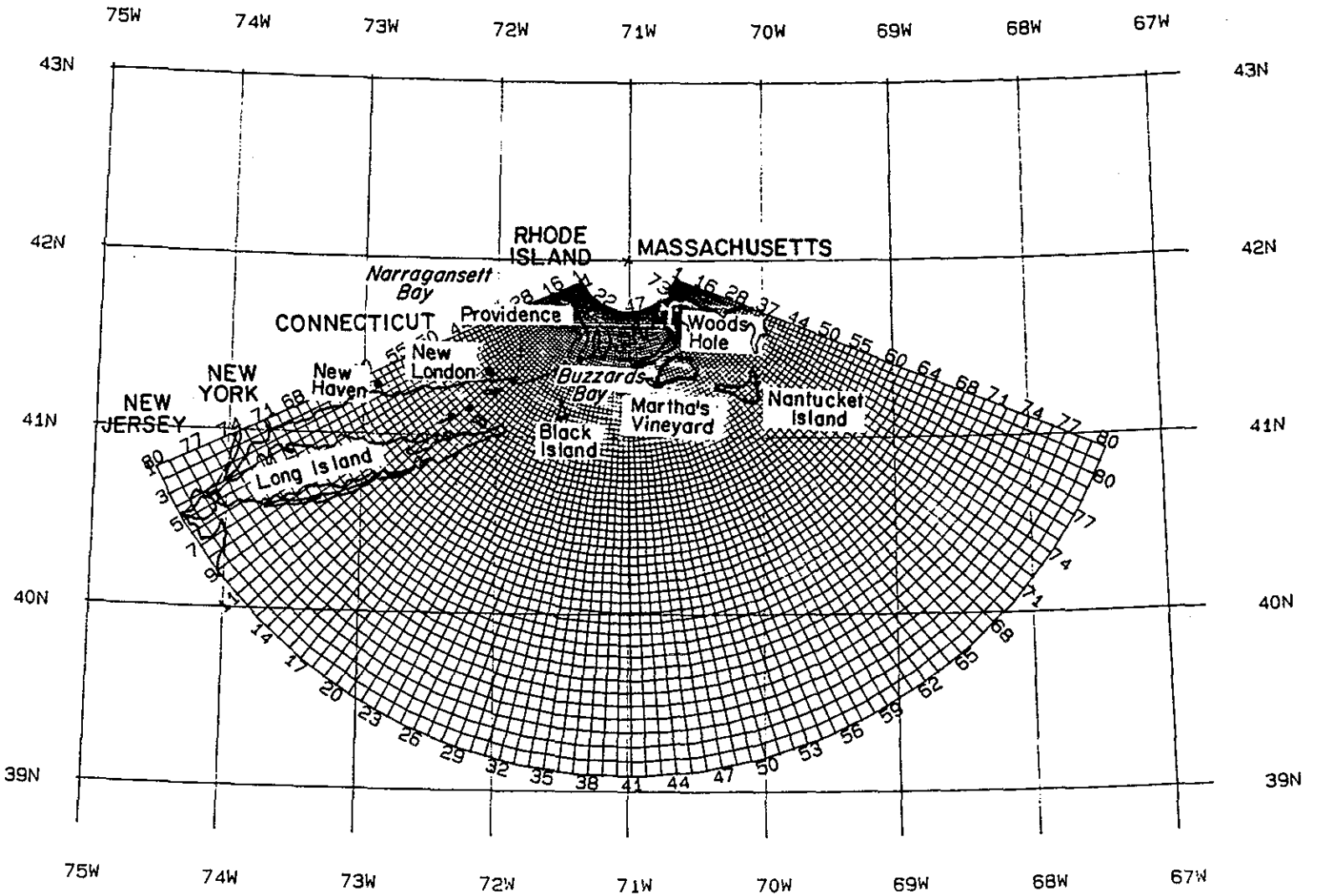

TRANSVERSE MERCATOR PROJECTION
SCALE 1: 3,400,000
TRUE AT 71W

NARRAGANSETT-BUZZARDS BAYS

FIGURE 1.

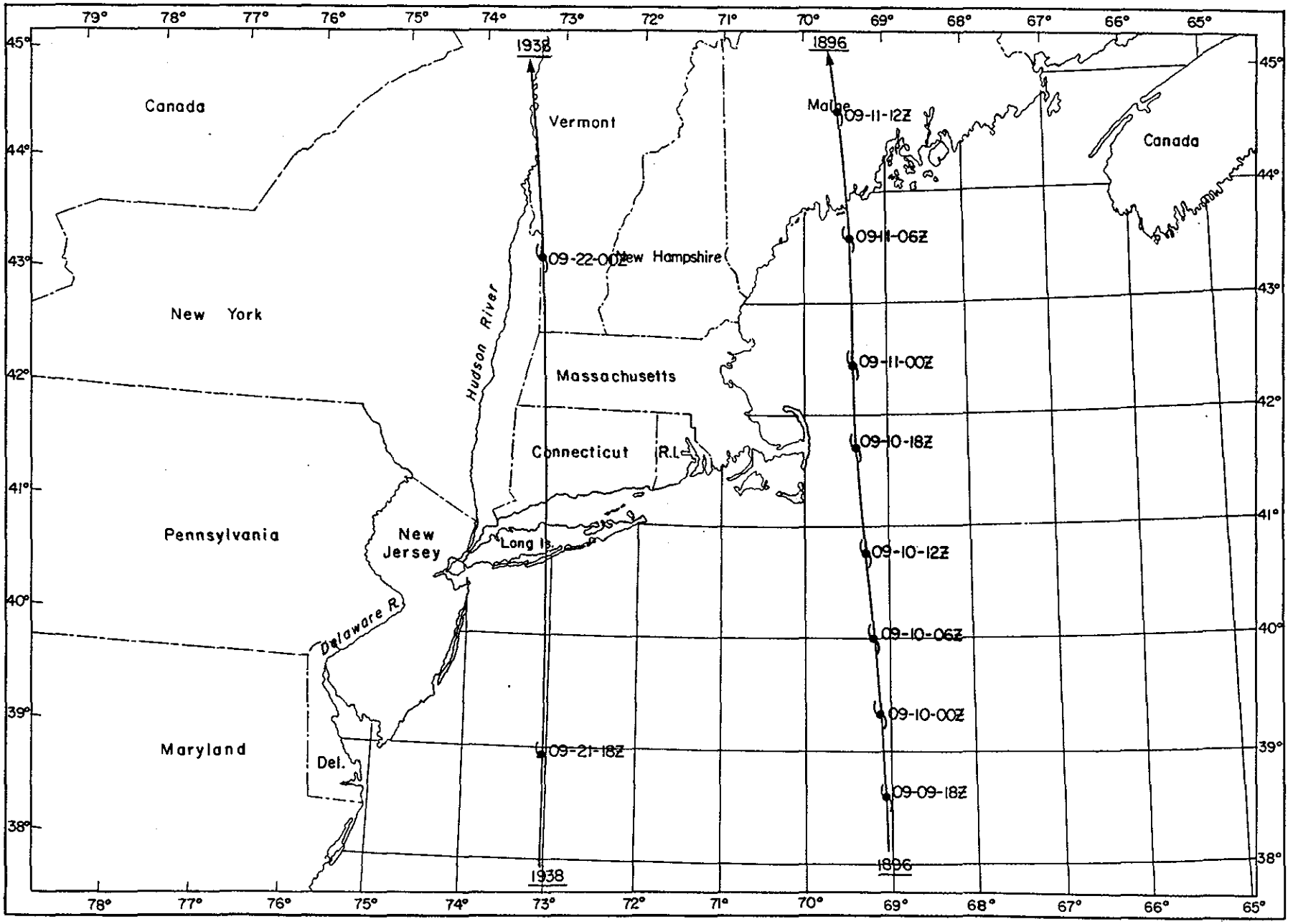
1938
1896
Canada
Vermont
Maine
09-11-12Z
Canada
09-11-06Z
09-22-00Z
New Hampshire
New York
Hudson River
09-11-00Z
Massachusetts
09-10-18Z
Connecticut
R.I.
Pennsylvania
New Jersey
Long Is.
09-10-12Z
Delaware R.
09-10-06Z
09-10-00Z
Maryland
Del.
09-21-18Z
09-09-18Z
1896
1938

FIGURE 2.

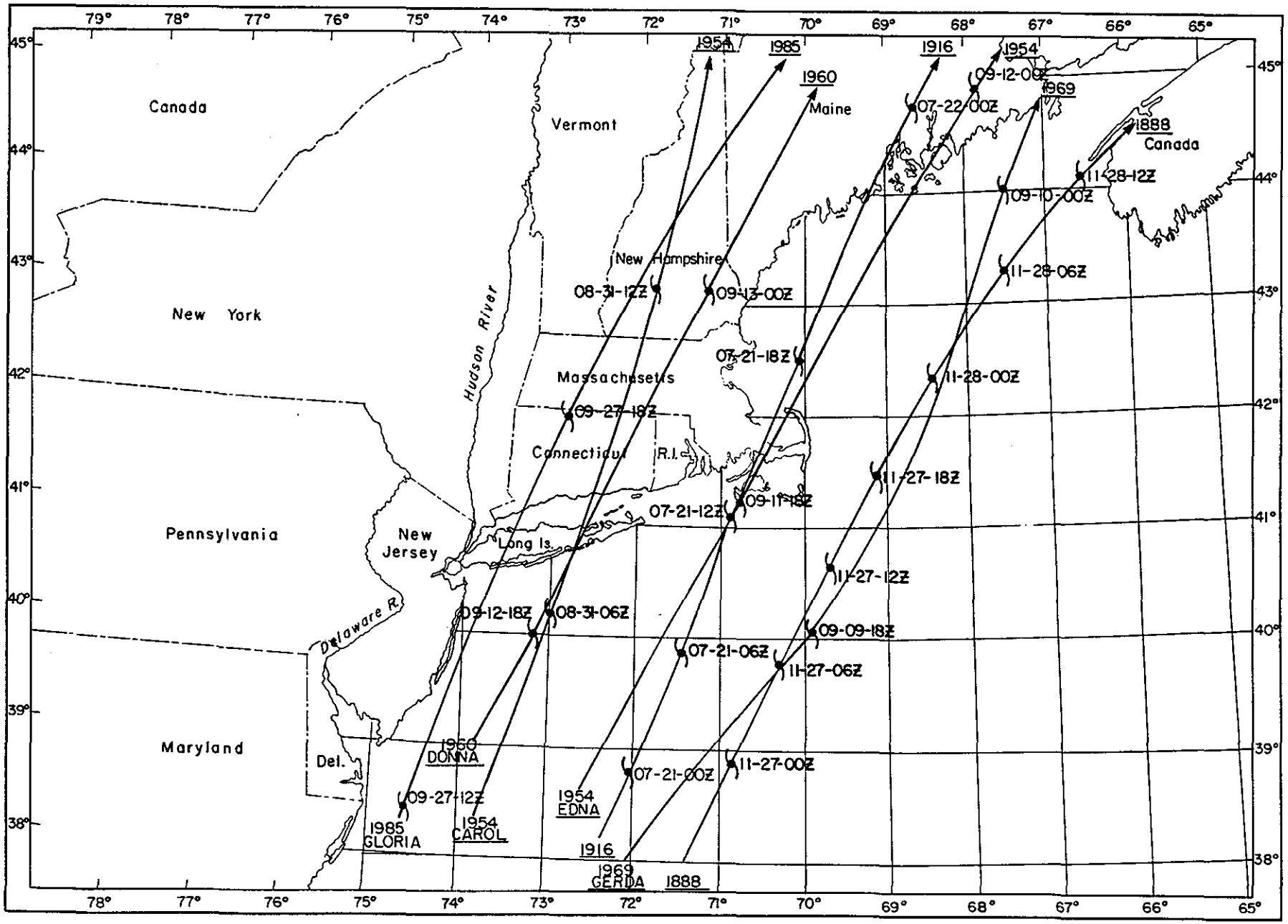
Canada
Vermont
Maine
New Hampshire
New York
Massachusetts
Connecticut
R.I.
Long Is.
New Jersey
Pennsylvania
Maryland
Del.
Hudson River
Delaware R.
1954
1985
1960
1916
1954
09-12-00Z
1969
07-22-00Z
1888
Canada
11-28-12Z
09-10-00Z
11-28-06Z
08-31-12Z
09-13-00Z
07-21-18Z
11-28-00Z
09-27-18Z
11-27-18Z
09-11-18Z
07-21-12Z
11-27-12Z
09-12-18Z
08-31-06Z
09-09-18Z
07-21-06Z
11-27-06Z
1960
DONNA
07-21-00Z
11-27-00Z
09-27-12Z
1954
EDNA
1985
GLORIA
1954
CAROL
1916
1969
GERDA
1888
79°
78°
77°
76°
75°
74°
73°
72°
71°
70°
69°
68°
67°
66°
65°
45°
44°
43°
42°
41°
40°
39°
38°

FIGURE 3.

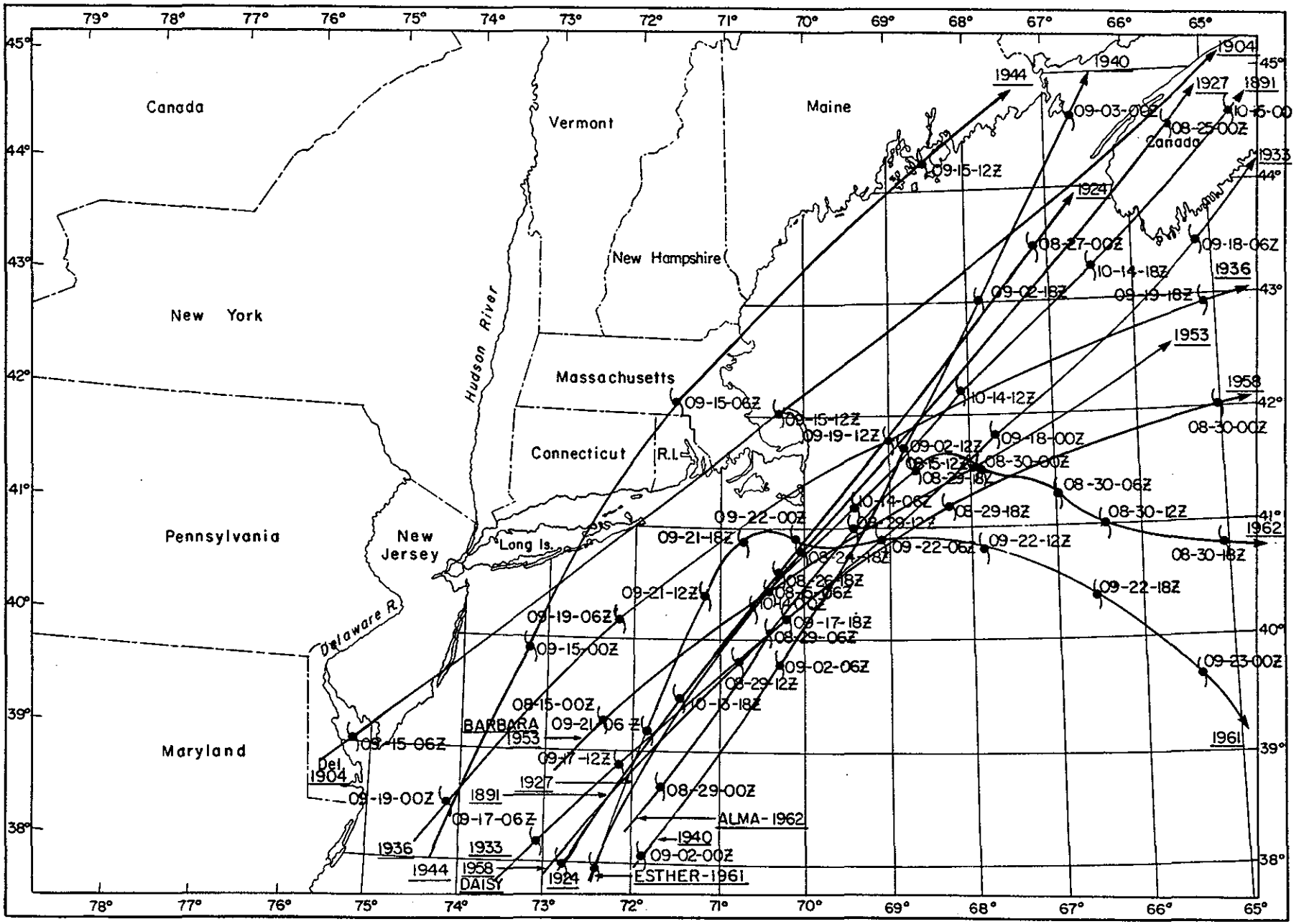
Canada
Vermont
Maine
New York
New Hampshire
Hudson River
Massachusetts
Connecticut
R.I.
Pennsylvania
New Jersey
Long Is.
Delaware R.
Maryland
Del
BARBARA 1953
DAISY
ALMA-1962
ESTHER-1961
1904
1940
1944
1927
1891
1933
1924
1936
1953
1958
1962
1961
09-15-06Z
09-15-12Z
09-19-12Z
09-02-12Z
09-18-00Z
08-30-00Z
08-30-06Z
08-30-12Z
08-30-18Z
09-22-00Z
09-21-18Z
09-22-06Z
09-22-12Z
09-22-18Z
09-23-00Z
09-21-12Z
09-19-06Z
09-15-00Z
08-15-00Z
09-21-06Z
09-17-12Z
09-19-00Z
09-17-06Z
08-29-00Z
09-02-00Z
09-03-06Z
08-25-00Z
09-15-12Z
08-27-00Z
10-14-18Z
09-02-18Z
09-19-18Z
09-18-06Z
10-14-12Z
08-29-18Z
08-30-06Z
10-14-06Z
08-29-12Z
08-26-18Z
09-17-18Z
08-29-06Z
09-02-06Z
08-29-12Z
10-15-18Z

FIGURE 4.

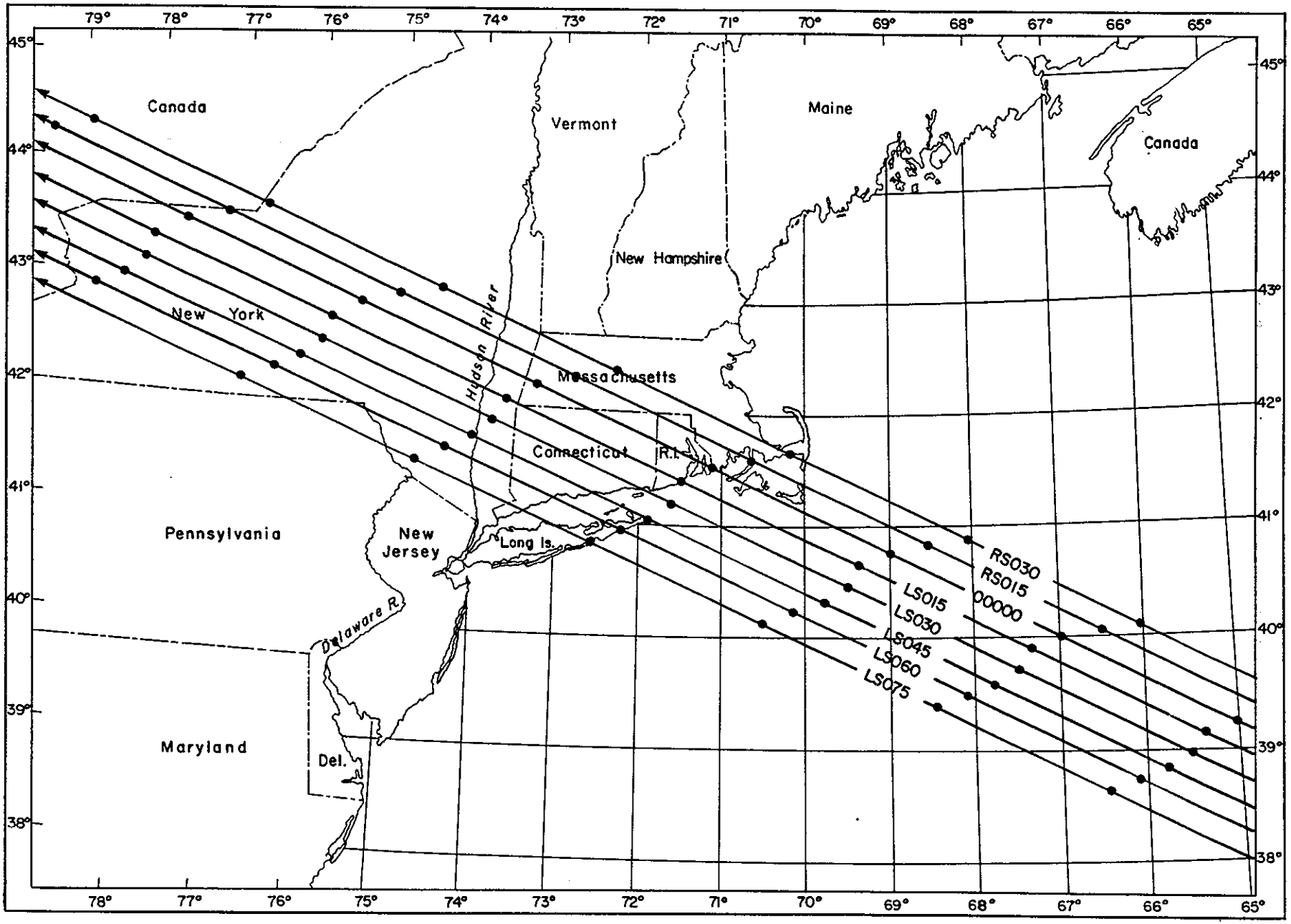
79° 78° 77° 76° 75° 74° 73° 72° 71° 70° 69° 68° 67° 66° 65°
45° 44° 43° 42° 41° 40° 39° 38°
Canada
Vermont
Maine
Canada
New Hampshire
New York
Hudson River
Massachusetts
Connecticut
R.I.
Pennsylvania
New Jersey
Long Is.
Delaware R.
Maryland
Del.
RS030
RS015
00000
LS015
LS030
LS045
LS060
LS075

FIGURE 5.

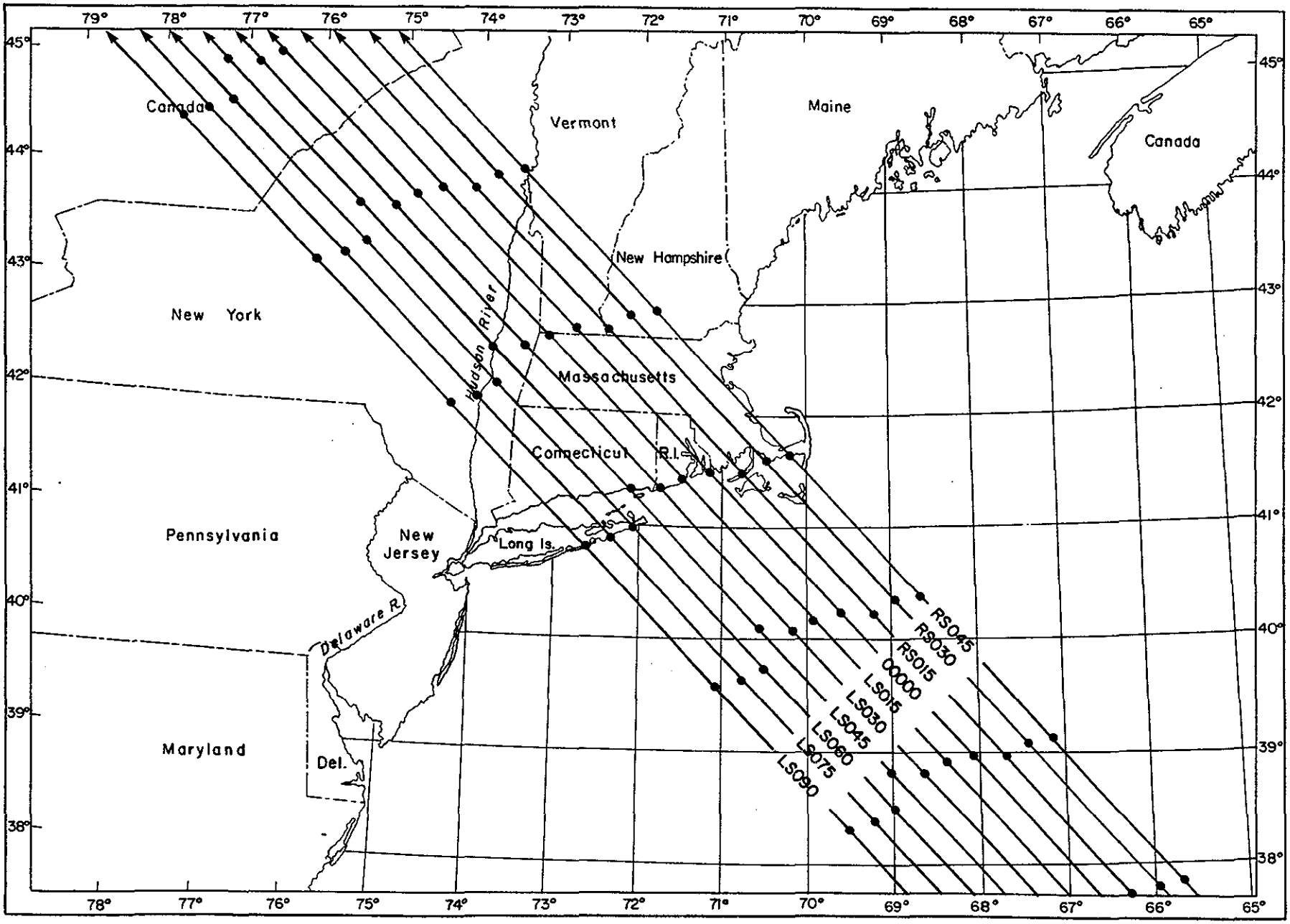
79°
78°
77°
76°
75°
74°
73°
72°
71°
70°
69°
68°
67°
66°
65°
45°
44°
43°
42°
41°
40°
39°
38°
Canada
Vermont
Maine
Canada
New Hampshire
New York
Hudson River
Massachusetts
Connecticut
R.I.
Pennsylvania
New Jersey
Long Is.
Delaware R.
Maryland
Del.
RS045
RS030
RS015
00000
LS015
LS030
LS045
LS060
LS075
LS090

FIGURE 6.

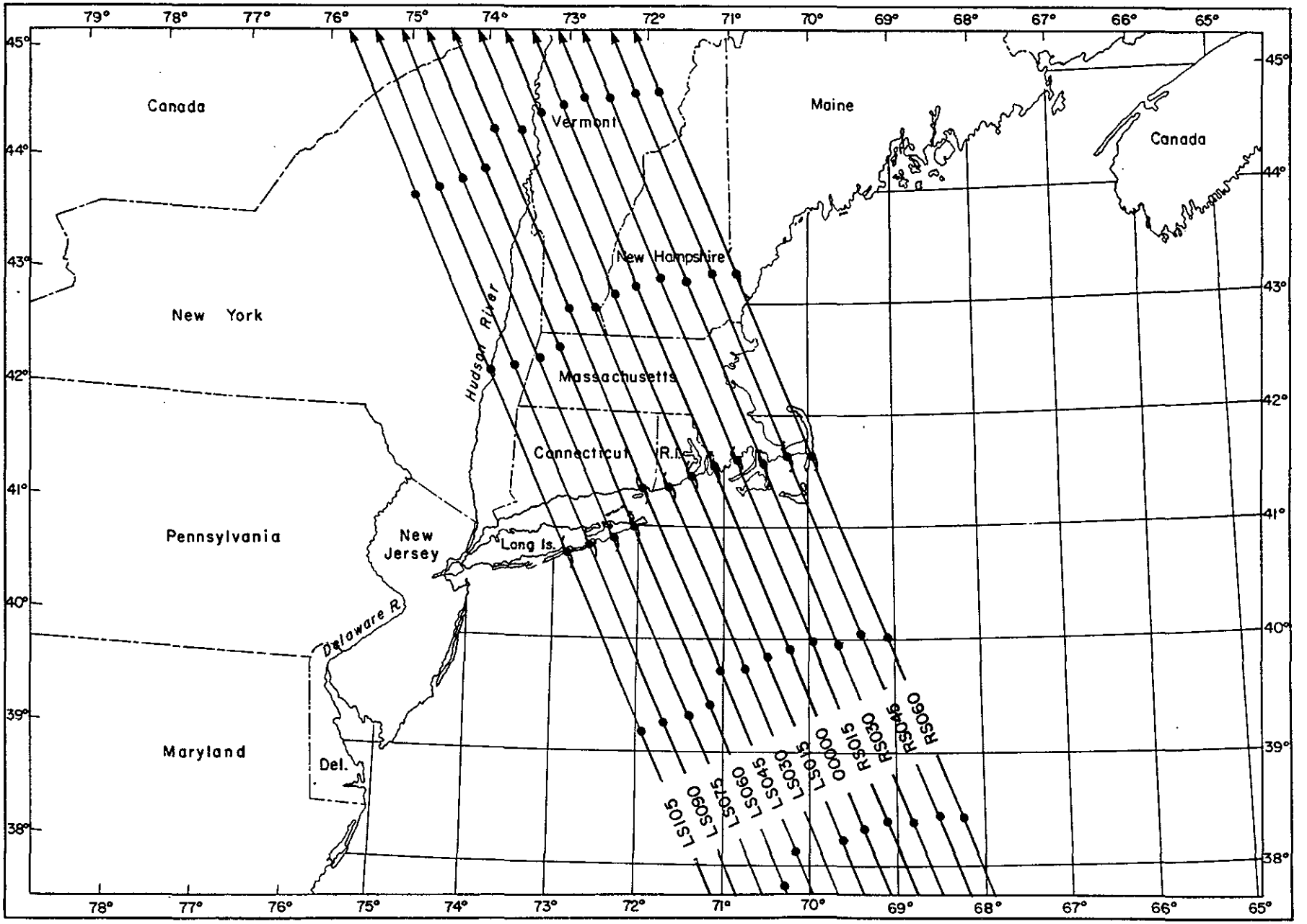
79°
78°
77°
76°
75°
74°
73°
72°
71°
70°
69°
68°
67°
66°
65°
45°
44°
43°
42°
41°
40°
39°
38°
Canada
Vermont
Maine
Canada
New Hampshire
New York
Hudson River
Massachusetts
Connecticut
R.I.
Pennsylvania
New Jersey
Long Is.
Delaware R.
Maryland
Del.
L5105
L5090
L5075
L5060
L5045
L5030
L5015
00000
R5015
R5030
R5045
R5060

FIGURE 7.

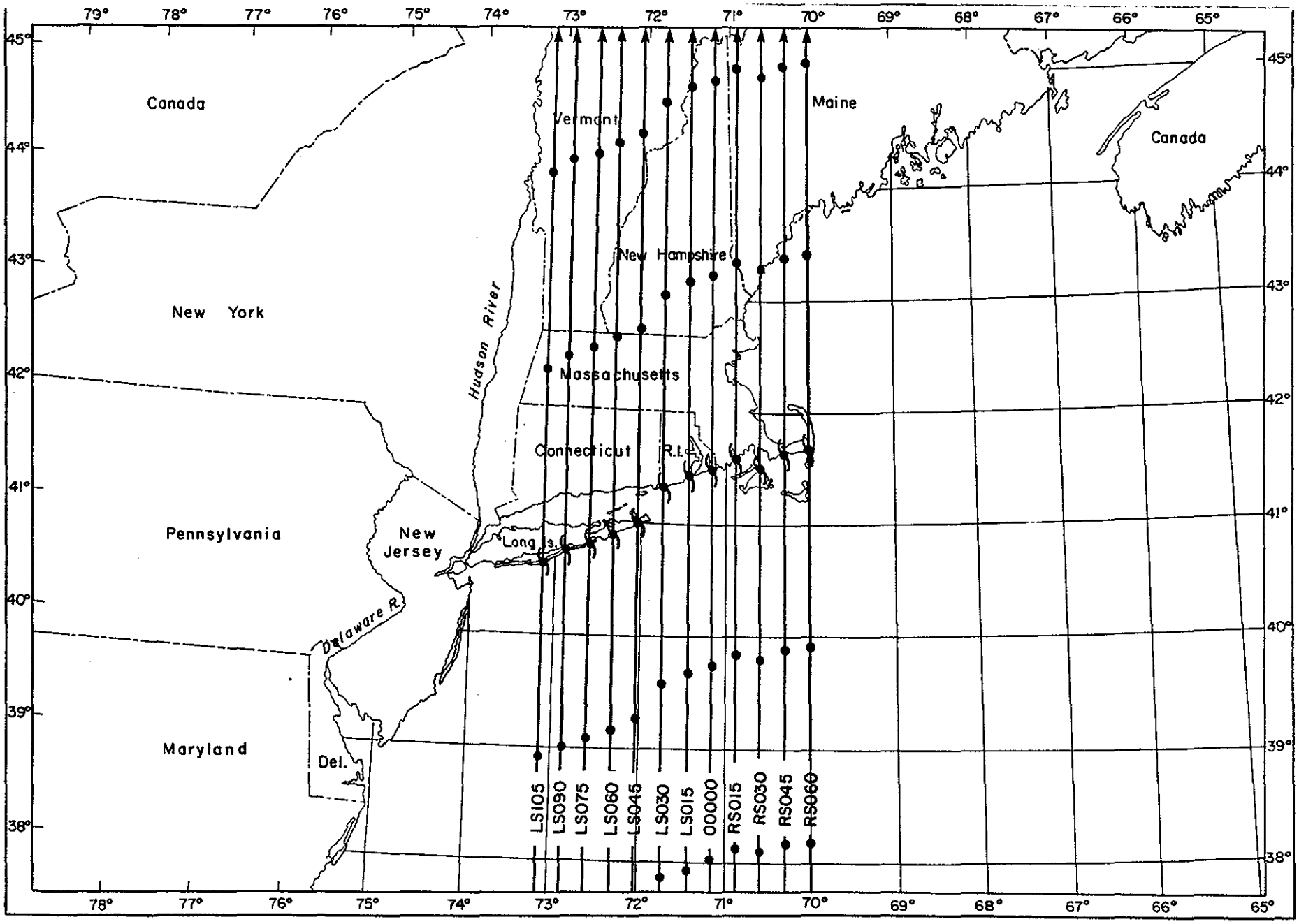
79°
78°
77°
76°
75°
74°
73°
72°
71°
70°
69°
68°
67°
66°
65°
45°
44°
43°
42°
41°
40°
39°
38°
Canada
Vermont
Maine
Canada
New Hampshire
New York
Hudson River
Massachusetts
Connecticut
R.I.
Pennsylvania
New Jersey
Long Is.
Delaware R.
Maryland
Del.
LS105
LS090
LS075
LS060
LS045
LS030
LS015
00000
RS015
RS030
RS045
RS060

FIGURE 8.

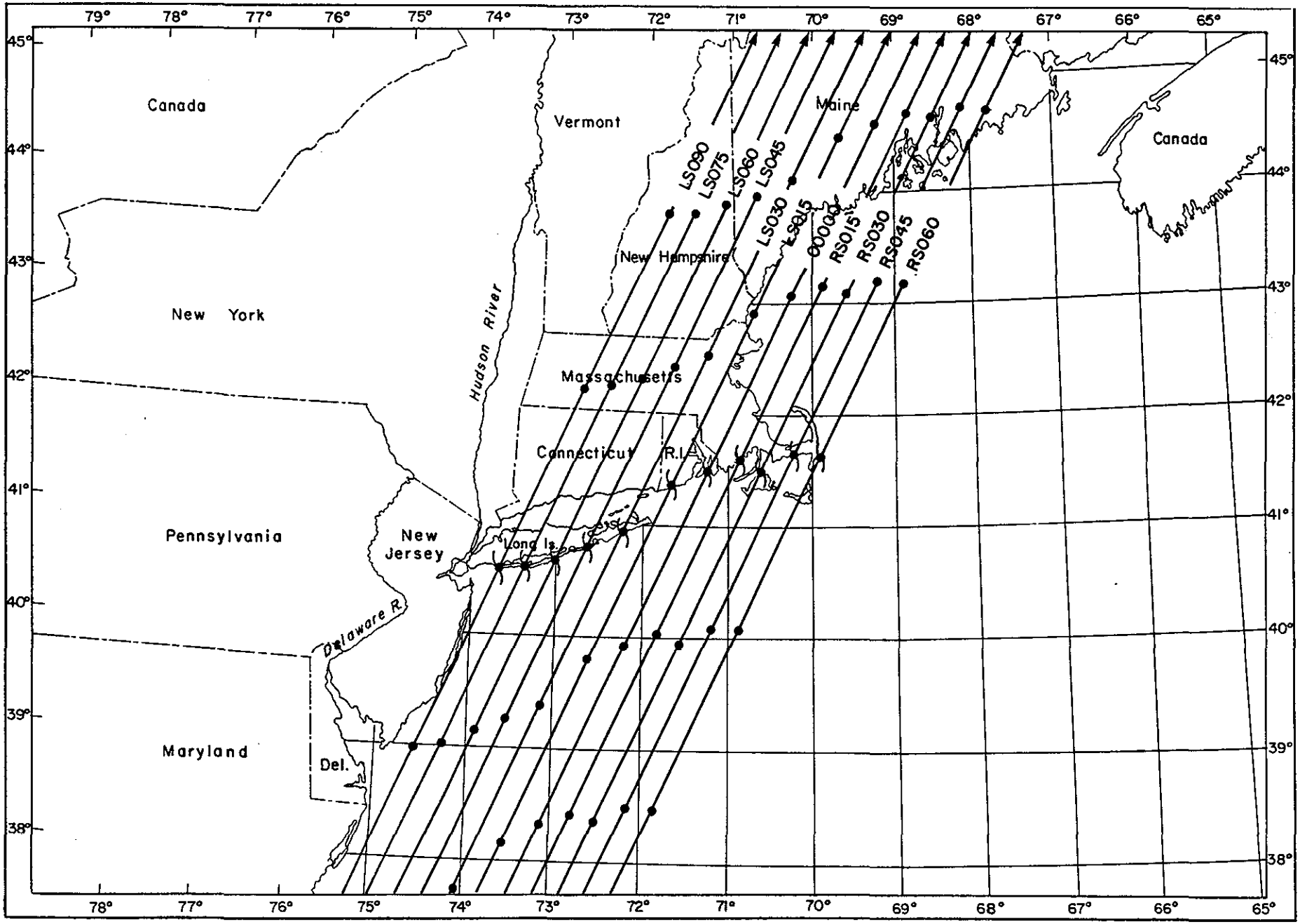
79° 78° 77° 76° 75° 74° 73° 72° 71° 70° 69° 68° 67° 66° 65°
45° 44° 43° 42° 41° 40° 39° 38°
Canada
Vermont
Maine
Canada
New Hampshire
New York
Massachusetts
Connecticut
R.I.
Pennsylvania
New Jersey
Long Is.
Maryland
Del.
Hudson River
Delaware R.
LS090
LS075
LS060
LS045
LS030
LS015
000000
RS015
RS030
RS045
RS060

FIGURE 9.

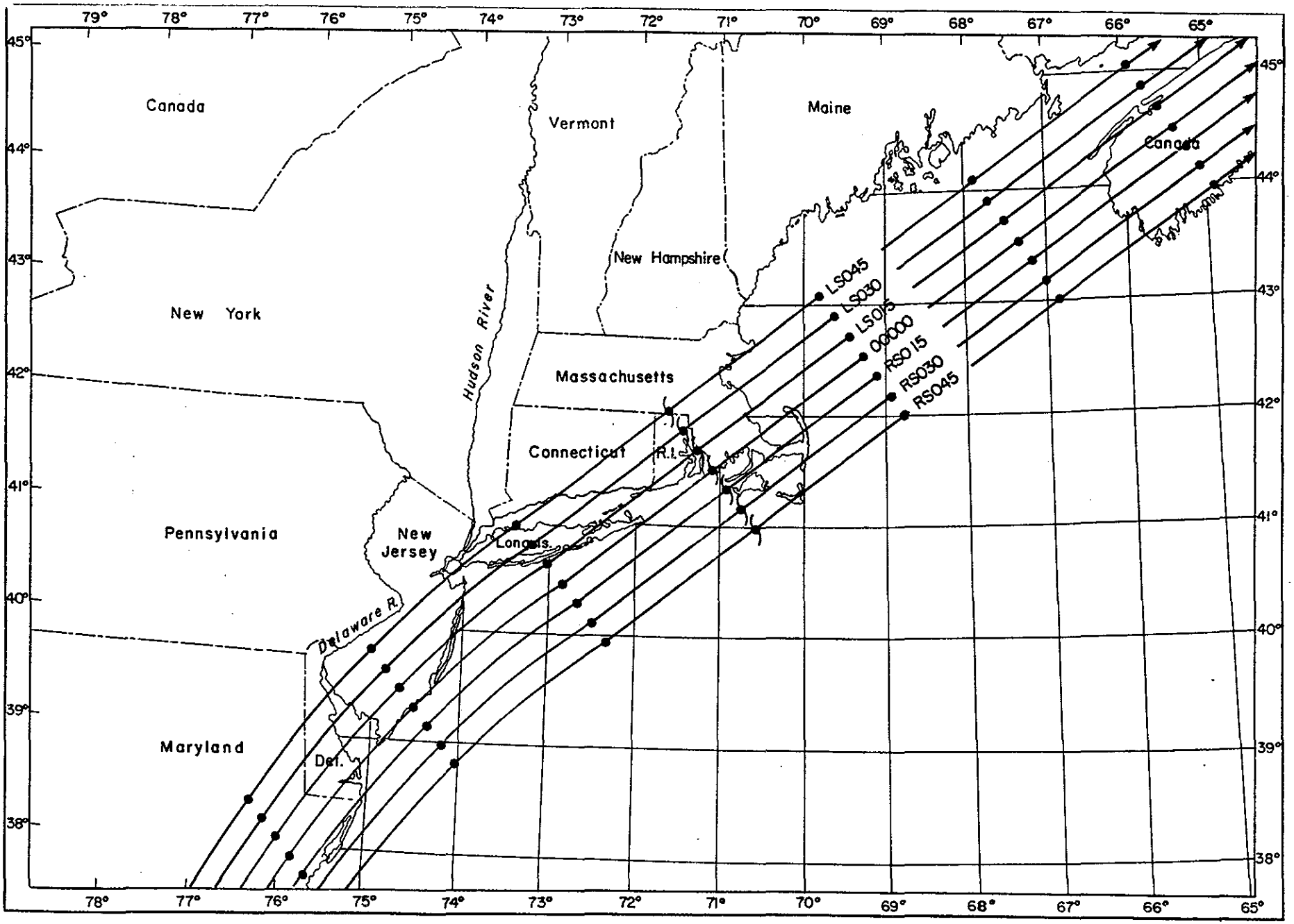
79°
78°
77°
76°
75°
74°
73°
72°
71°
70°
69°
68°
67°
66°
65°
45°
44°
43°
42°
41°
40°
39°
38°
Canada
Vermont
Maine
New Hampshire
New York
Massachusetts
Connecticut
R.I.
Pennsylvania
New Jersey
Maryland
Del.
Hudson River
Delaware R.
Long Is.
LS045
LS030
LS015
00000
RS015
RS030
RS045

FIGURE 10.

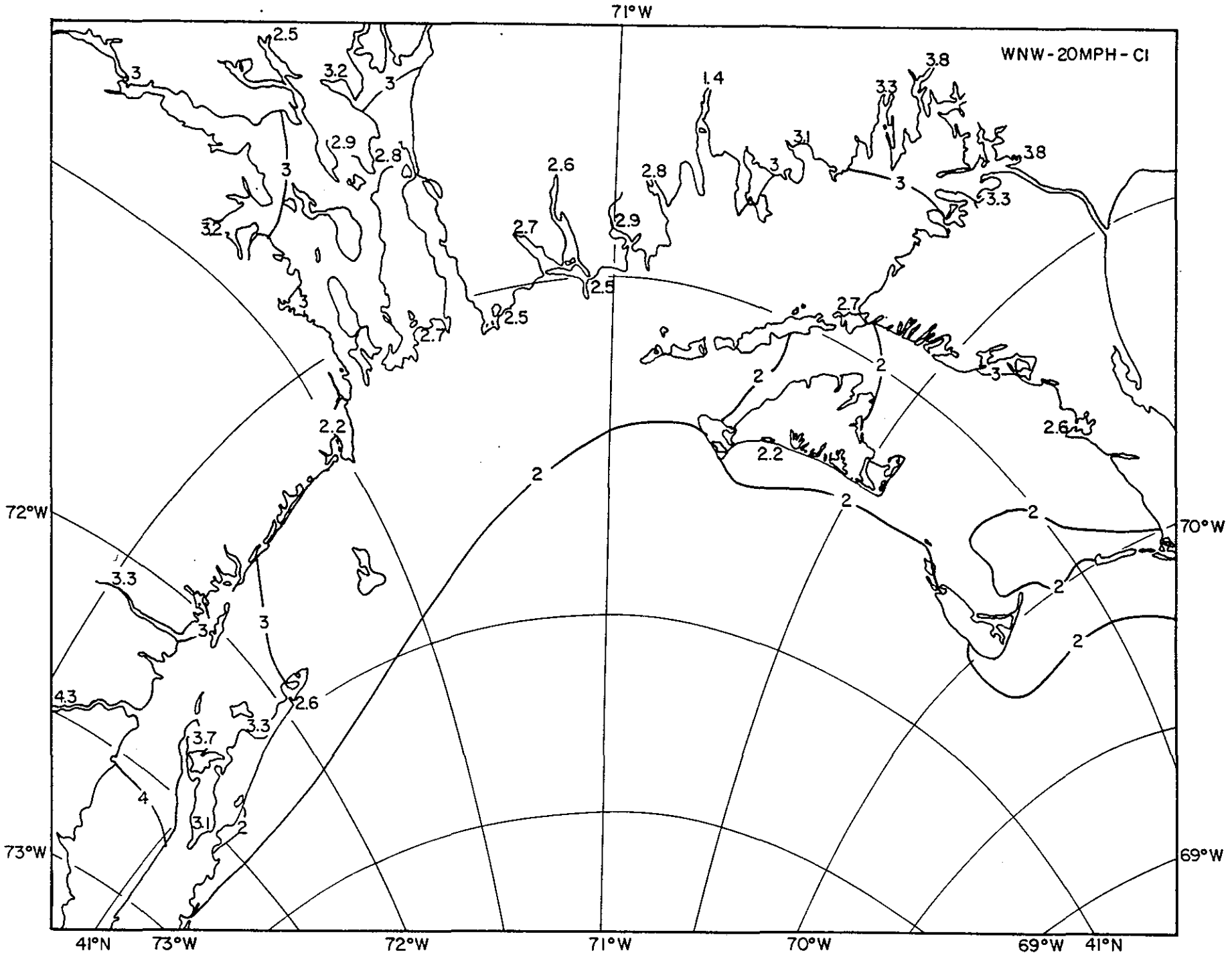
71°W
WNW-20MPH-CI
72°W
70°W
73°W
69°W
41°N
73°W
72°W
71°W
70°W
69°W
41°N

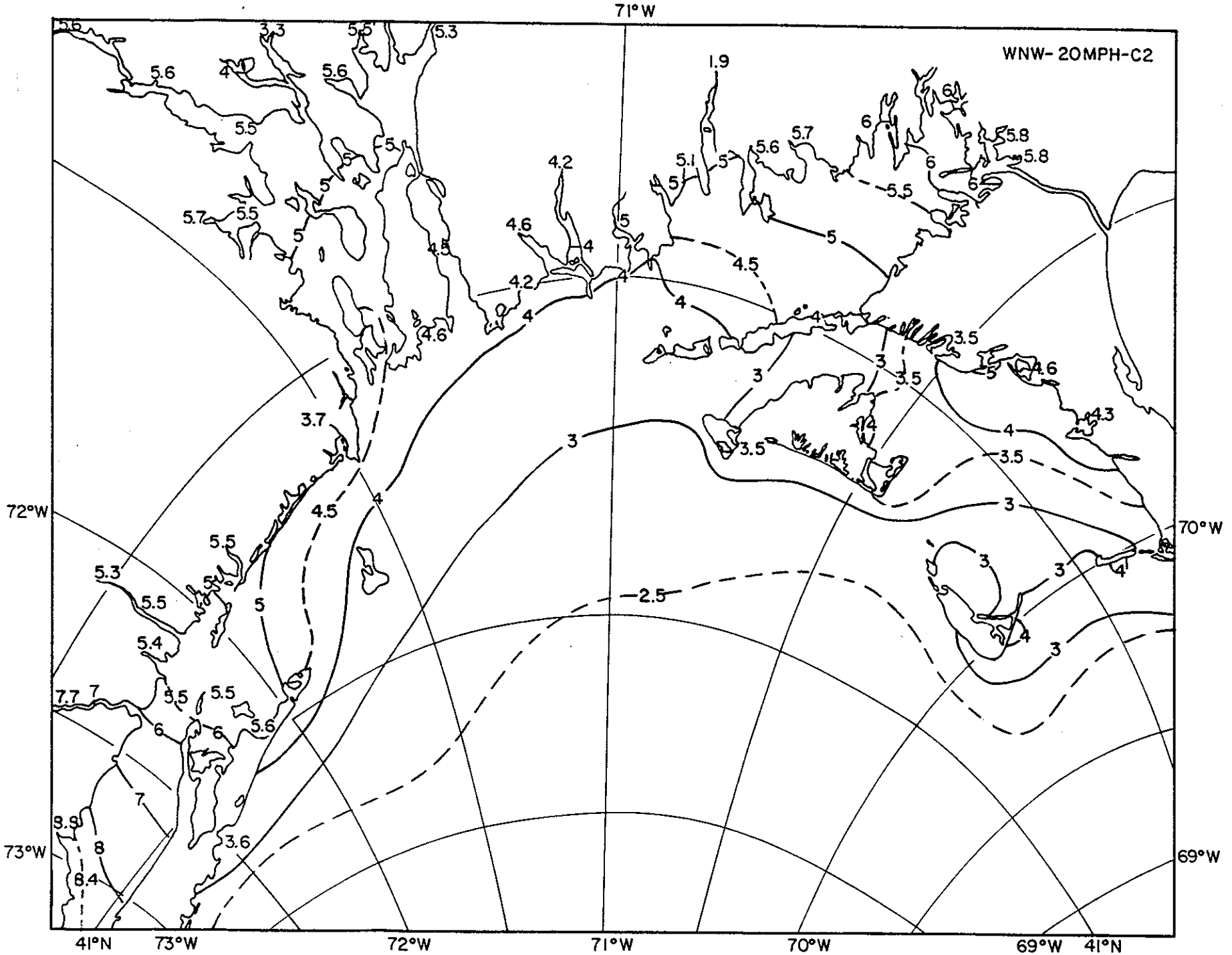
71°W
WNW- 20MPH-C2
72°W
70°W
73°W
69°W
41°N
73°W
72°W
71°W
70°W
69°W
41°N
2.5

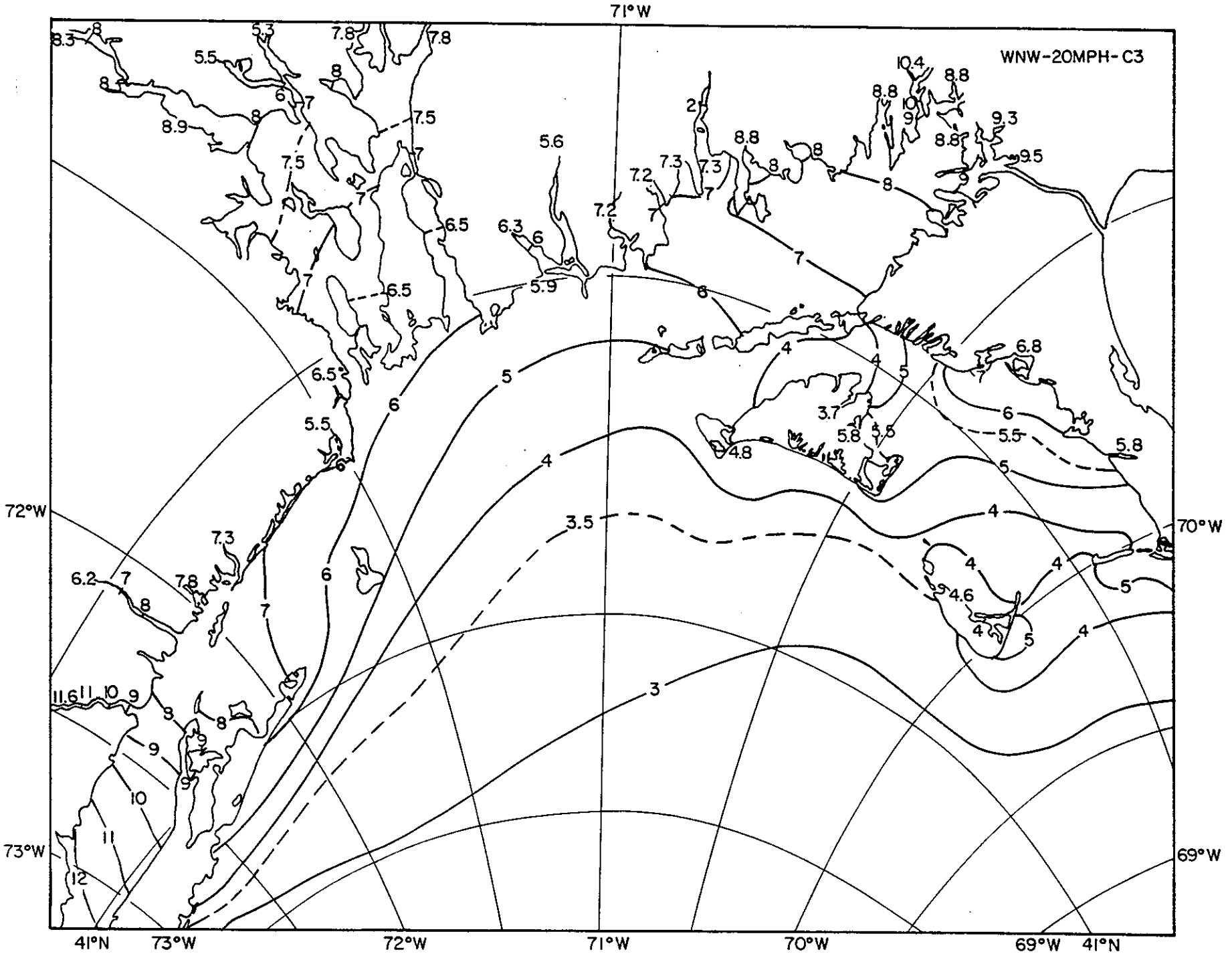
71°W
WNW-20MPH-C3
72°W
70°W
73°W
69°W
41°N
73°W
72°W
71°W
70°W
69°W
41°N

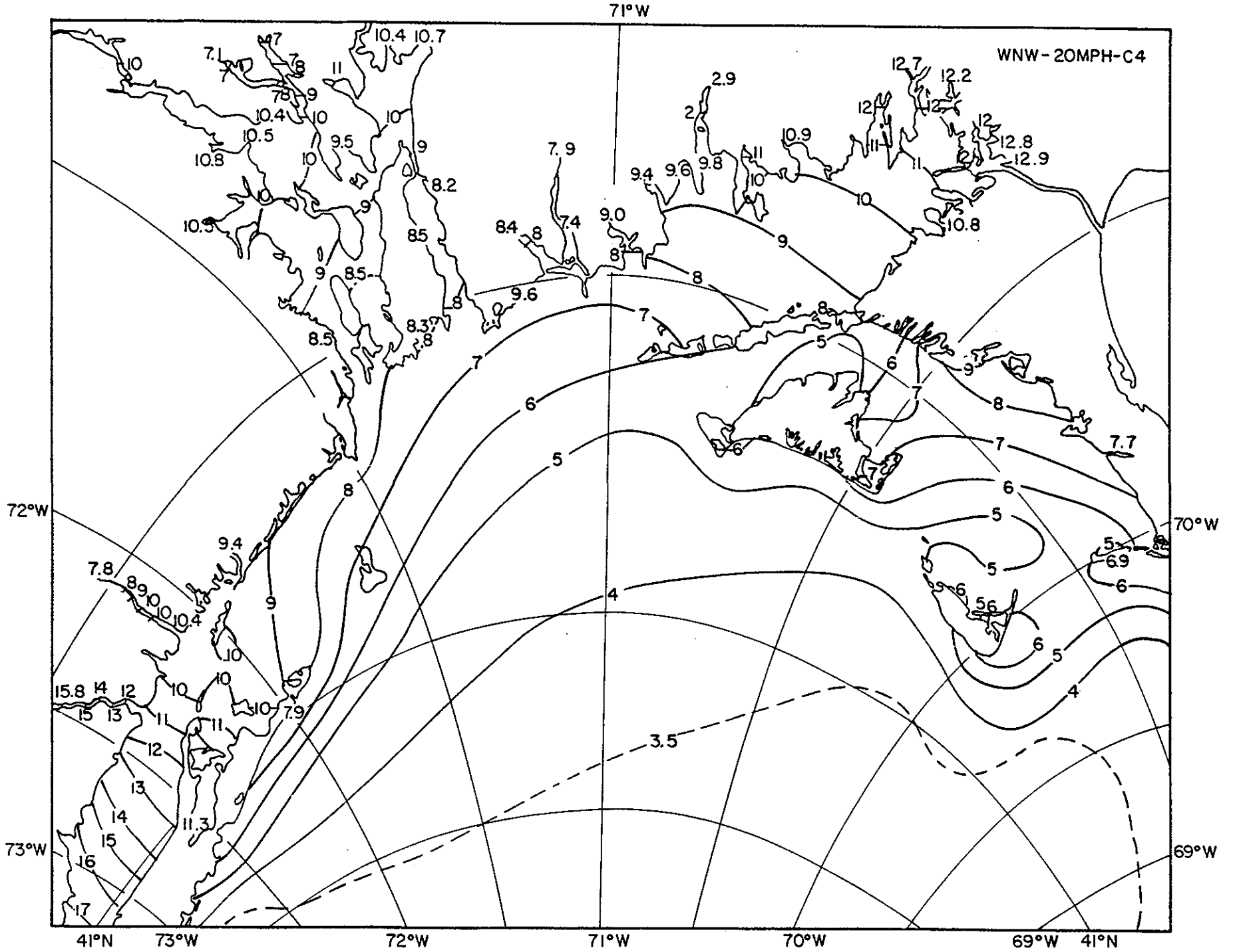
71°W
WNW-20MPH-C4
72°W
70°W
73°W
69°W
41°N
73°W
72°W
71°W
70°W
69°W
41°N
3.5

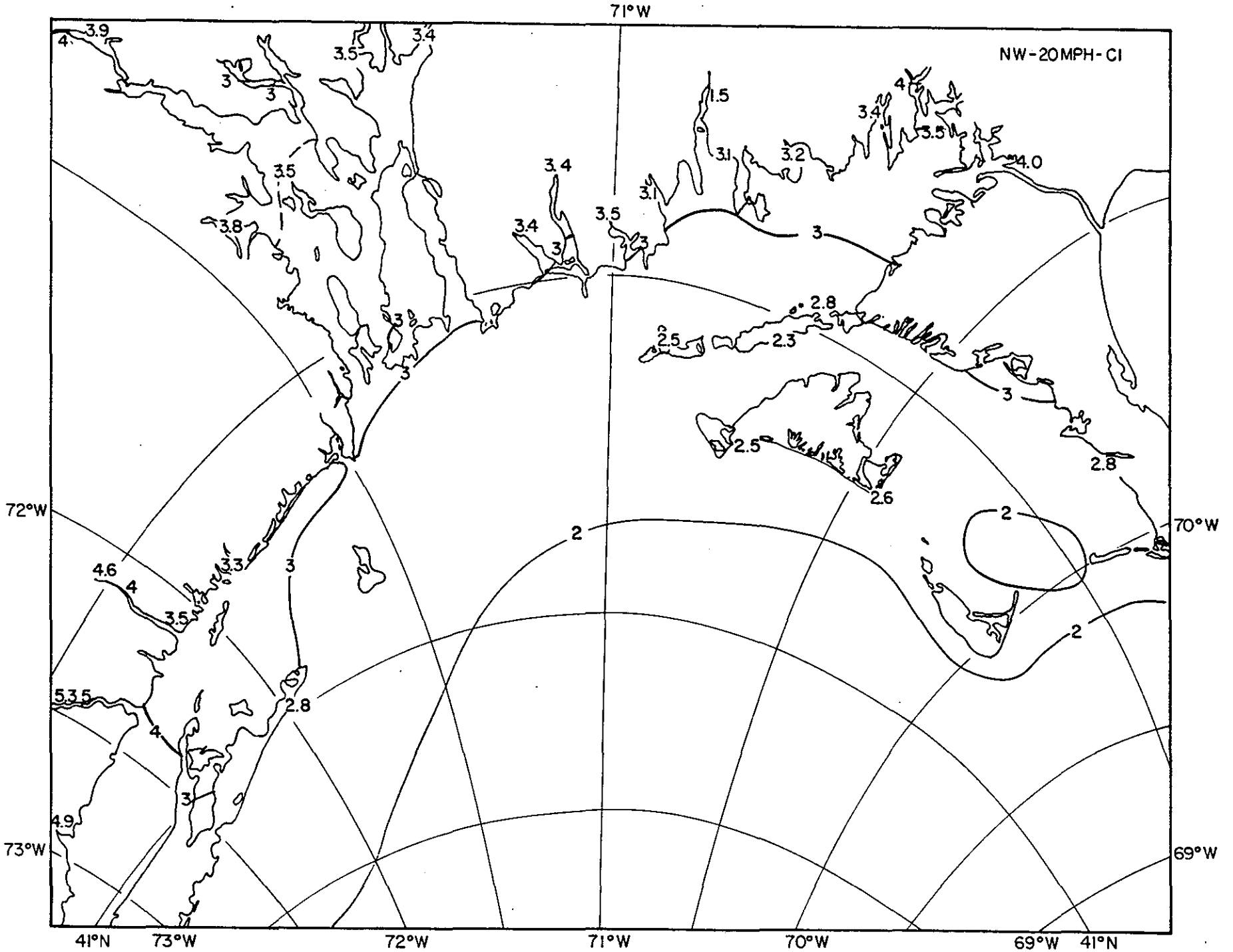
71°W
NW-20MPH-CI
72°W
70°W
73°W
69°W
41°N
73°W
72°W
71°W
70°W
69°W
41°N

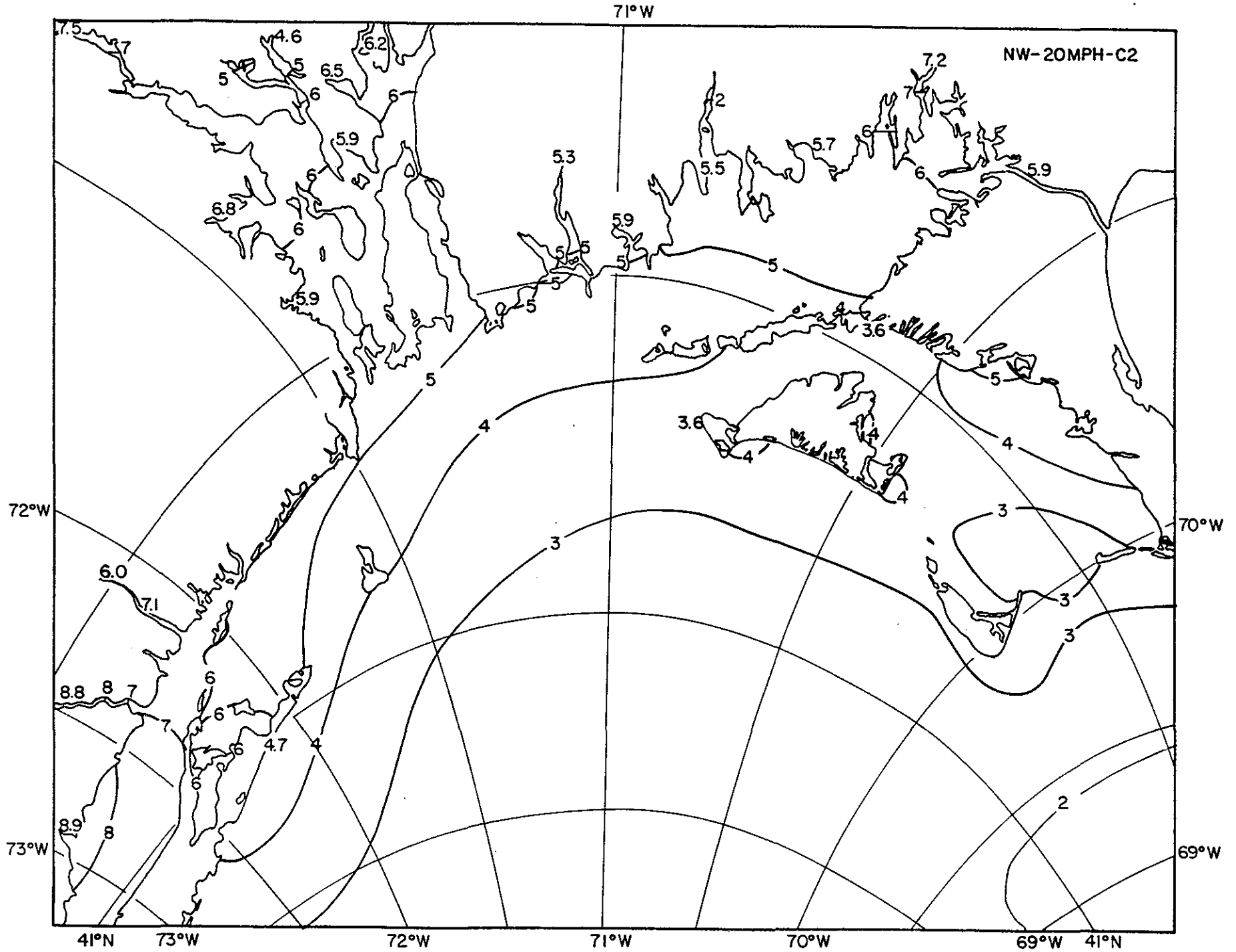
NW-20MPH-C2
71°W
72°W
73°W
70°W
69°W
41°N
73°W
72°W
71°W
70°W
69°W
41°N

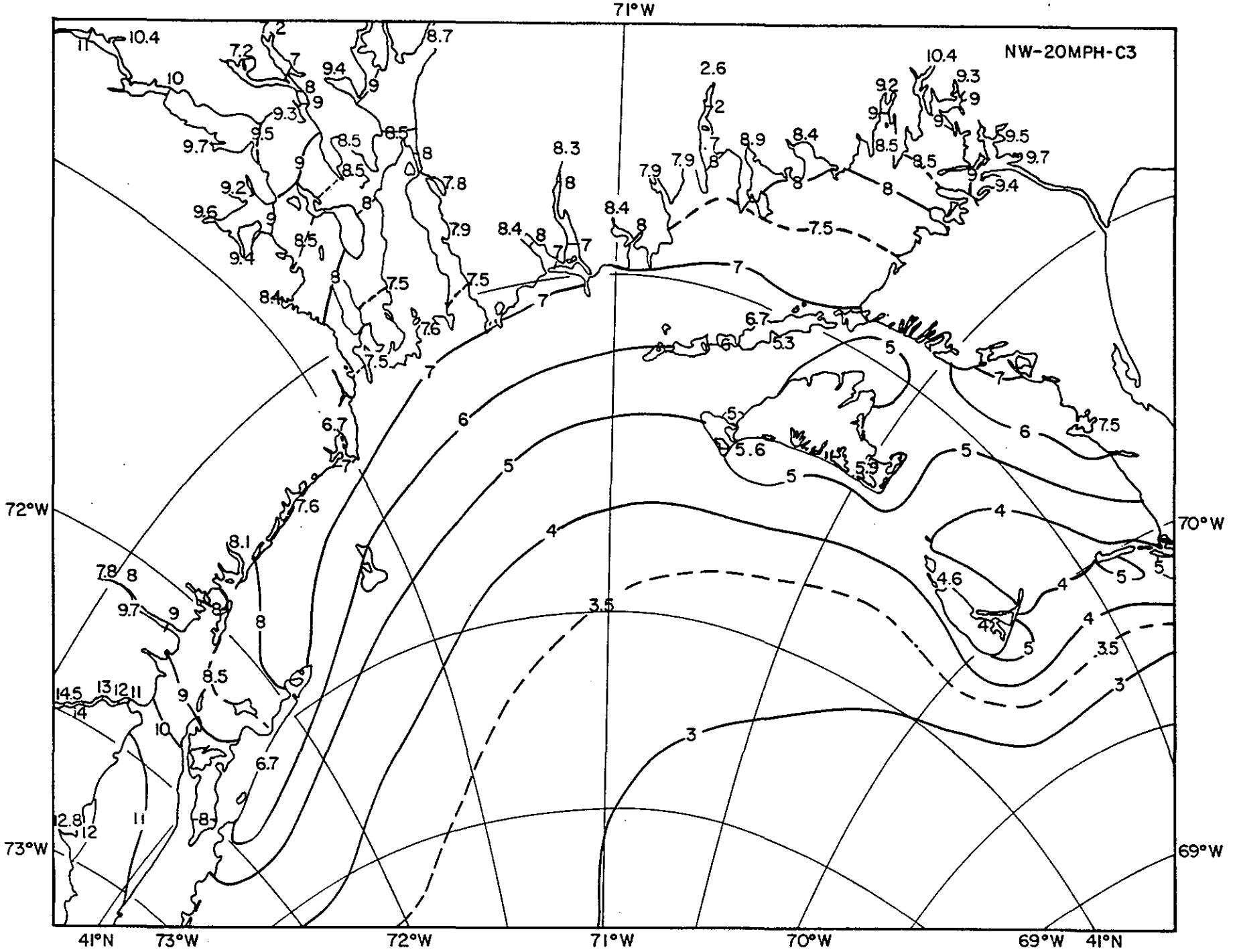
NW-20MPH-C3
71°W
72°W
70°W
73°W
69°W
41°N
73°W
72°W
71°W
70°W
69°W
41°N

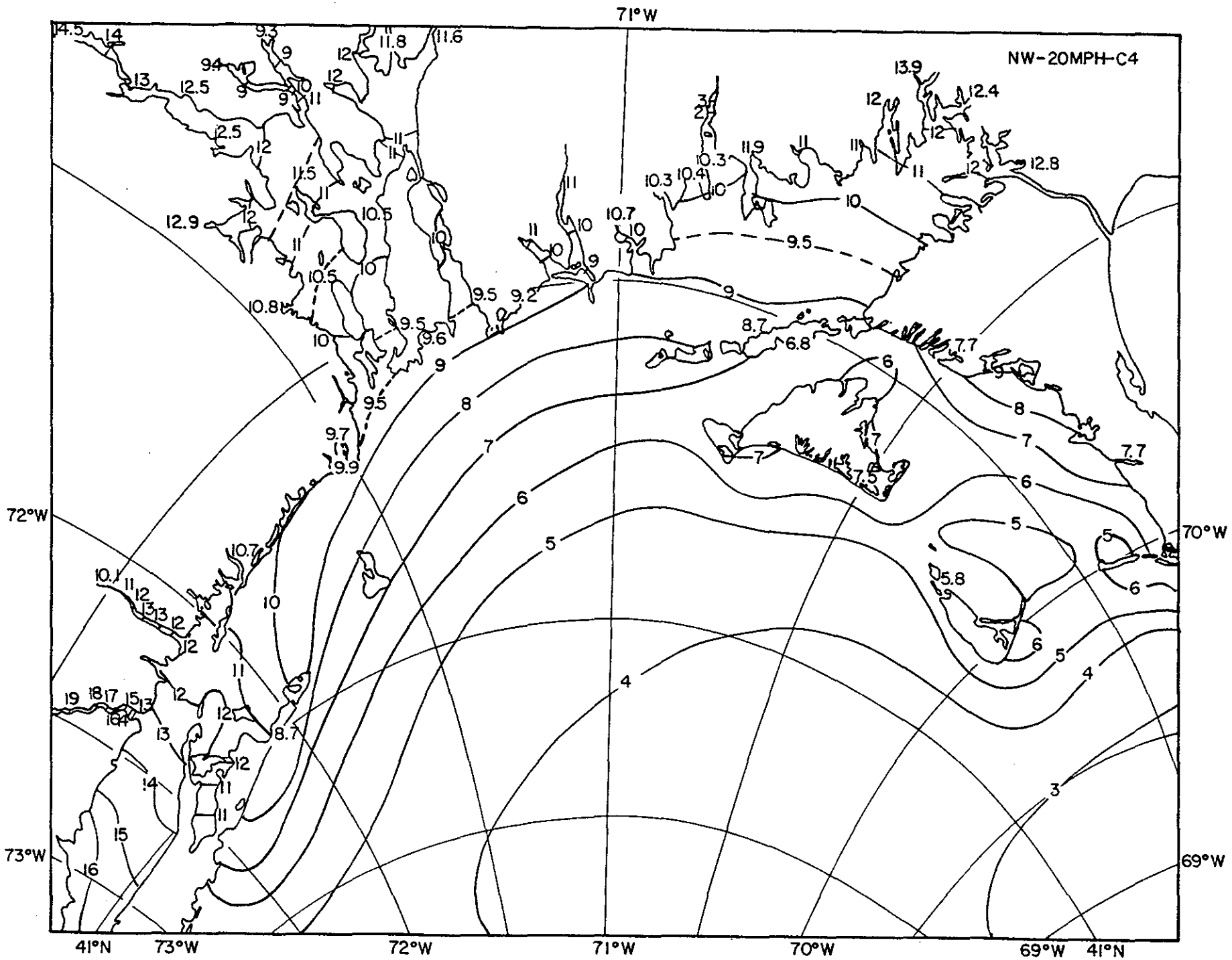
NW-20MPH-C4
71°W
72°W
70°W
73°W
69°W
41°N
73°W
72°W
71°W
70°W
69°W
41°N

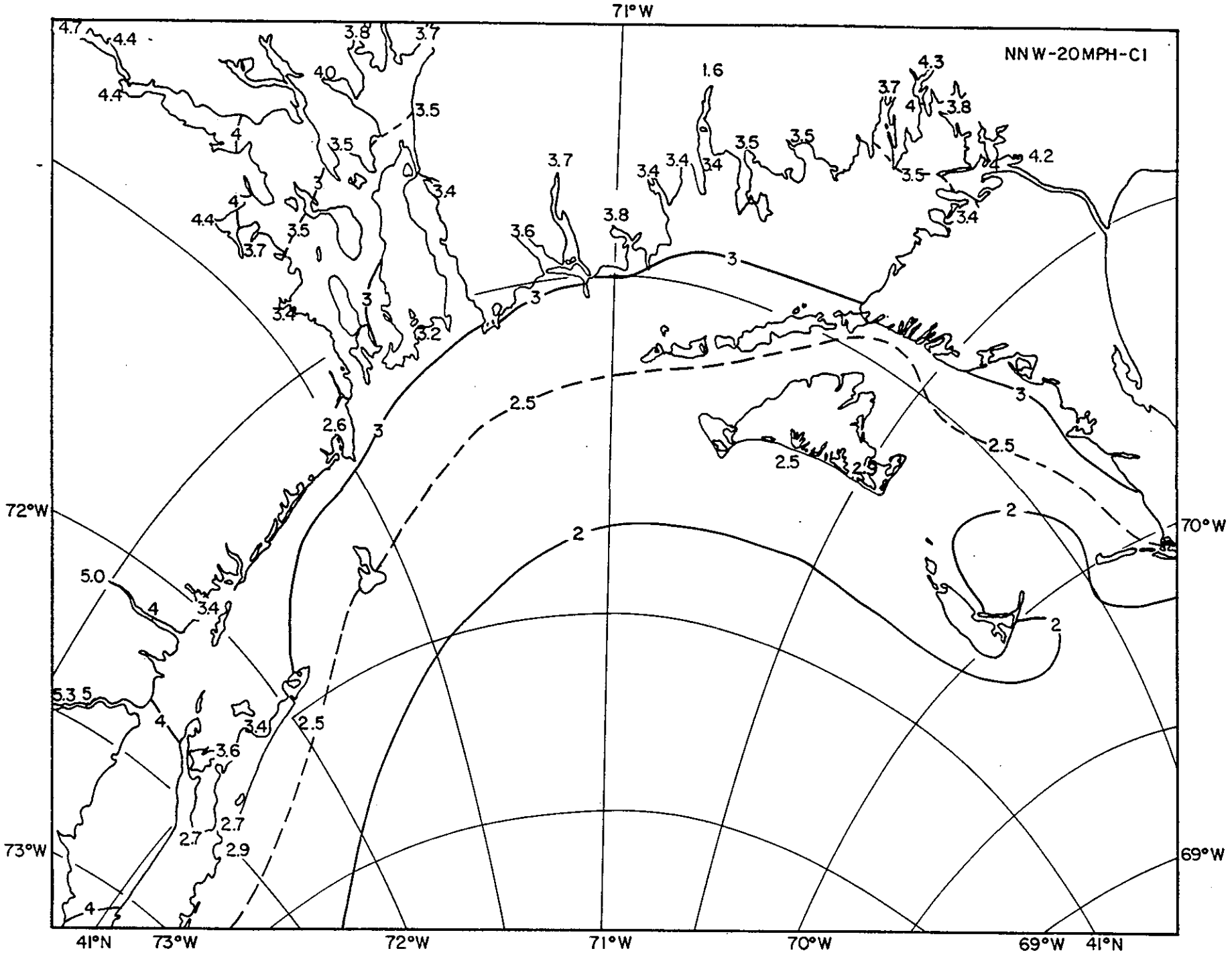
71°W
NNW-20MPH-CI
72°W
70°W
73°W
69°W
41°N
73°W
72°W
71°W
70°W
69°W
41°N

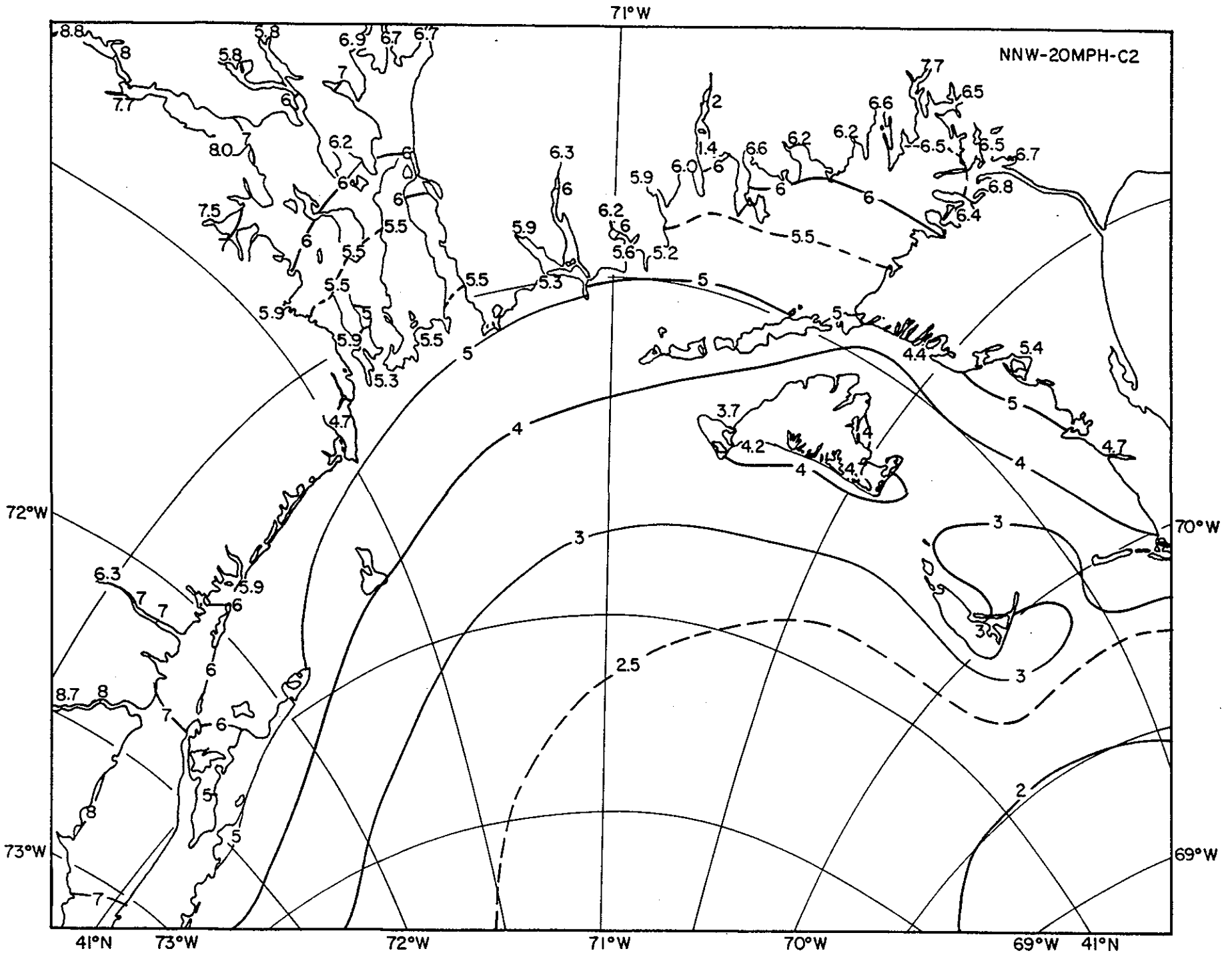
NNW-20MPH-C2
71°W
72°W
70°W
73°W
69°W
41°N
73°W
72°W
71°W
70°W
69°W
41°N

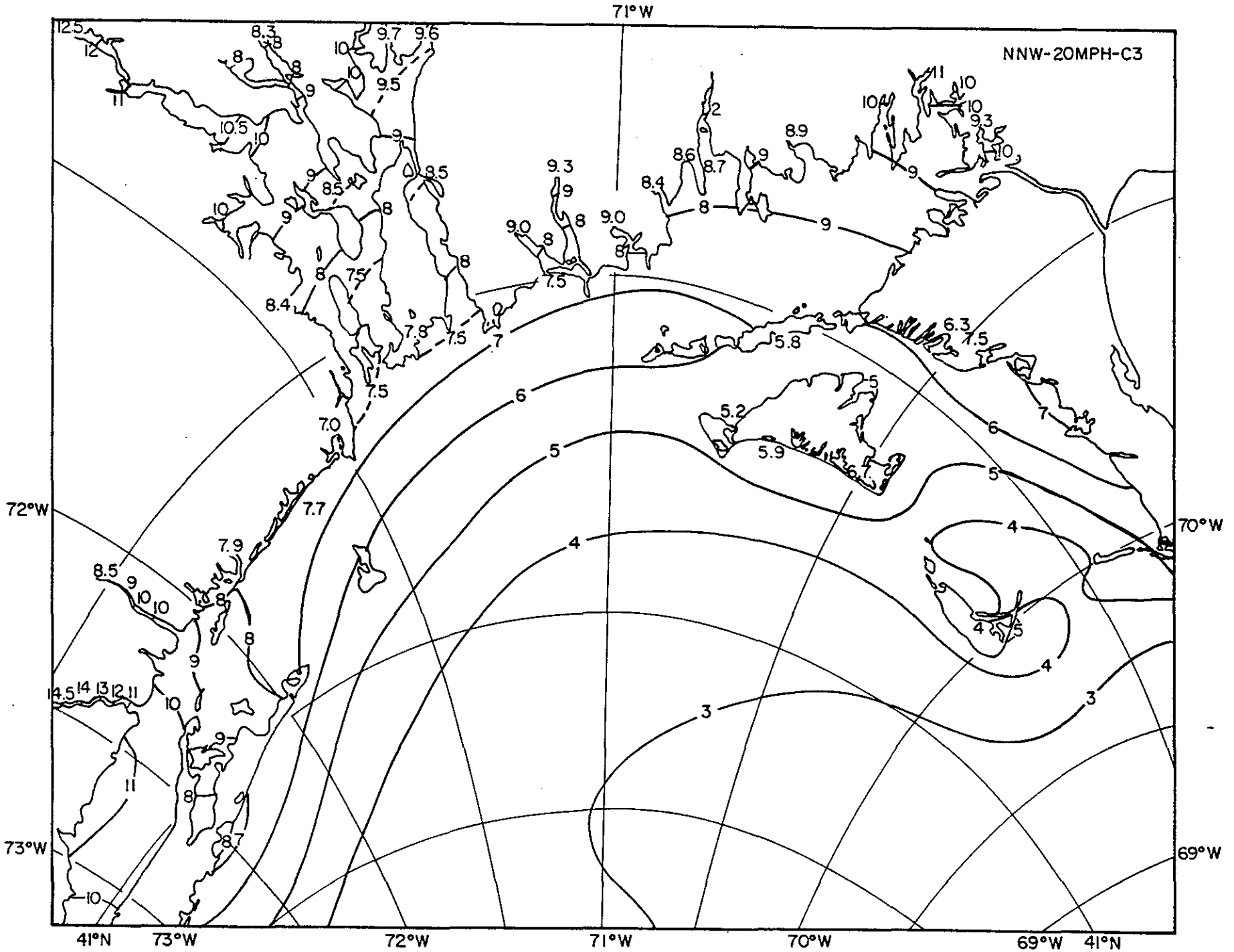
NNW-20MPH-C3
71°W
72°W
73°W
70°W
69°W
41°N

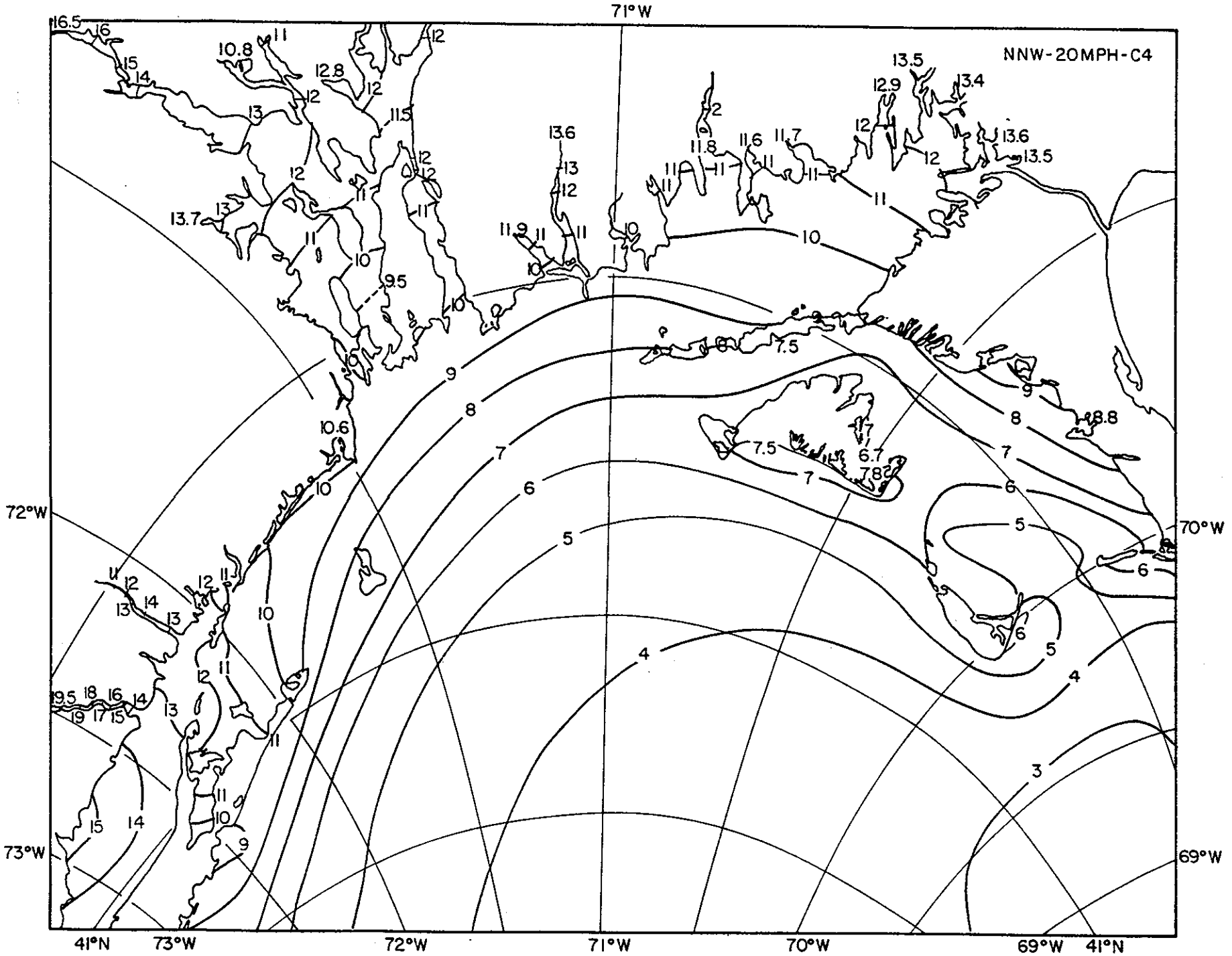
NNW-20MPH-C4
71°W
72°W
73°W
70°W
69°W
41°N
73°W
72°W
71°W
70°W
69°W
41°N

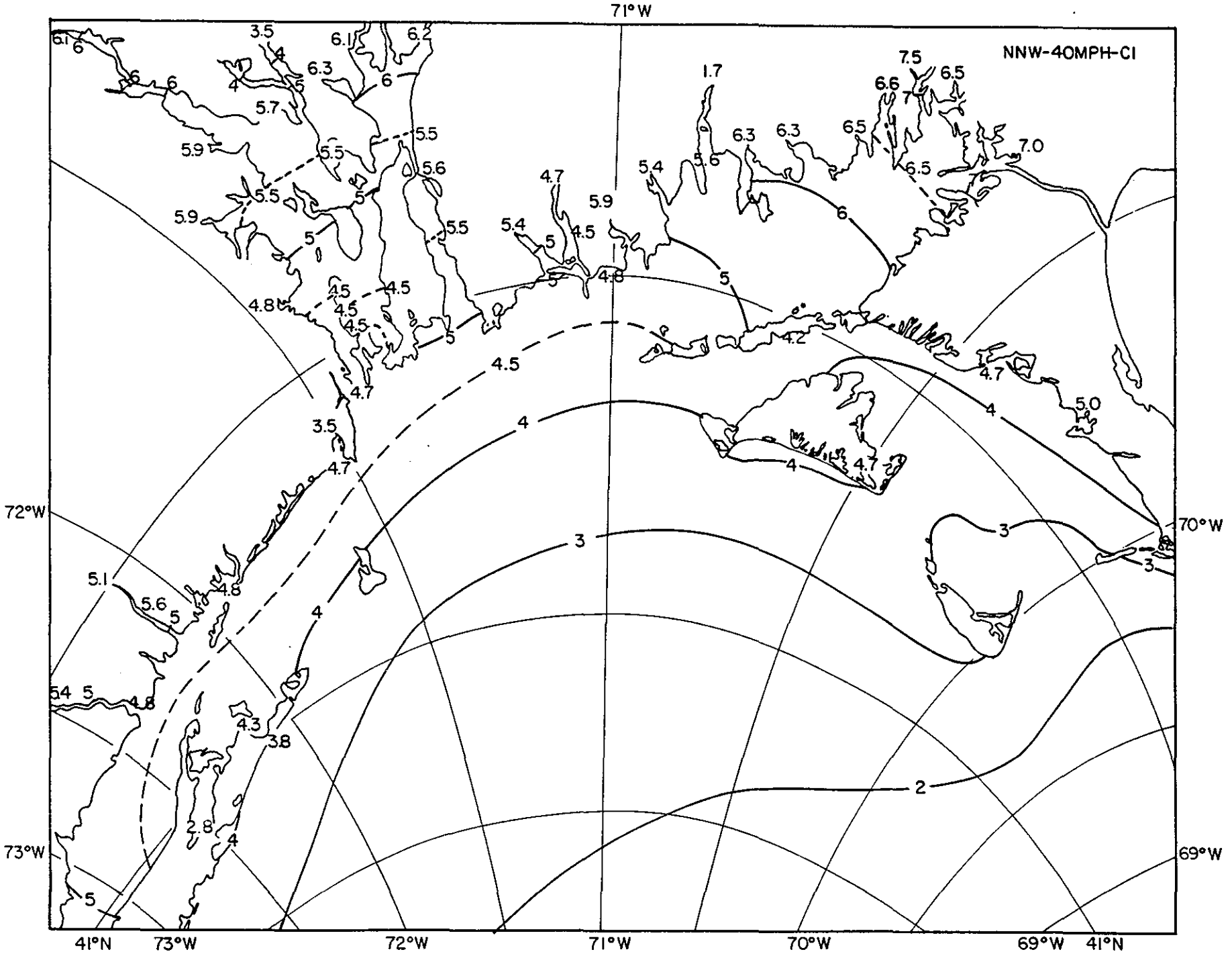
NNW-40MPH-CI
71°W
72°W
73°W
70°W
69°W
41°N
73°W
72°W
71°W
70°W
69°W
41°N

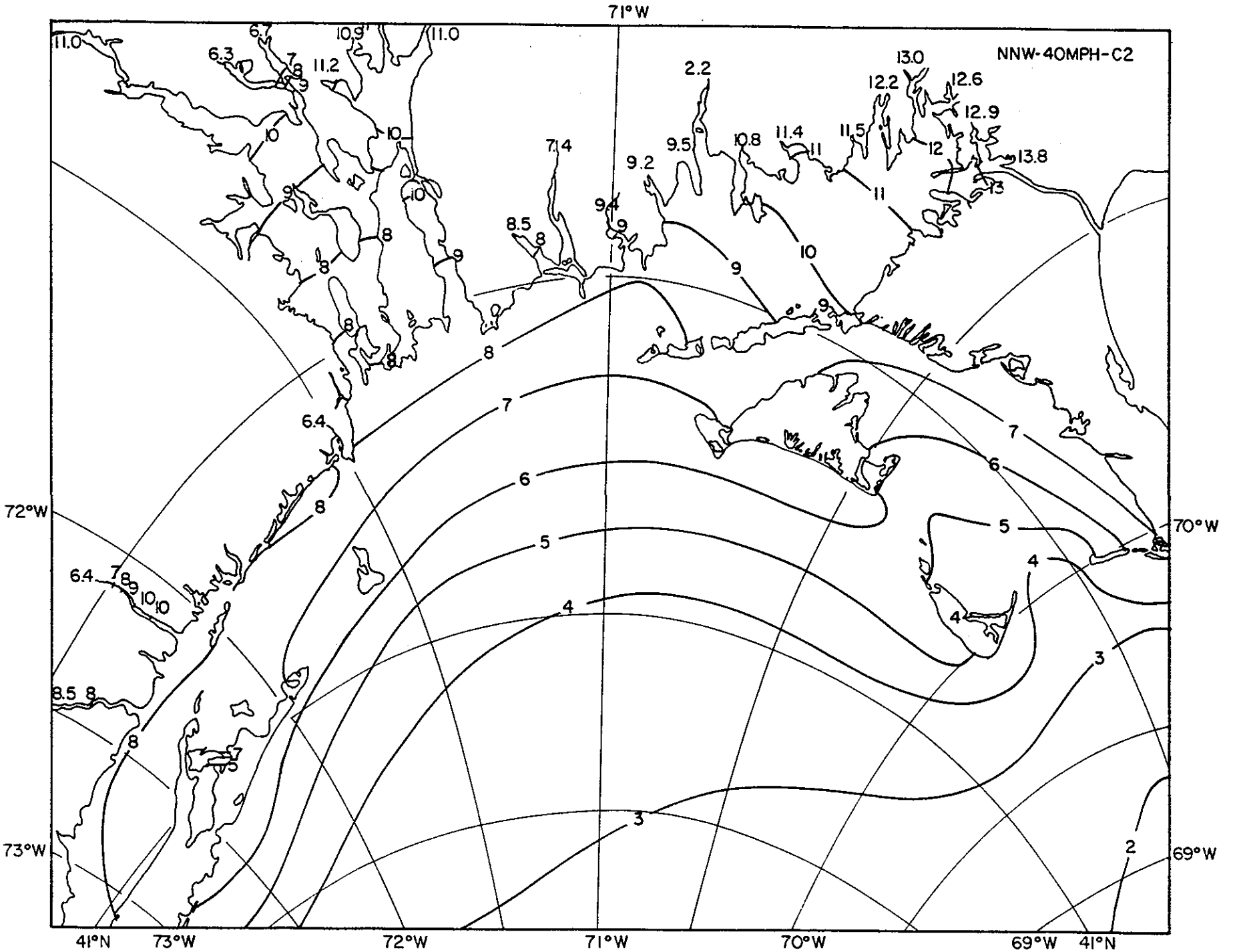
NNW-40MPH-C2
71°W
72°W
73°W
70°W
69°W
41°N
73°W
72°W
71°W
70°W
69°W
41°N

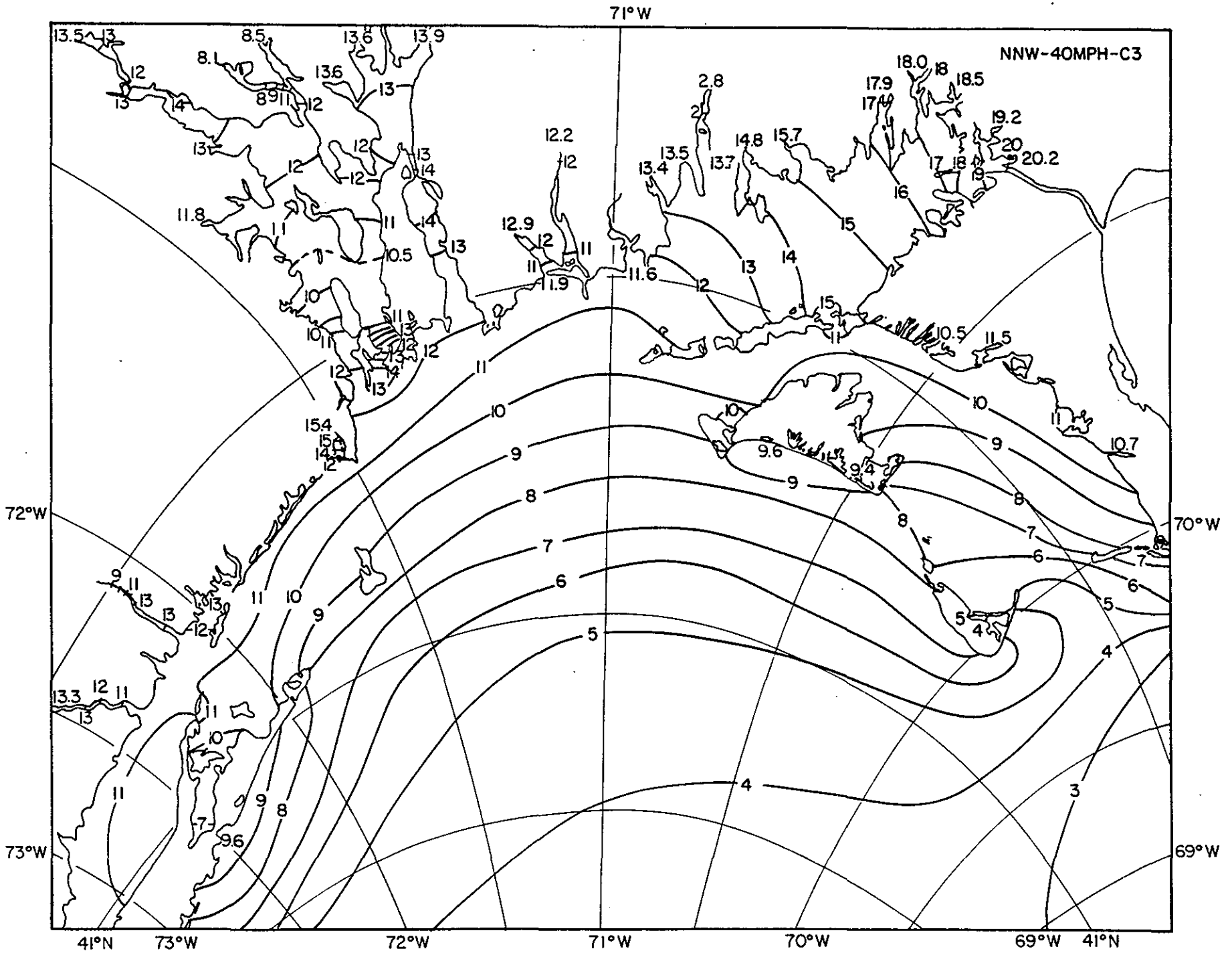
NNW-40MPH-C3
71°W
72°W
70°W
73°W
69°W
41°N
73°W
72°W
71°W
70°W
69°W
41°N

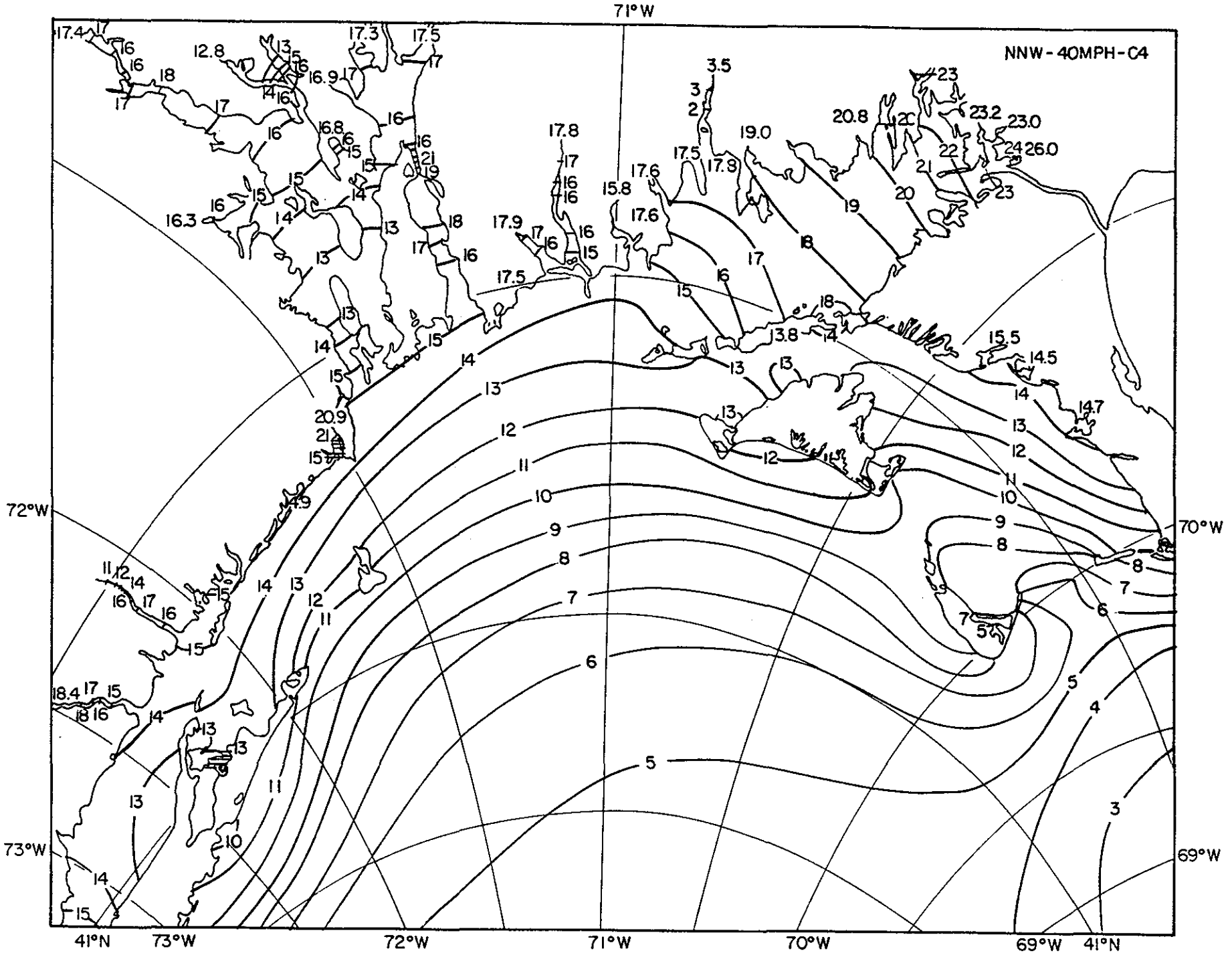
NNW - 40MPH - C4
71°W
72°W
70°W
73°W
69°W
41°N
73°W
72°W
71°W
70°W
69°W
41°N

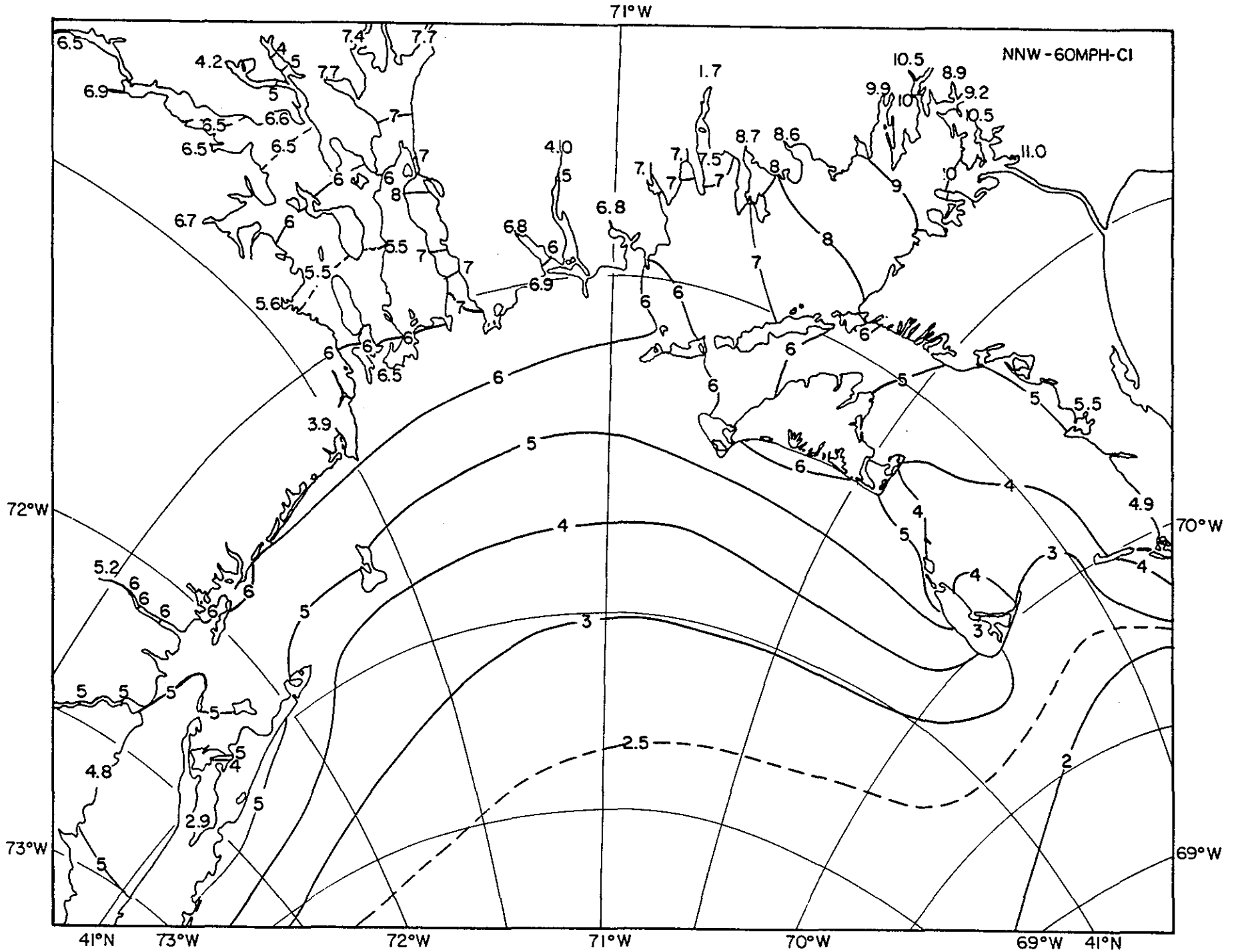
71°W
NNW-60MPH-CI
72°W
70°W
73°W
69°W
41°N
73°W
72°W
71°W
70°W
69°W
41°N
2.5

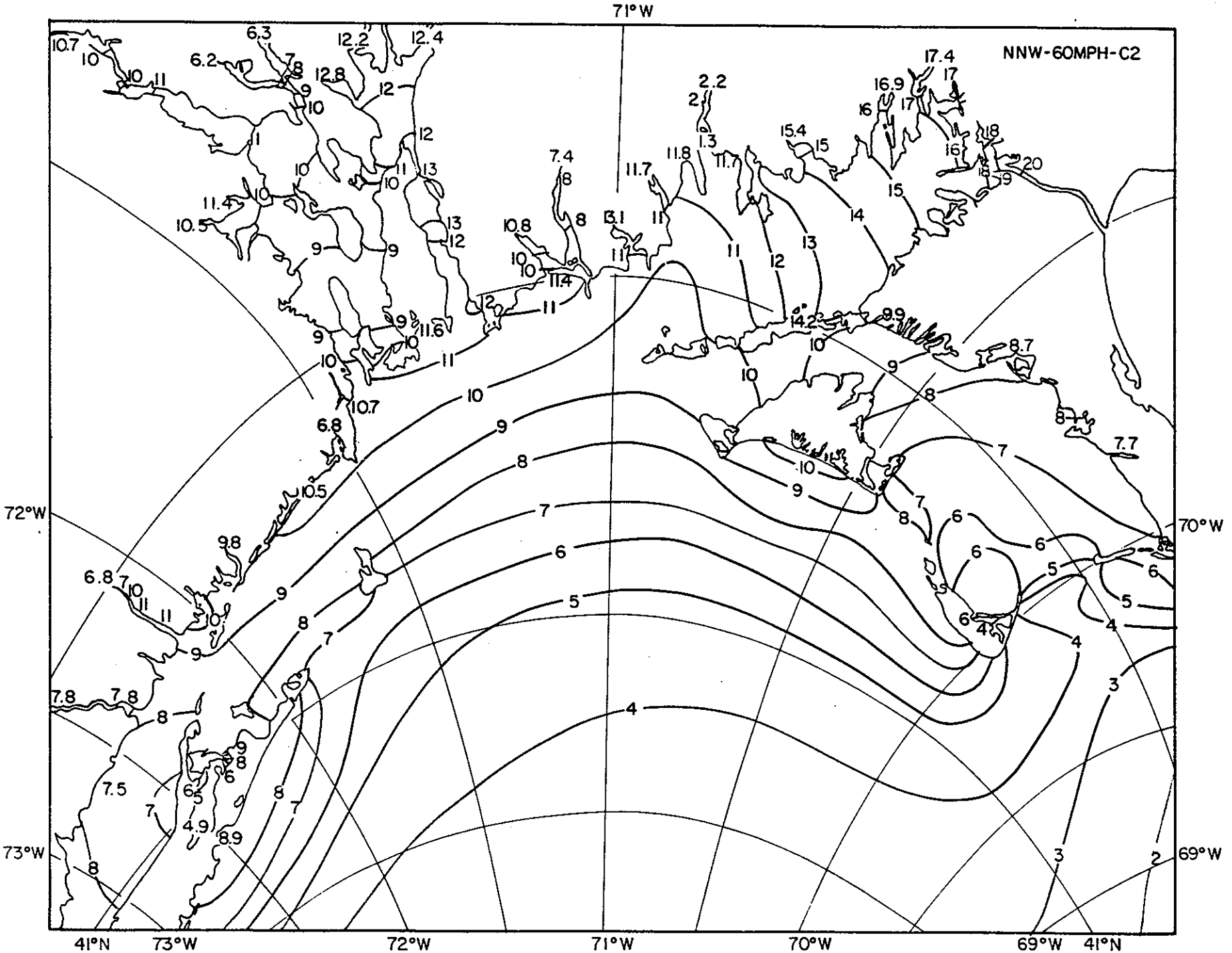
NNW-60MPH-C2
71°W
72°W
70°W
73°W
69°W
41°N
73°W
72°W
71°W
70°W
69°W
41°N

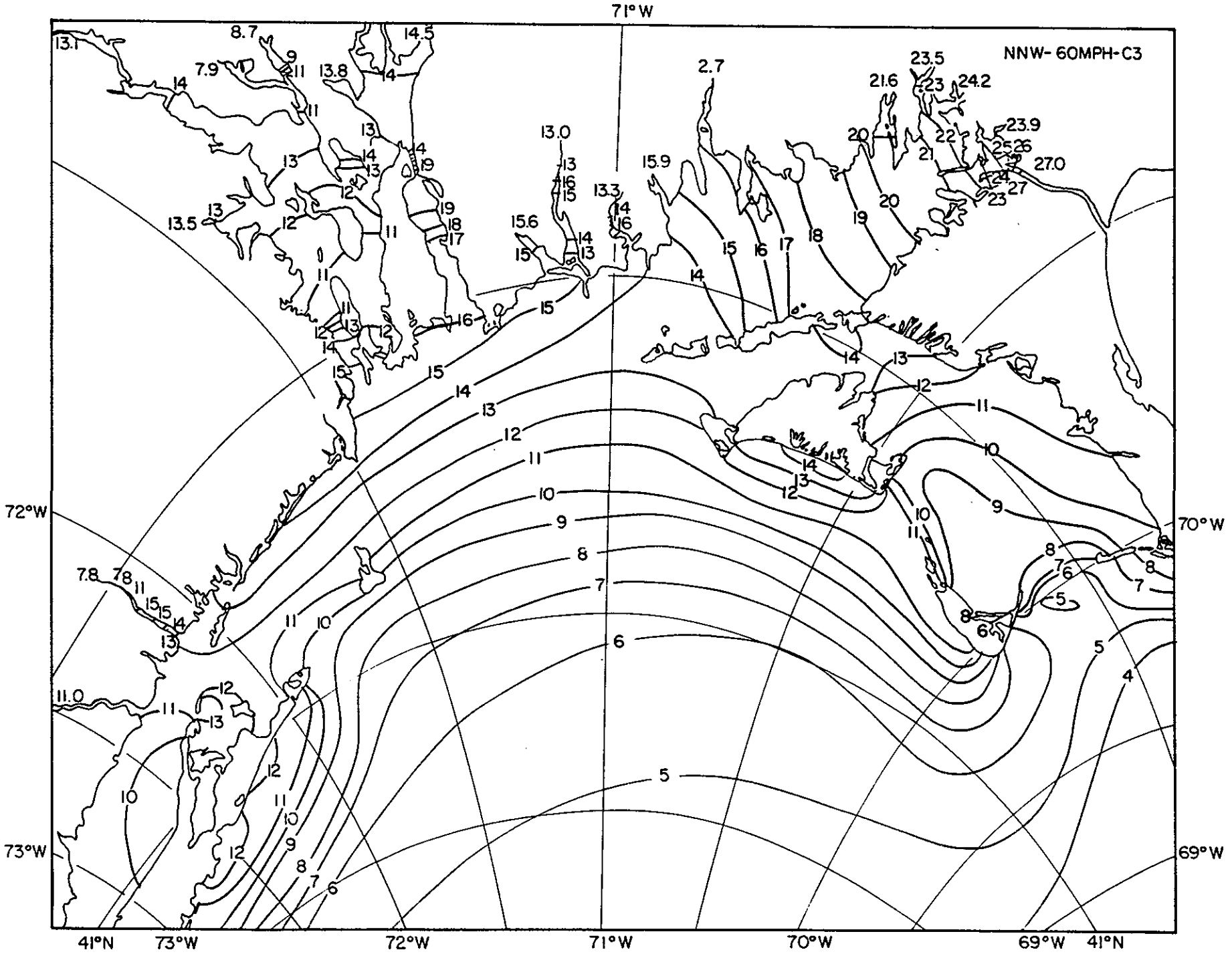
NNW- 60MPH-C3
71°W
72°W
70°W
73°W
69°W
41°N
73°W
72°W
71°W
70°W
69°W
41°N

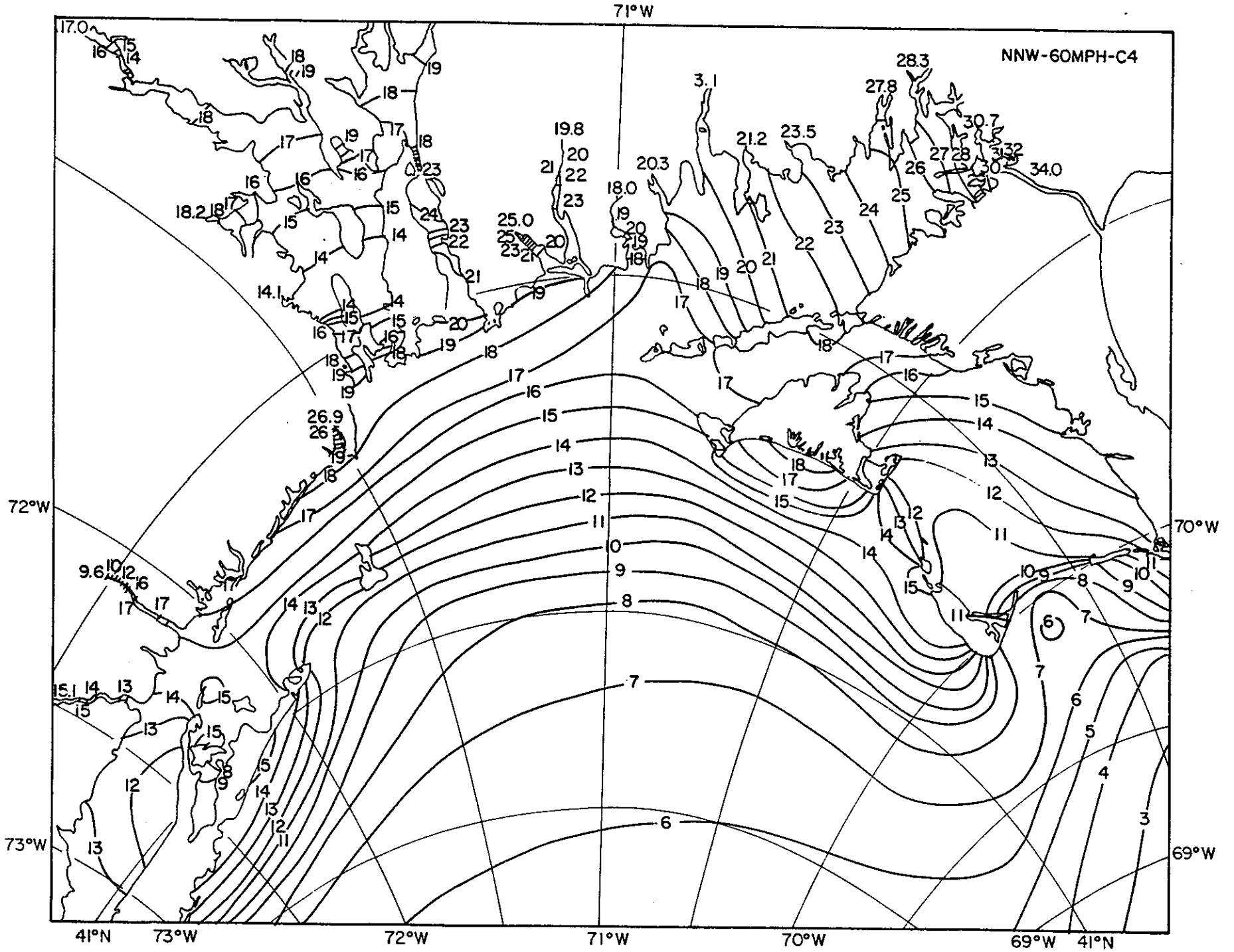
NNW-60MPH-C4
71°W
72°W
73°W
70°W
69°W
41°N

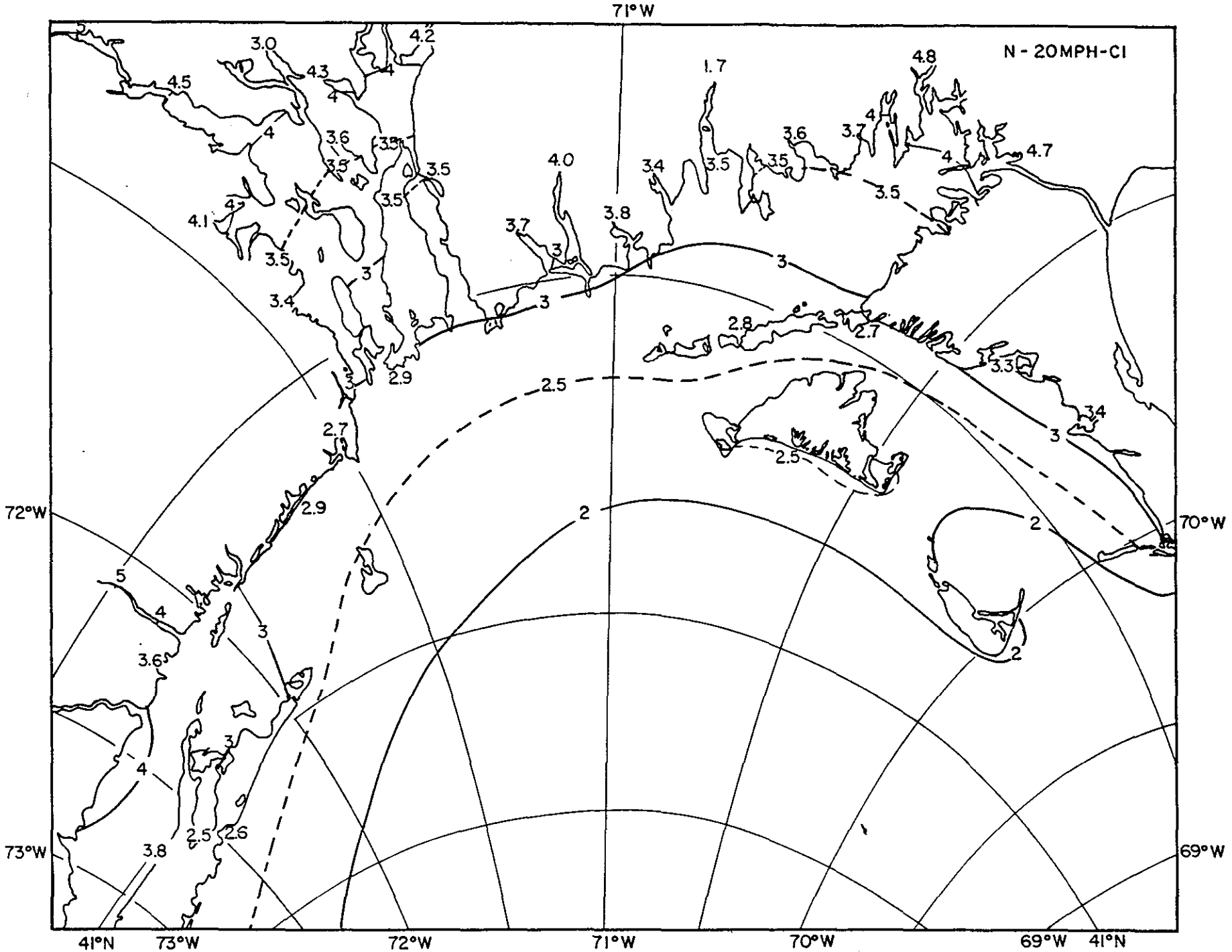
71°W
N - 20MPH-CI
72°W
70°W
73°W
69°W
41°N
73°W
72°W
71°W
70°W
69°W
41°N

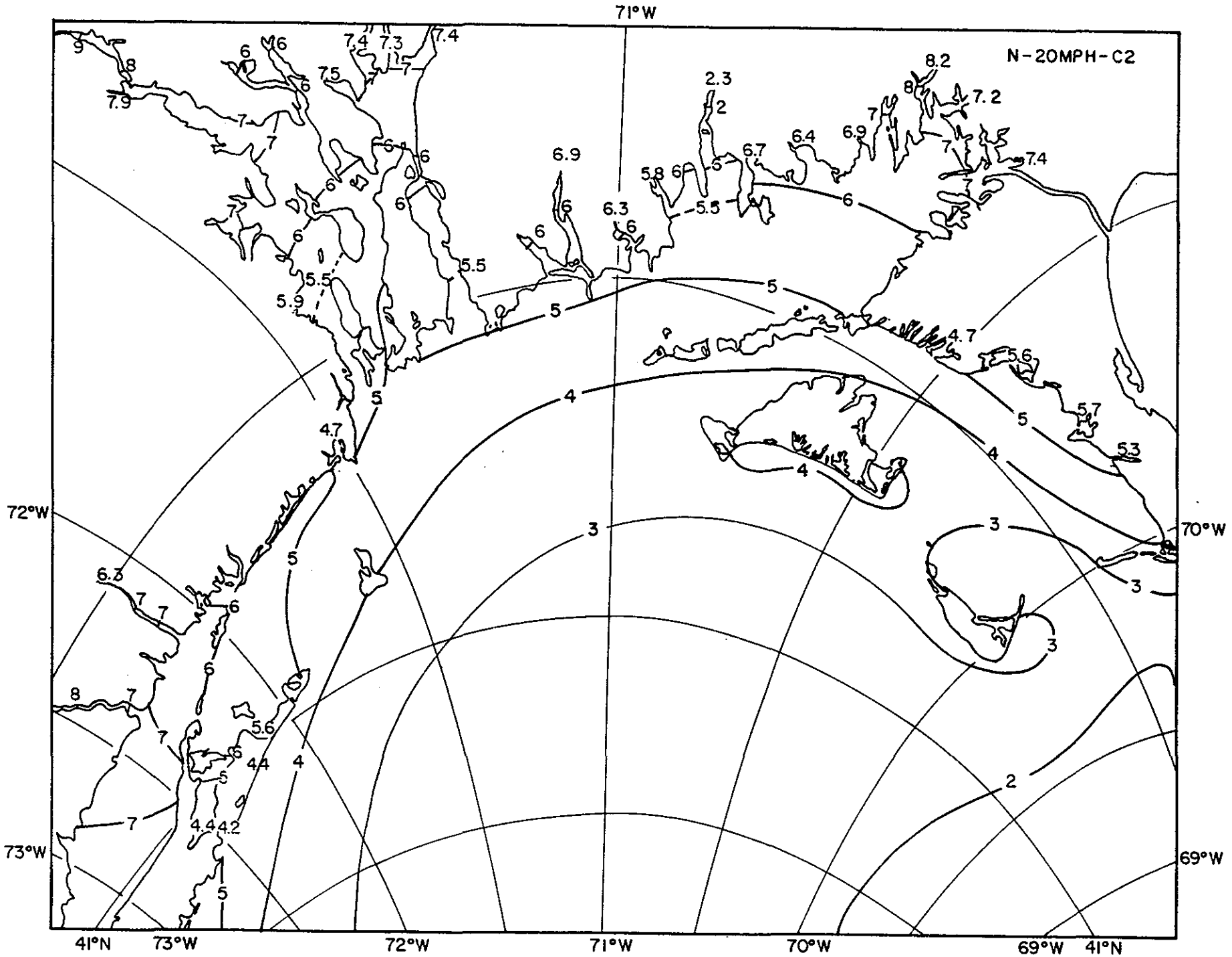
71°W
N-20MPH-C2
72°W
70°W
73°W
69°W
41°N
73°W
72°W
71°W
70°W
69°W
41°N

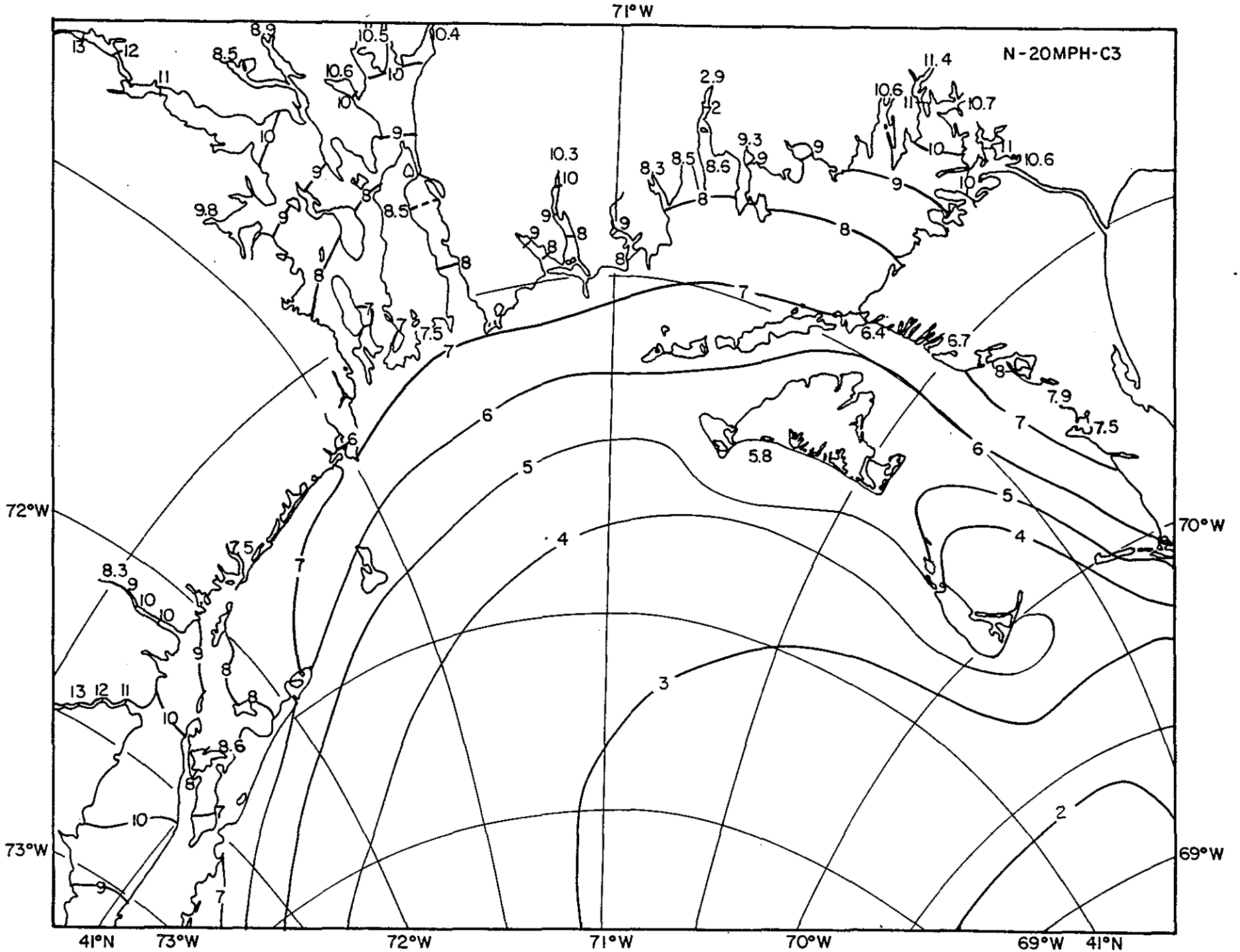
71°W
N-20MPH-C3
72°W
70°W
73°W
69°W
41°N
73°W
72°W
71°W
70°W
69°W
41°N

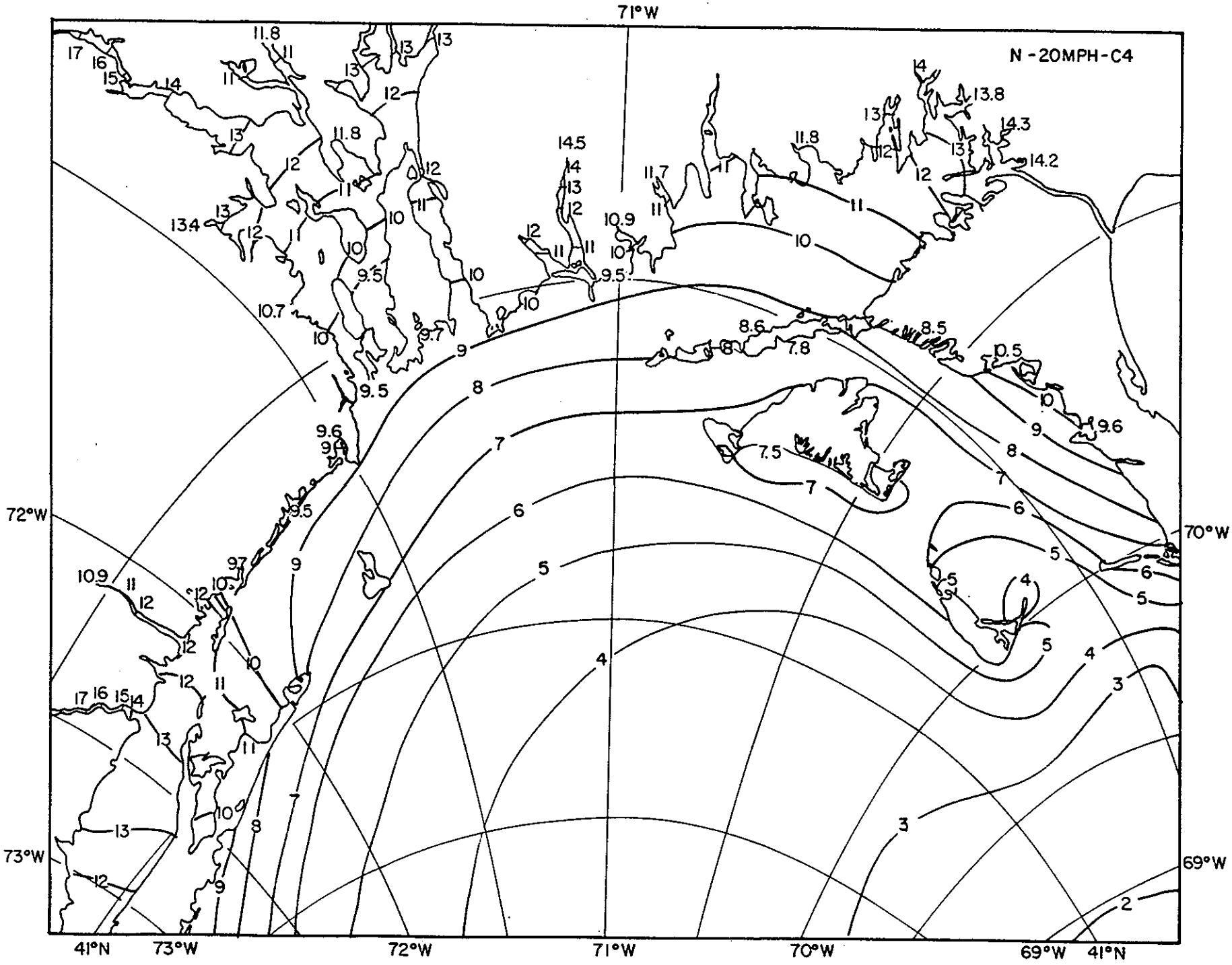
71°W
N - 20MPH - C4
72°W
70°W
73°W
69°W
41°N
73°W
72°W
71°W
70°W
69°W
41°N

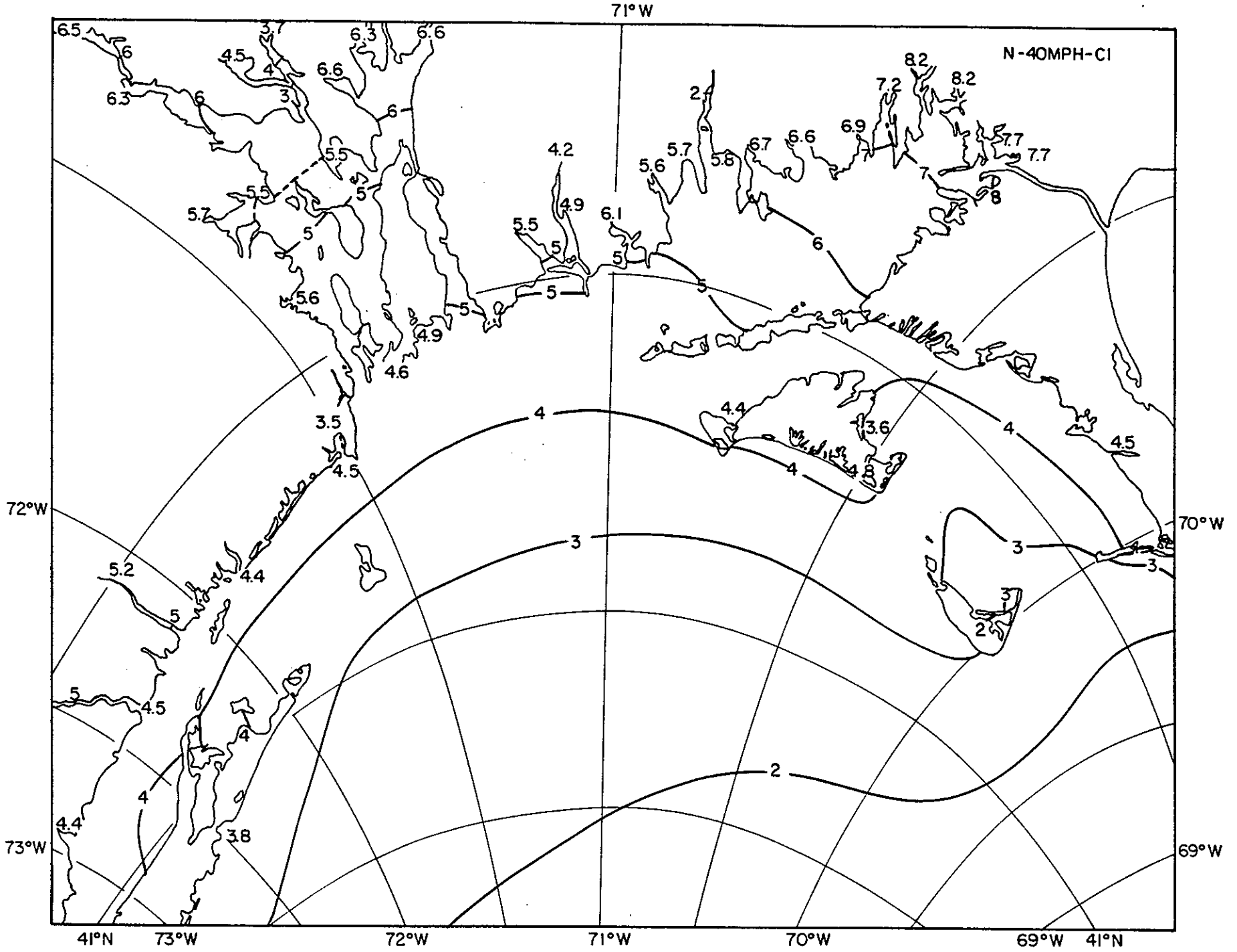
71°W
N-40MPH-CI
72°W
70°W
73°W
69°W
41°N
73°W
72°W
71°W
70°W
69°W
41°N

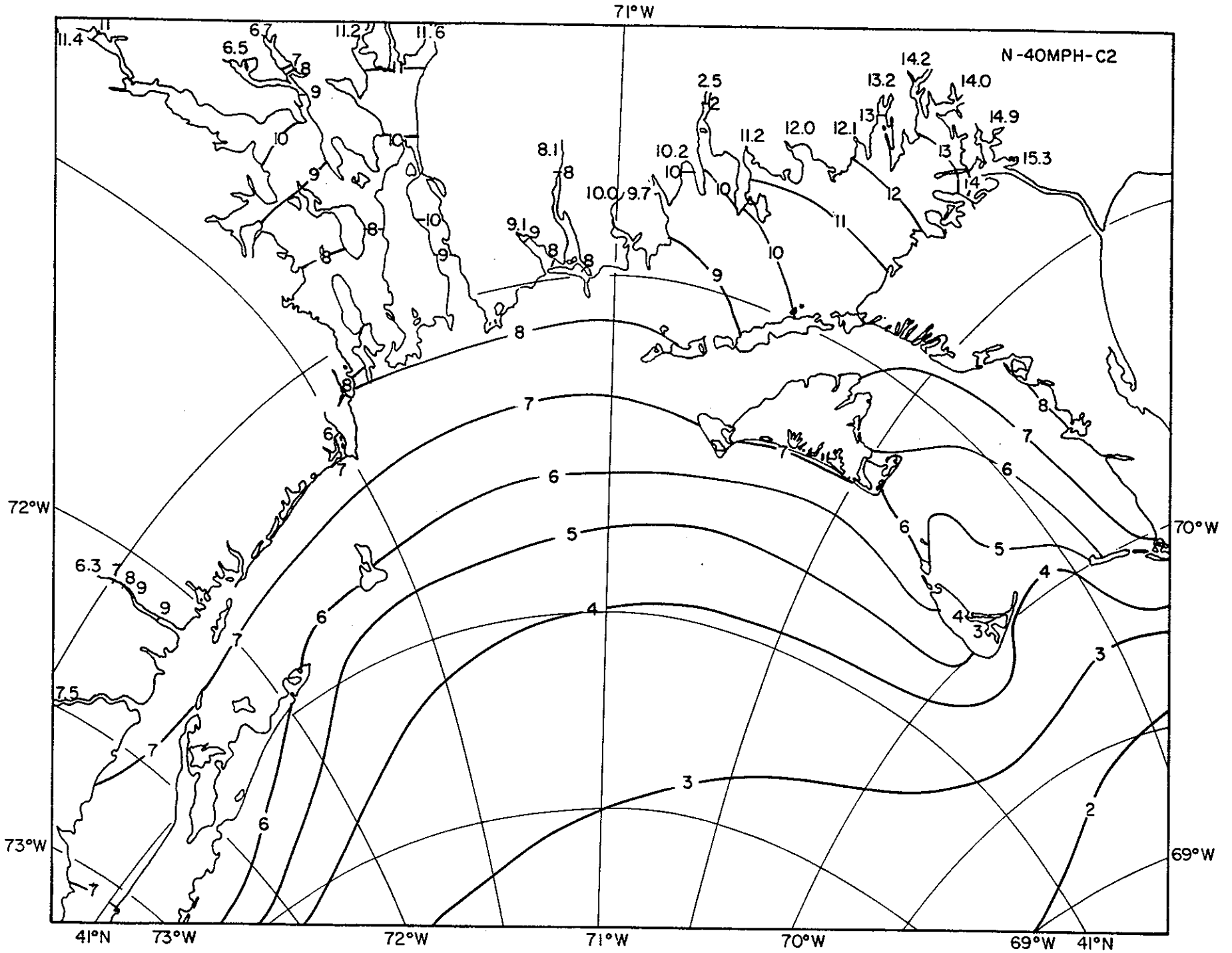
71°W
N-40MPH-C2
72°W
70°W
73°W
69°W
41°N
73°W
72°W
71°W
70°W
69°W
41°N

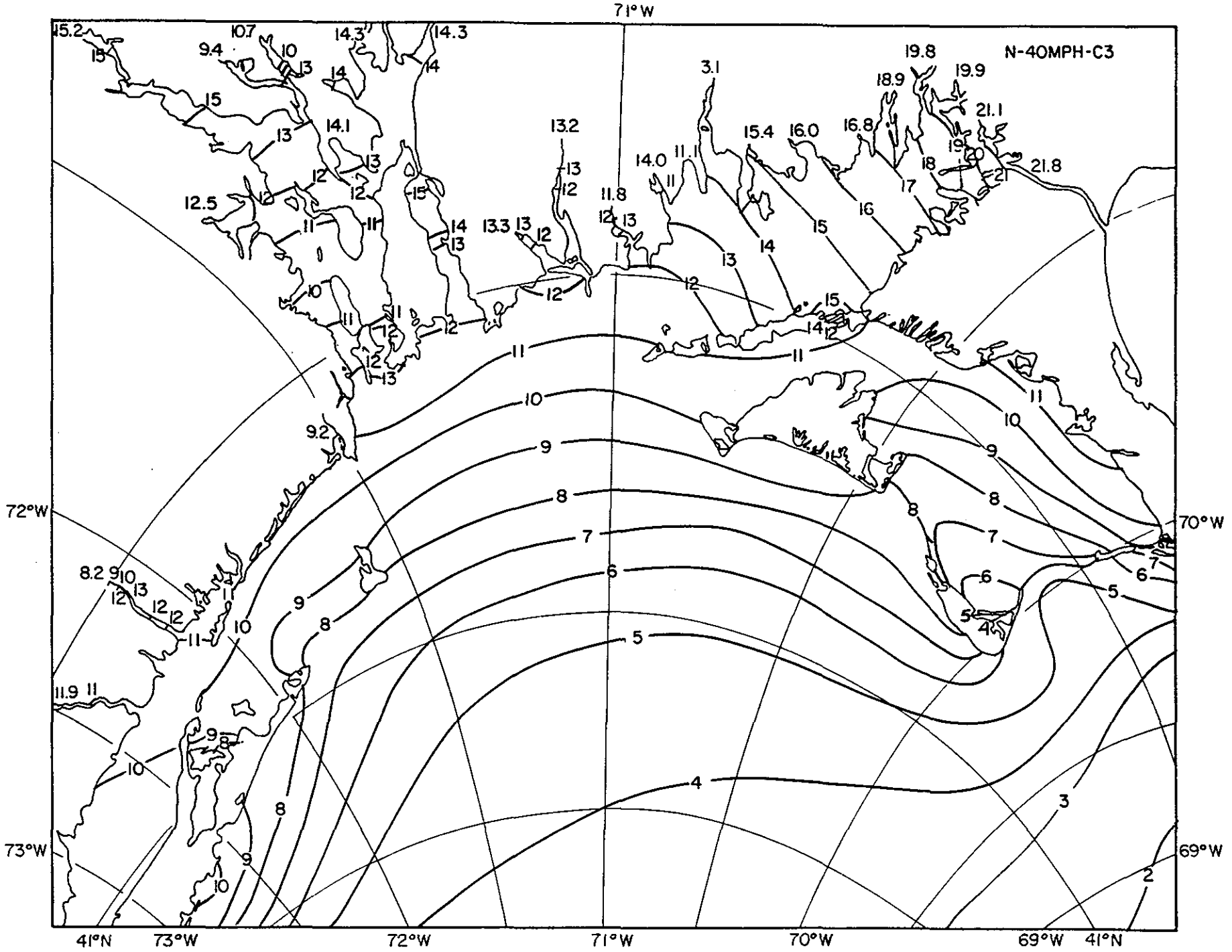
71°W
N-40MPH-C3
72°W
70°W
73°W
69°W
41°N
73°W
72°W
71°W
70°W
69°W
41°N

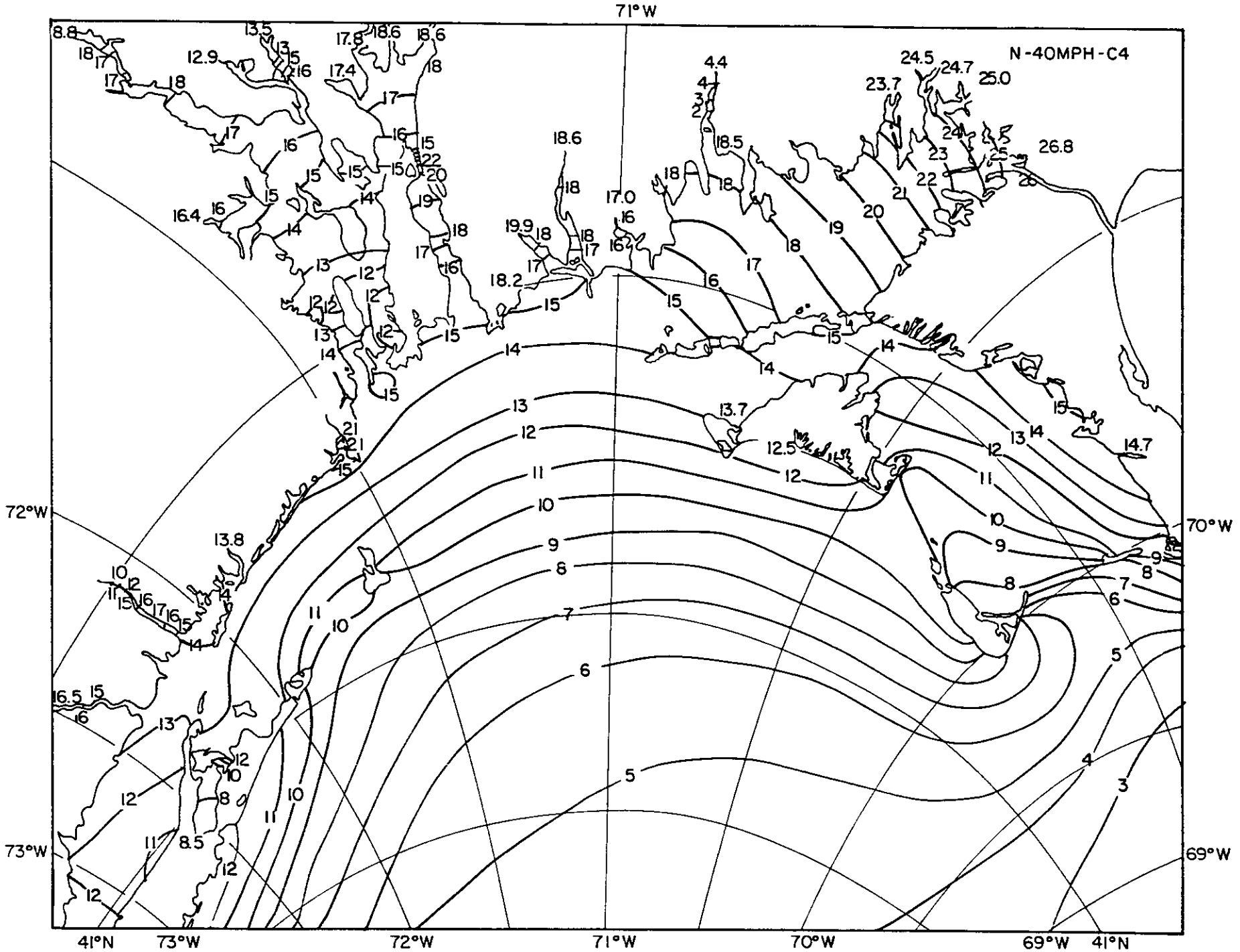
71°W
N-40MPH-C4
72°W
70°W
73°W
69°W
41°N
73°W
72°W
71°W
70°W
69°W
41°N

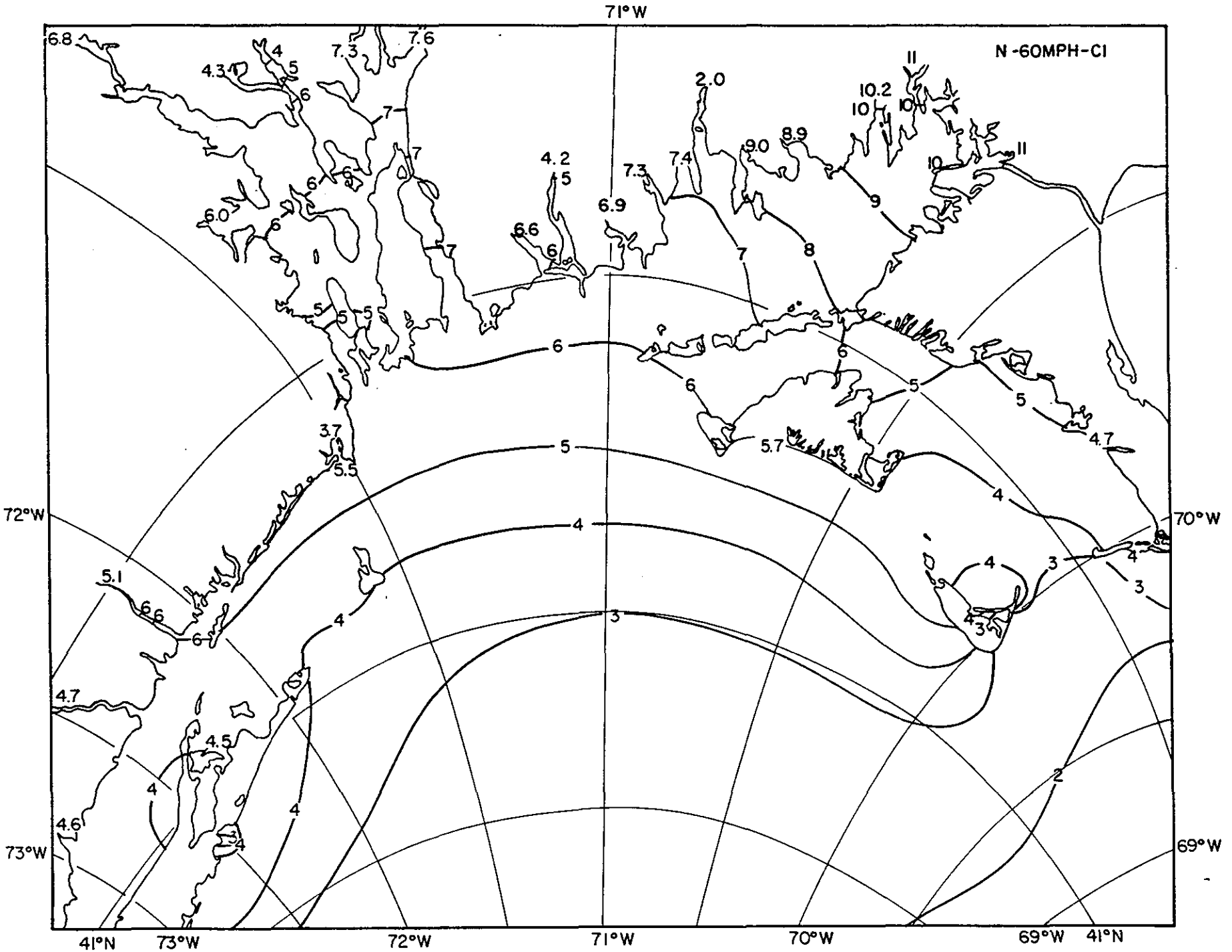
71°W
N-60MPH-CI
72°W
70°W
73°W
69°W
41°N
73°W
72°W
71°W
70°W
69°W
41°N

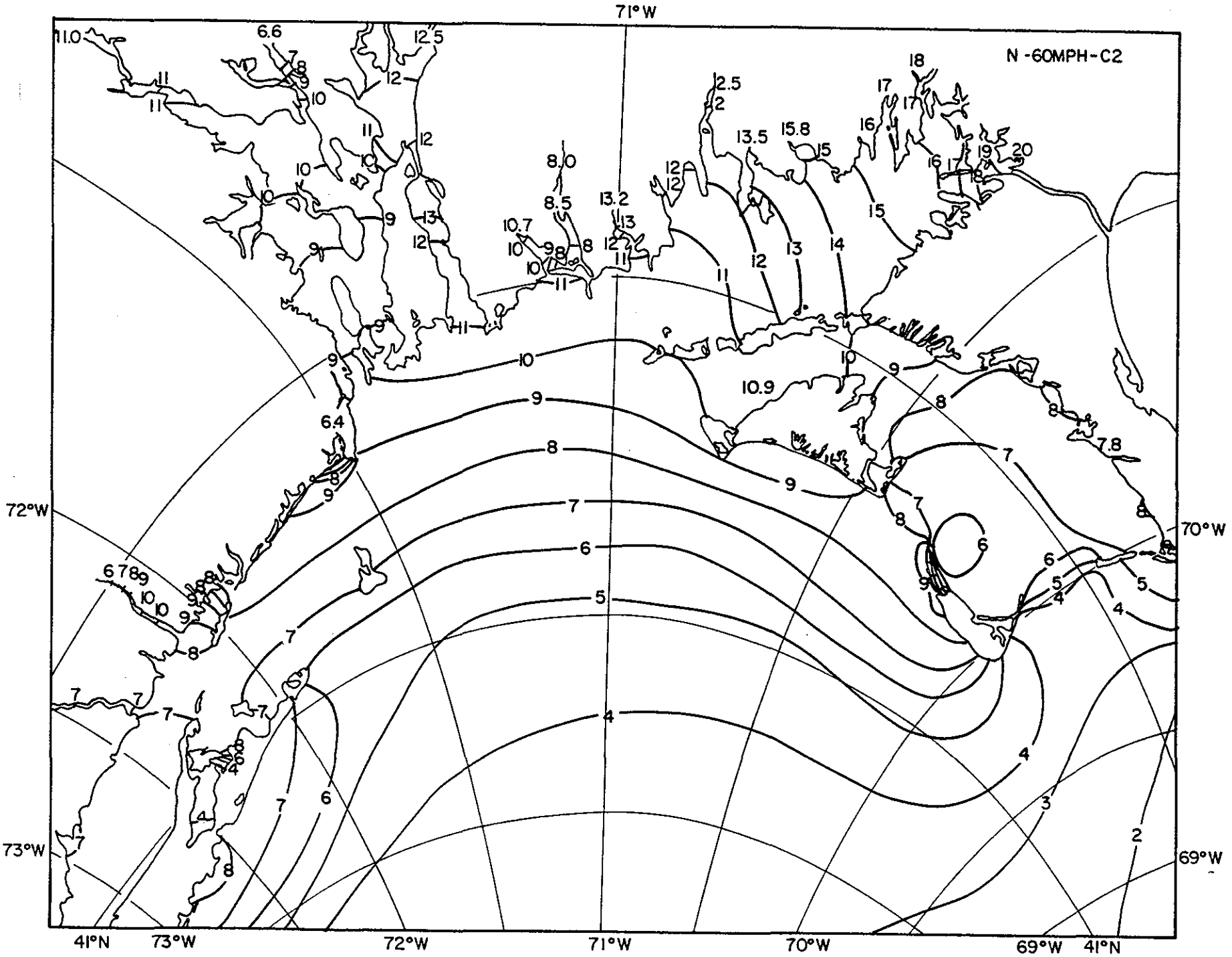
71°W
N -60MPH-C2
72°W
70°W
73°W
69°W
41°N
73°W
72°W
71°W
70°W
69°W
41°N

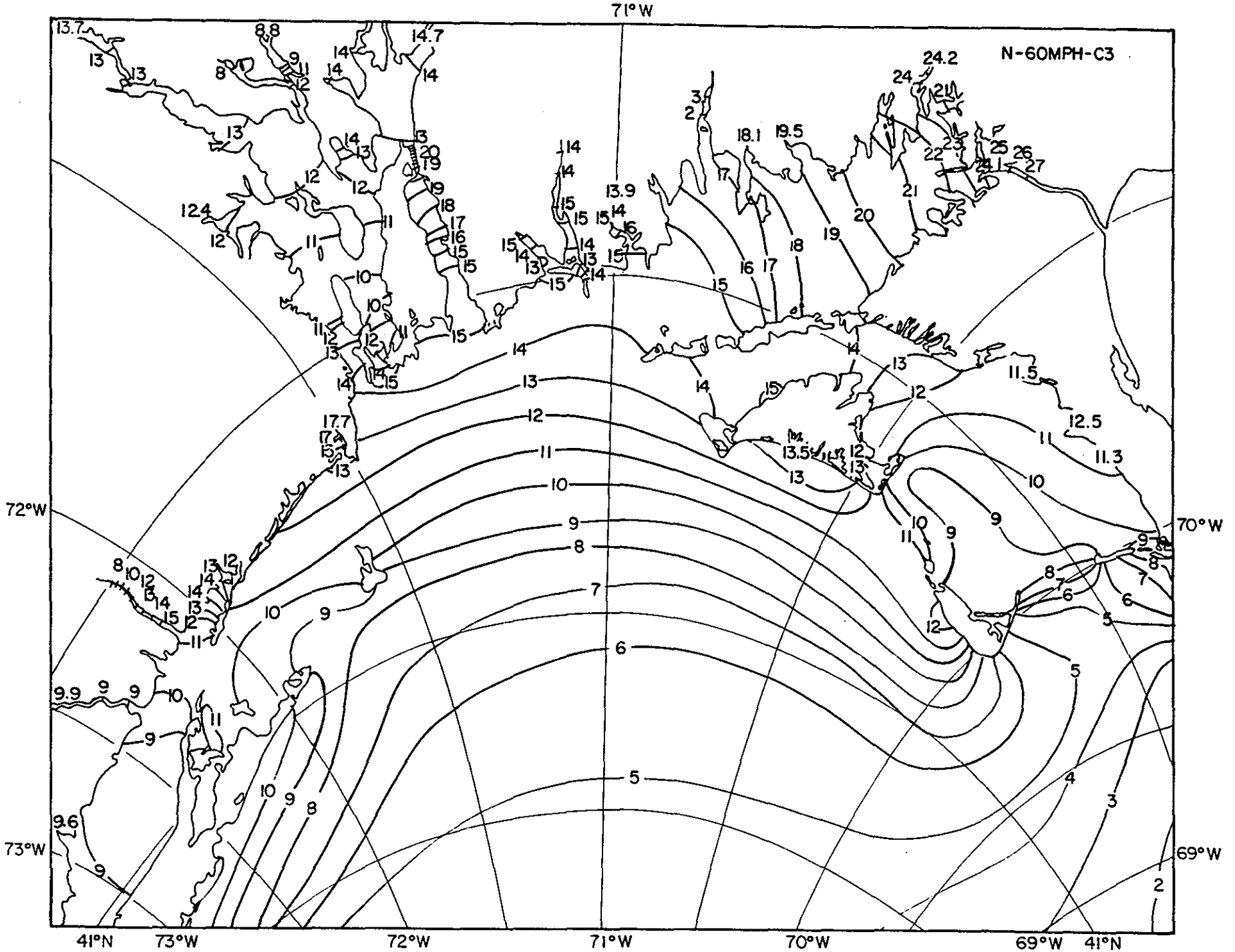
N-60MPH-C3
71°W
72°W
73°W
70°W
69°W
41°N
73°W
72°W
71°W
70°W
69°W
41°N

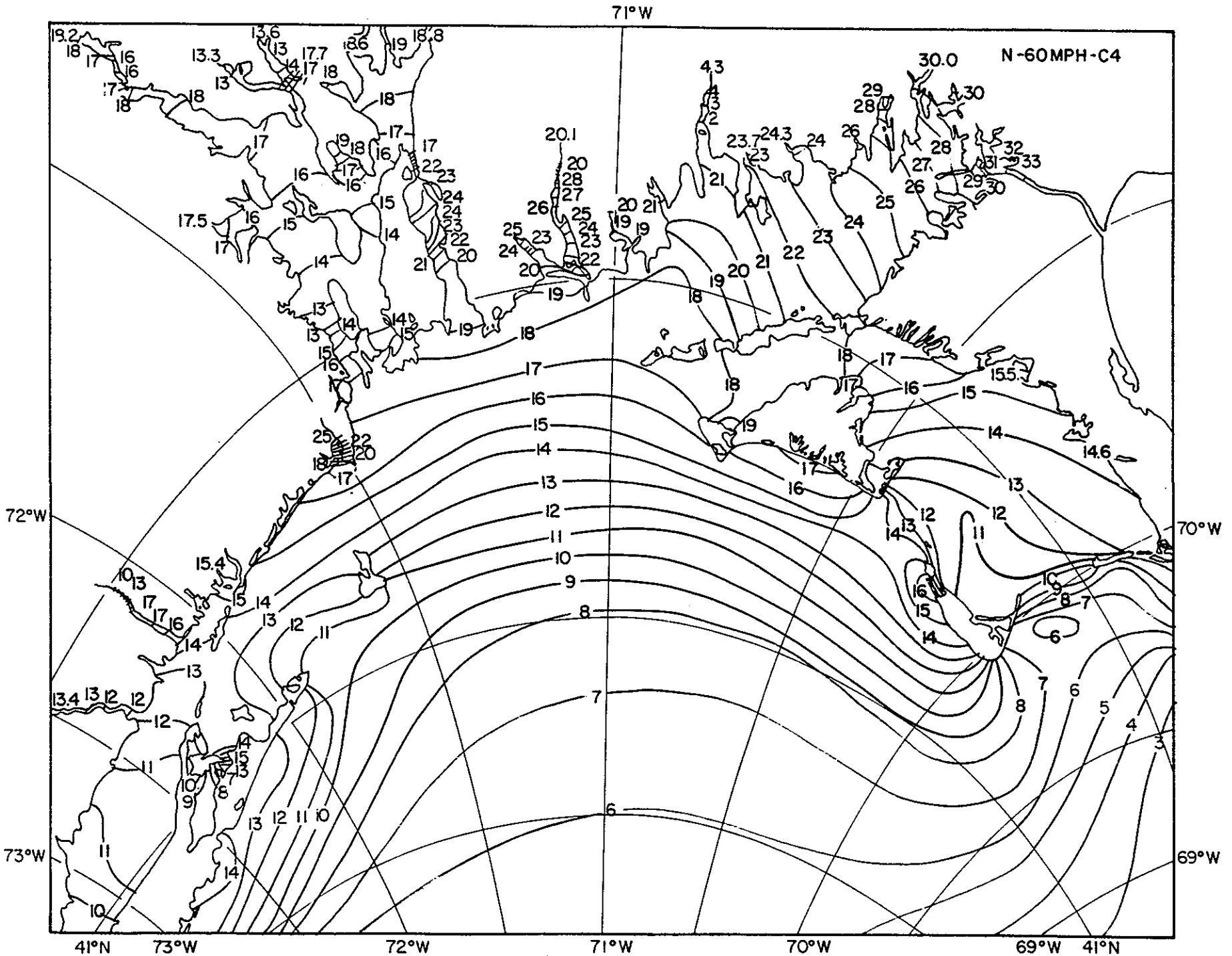
71°W
N-60MPH-C4
72°W
70°W
73°W
69°W
41°N
73°W
72°W
71°W
70°W
69°W
41°N

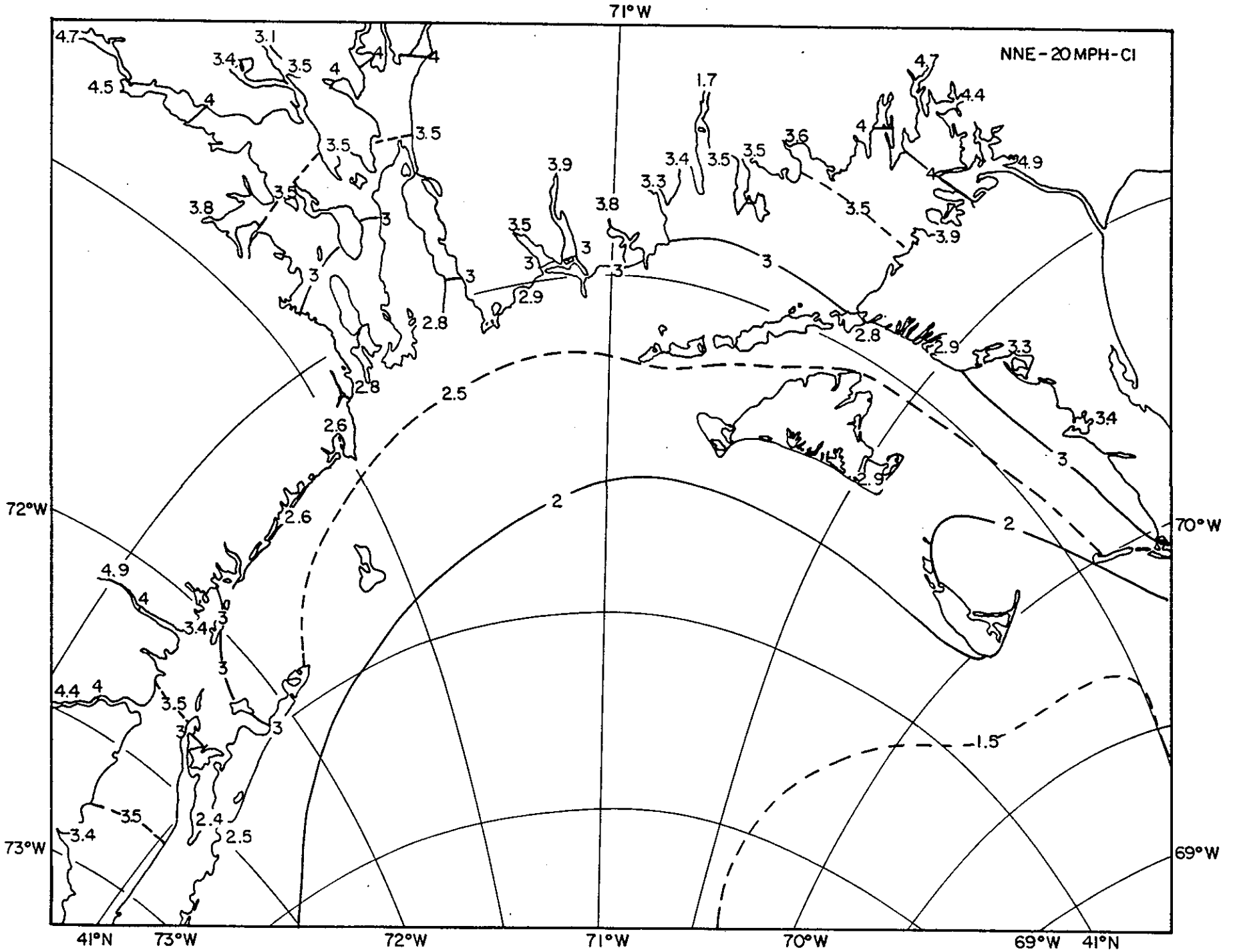
71°W
NNE-20 MPH-CI
72°W
70°W
73°W
69°W
41°N
73°W
72°W
71°W
70°W
69°W
41°N
1.5
2
2.5
3
3.5
4

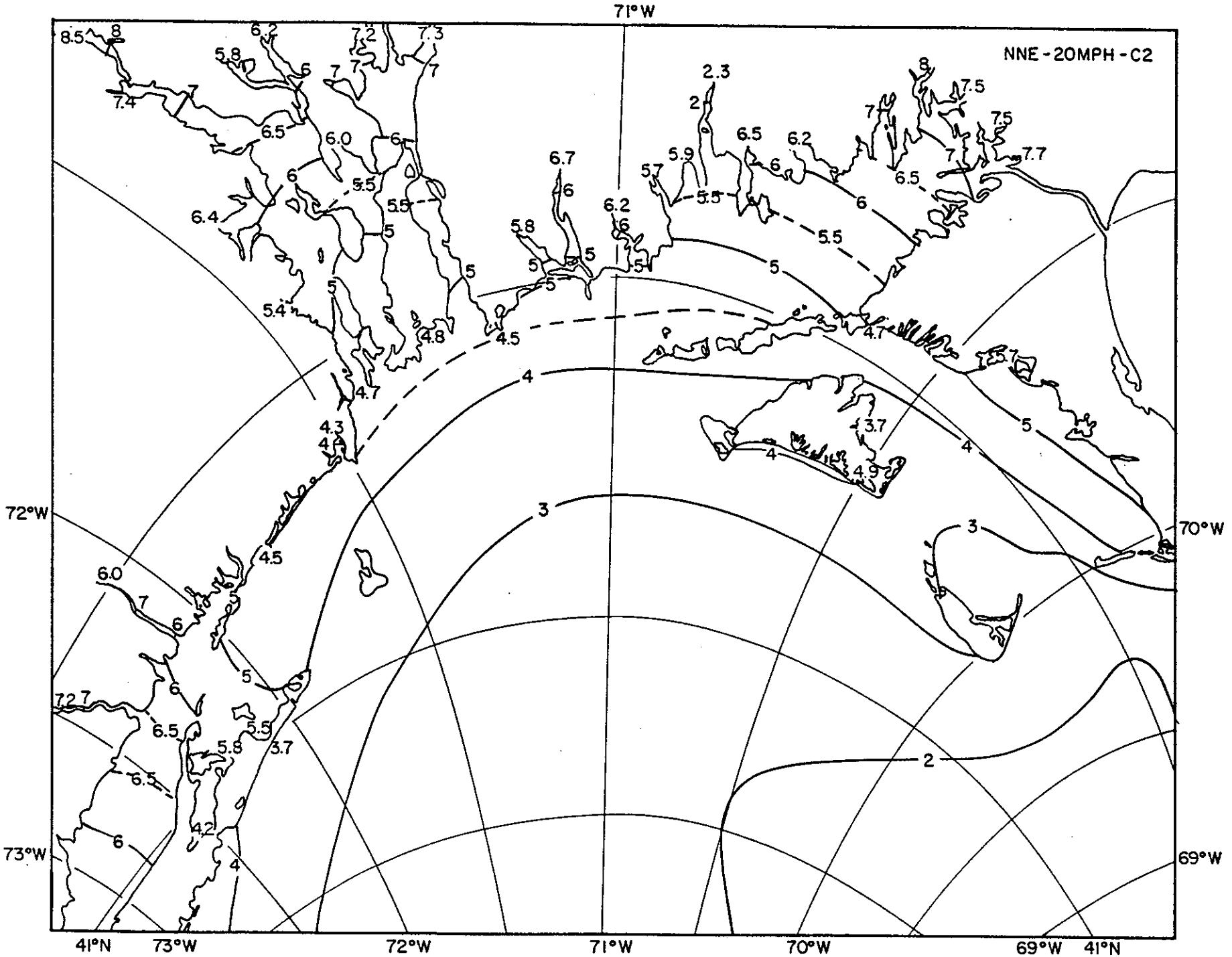
NNE - 20MPH - C2
71°W
72°W
70°W
73°W
69°W
41°N
73°W
72°W
71°W
70°W
69°W
41°N

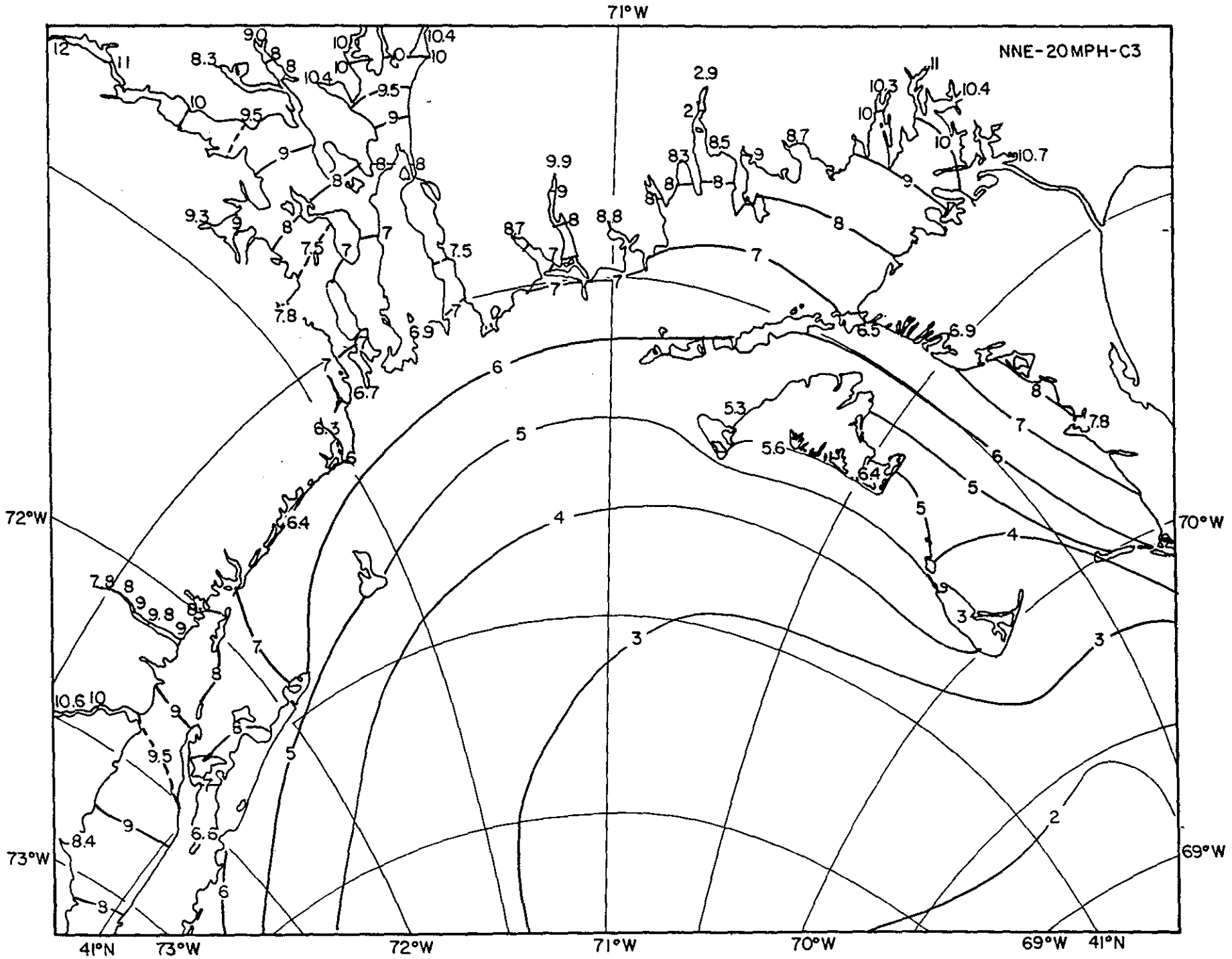
71°W
NNE-20MPH-C3
72°W
70°W
73°W
69°W
41°N
73°W
72°W
71°W
70°W
69°W
41°N

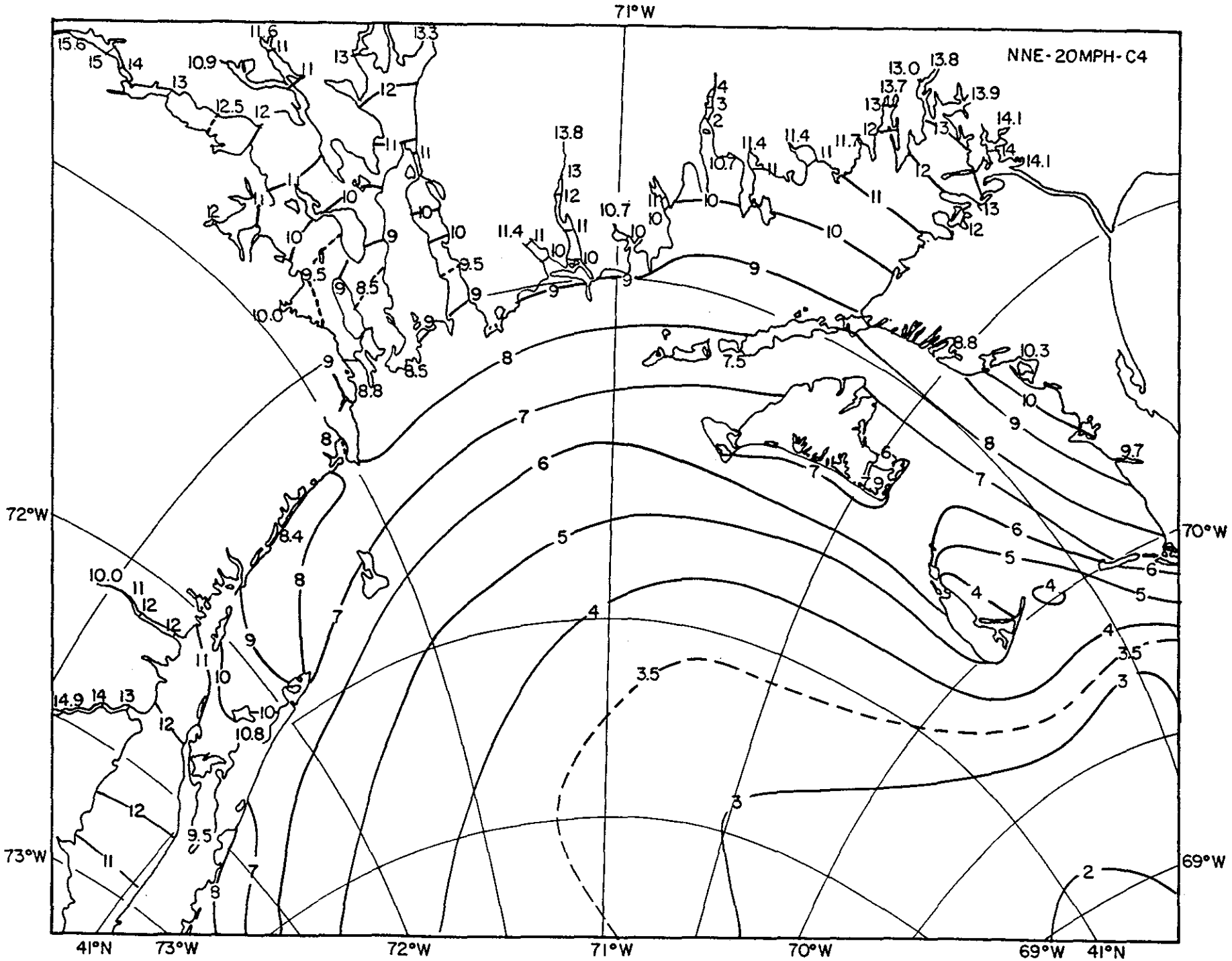
NNE-20MPH-C4
71°W
72°W
73°W
70°W
69°W
41°N
73°W
72°W
71°W
70°W
69°W
41°N

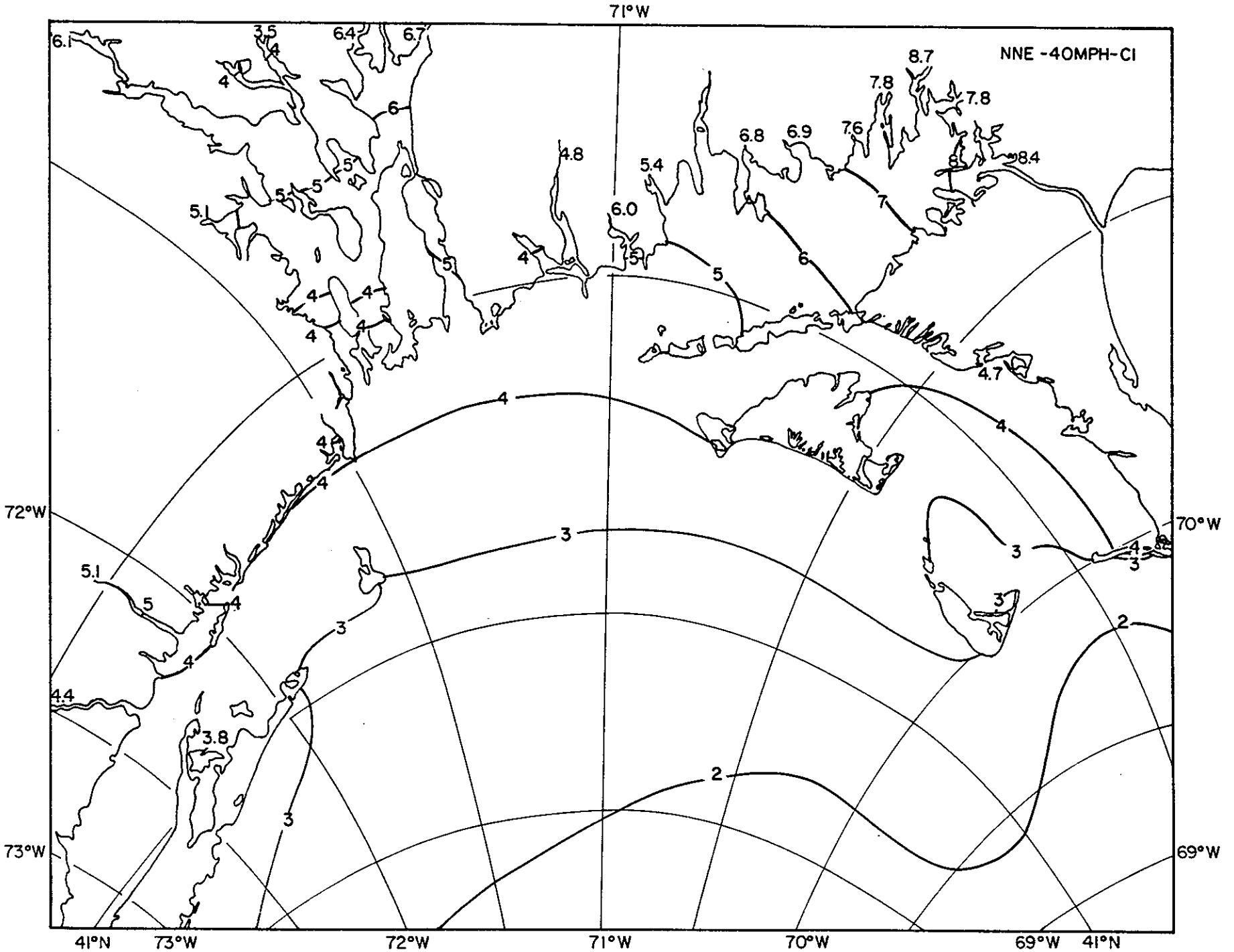
NNE -40MPH-CI
71°W
72°W
73°W
70°W
69°W
41°N
6.1
3.5
6.4
6.7
8.7
7.8
7.8
6.8
6.9
7.6
8.4
4.8
5.4
6.0
5.1
4.7
4.4
3.8

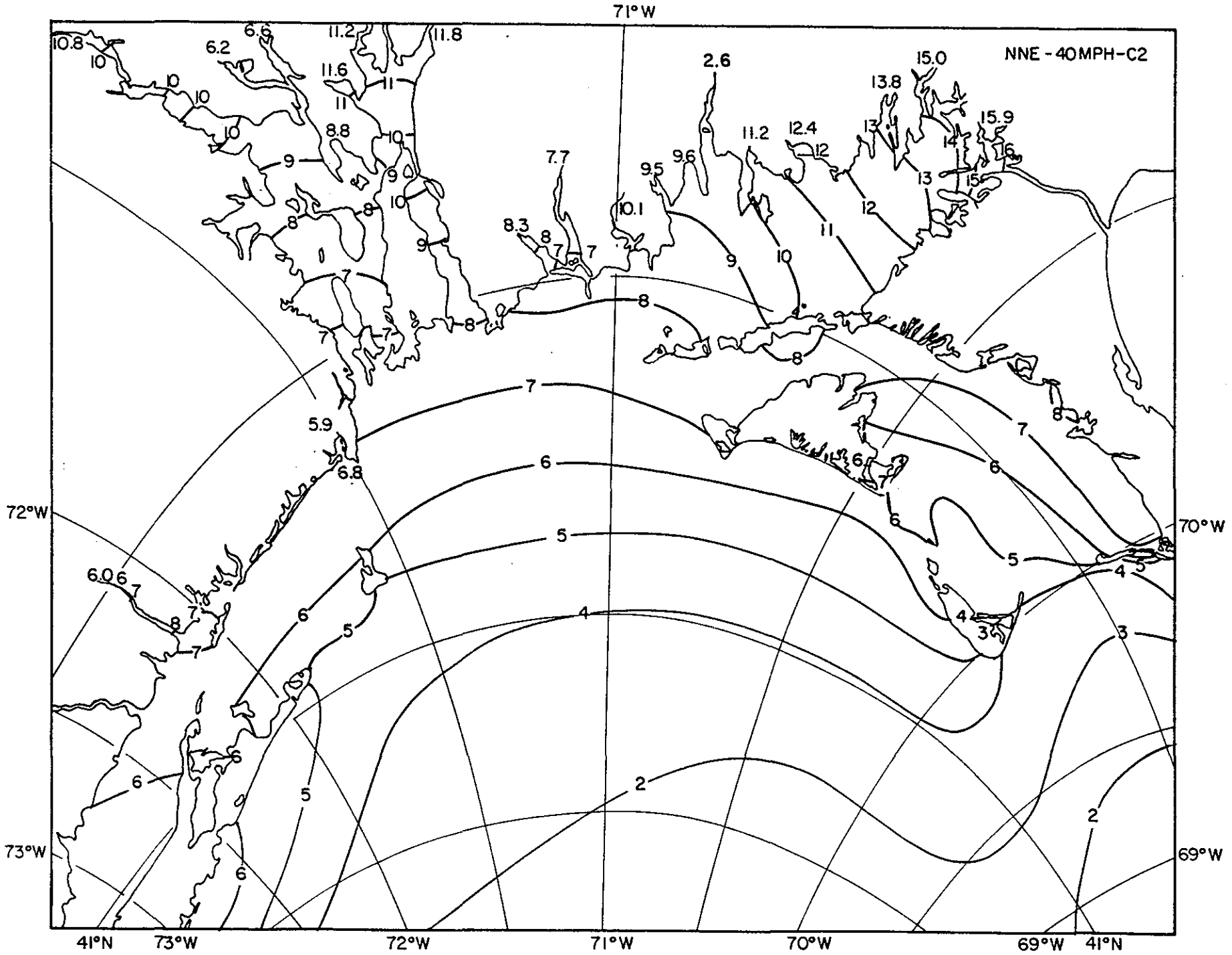
NNE - 40MPH - C2
71°W
72°W
70°W
73°W
69°W
41°N
73°W
72°W
71°W
70°W
69°W
41°N

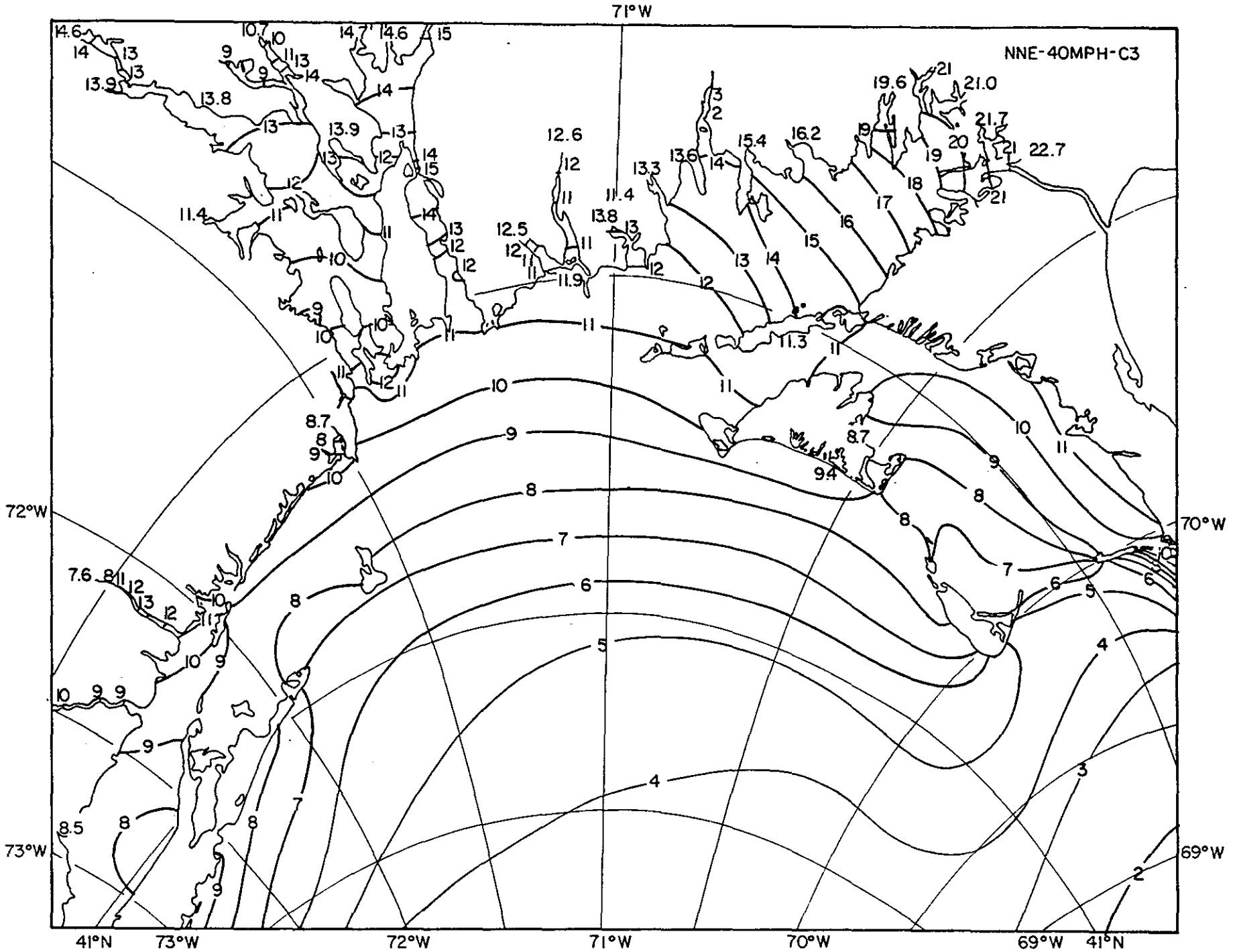
NNE-40MPH-C3
71°W
72°W
70°W
73°W
69°W
41°N
73°W
72°W
71°W
70°W
69°W
41°N

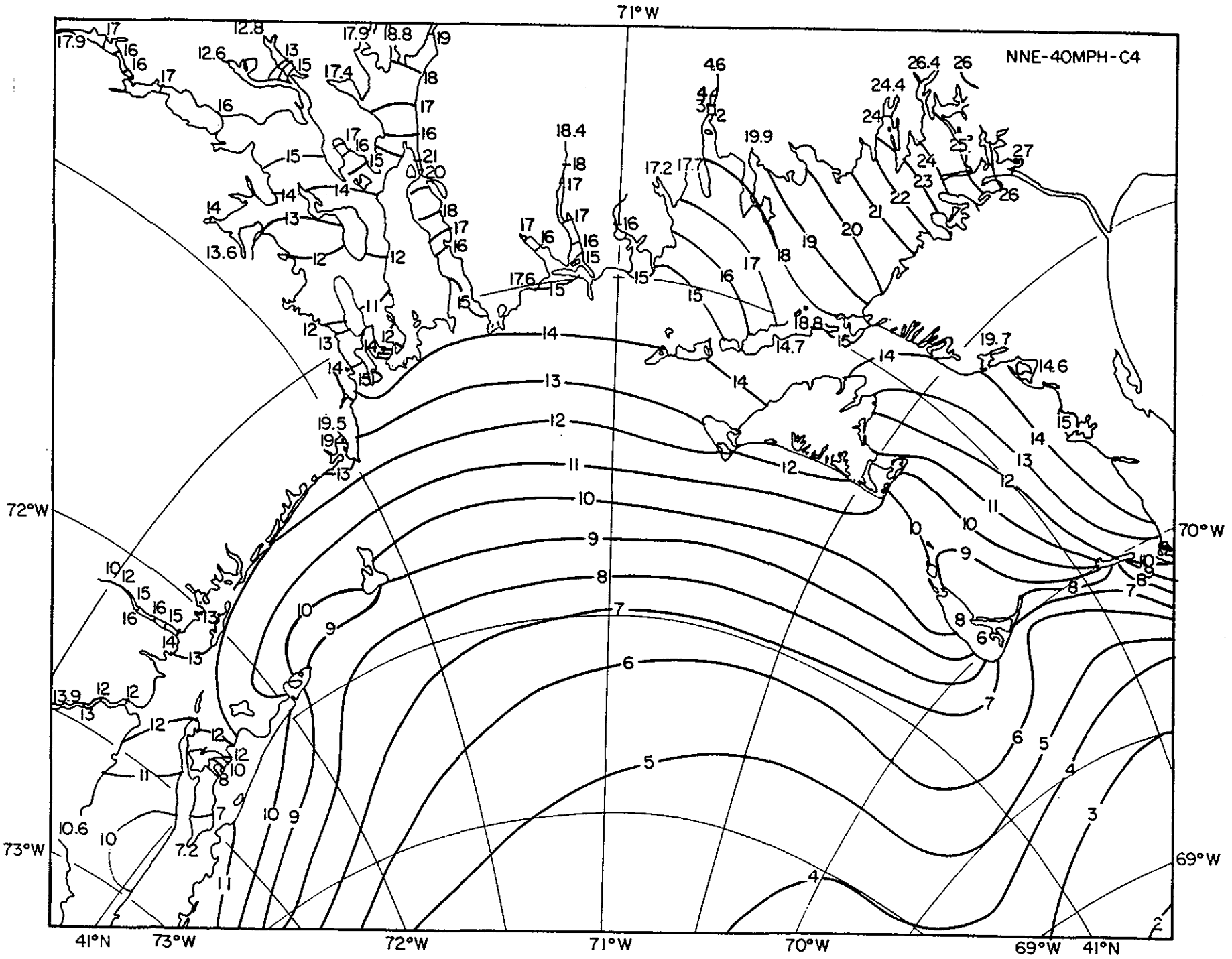
NNE-40MPH-C4
71°W
72°W
70°W
73°W
69°W
41°N
73°W
72°W
71°W
70°W
69°W
41°N

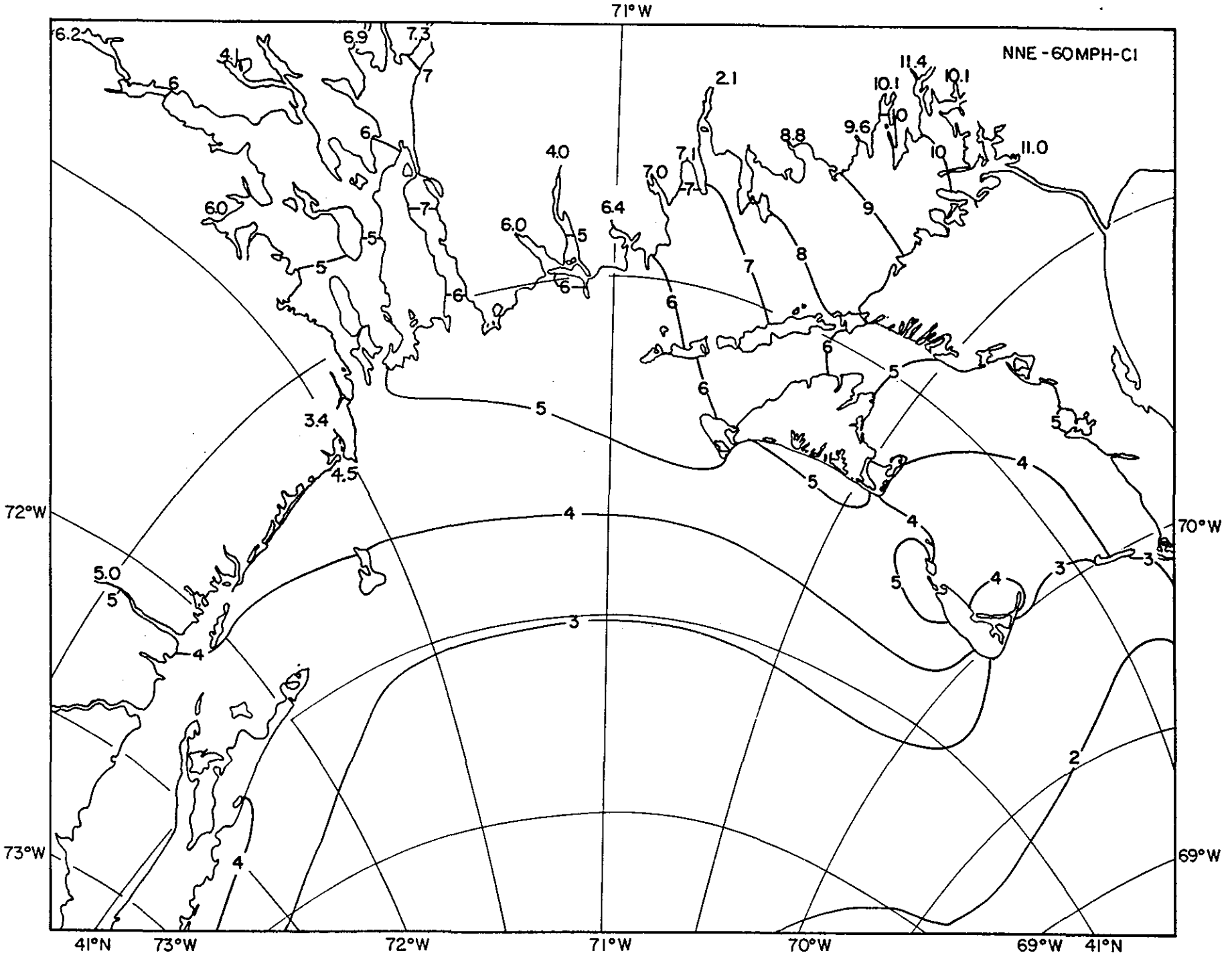
NNE - 60MPH - C1
71°W
72°W
73°W
70°W
69°W
41°N
41°N
73°W
72°W
71°W
70°W
69°W

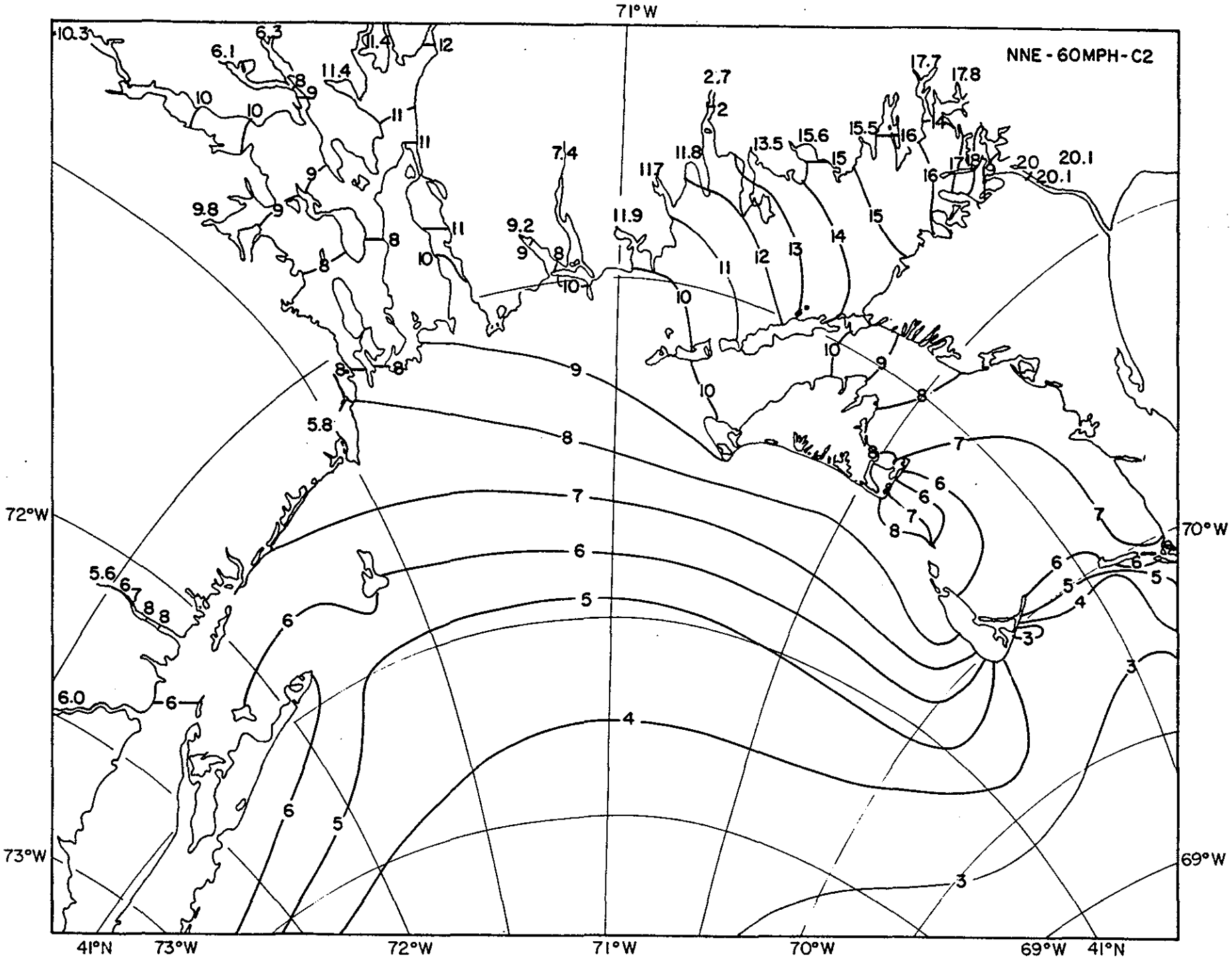
NNE - 60MPH - C2
71°W
72°W
70°W
73°W
69°W
41°N
73°W
72°W
71°W
70°W
69°W
41°N

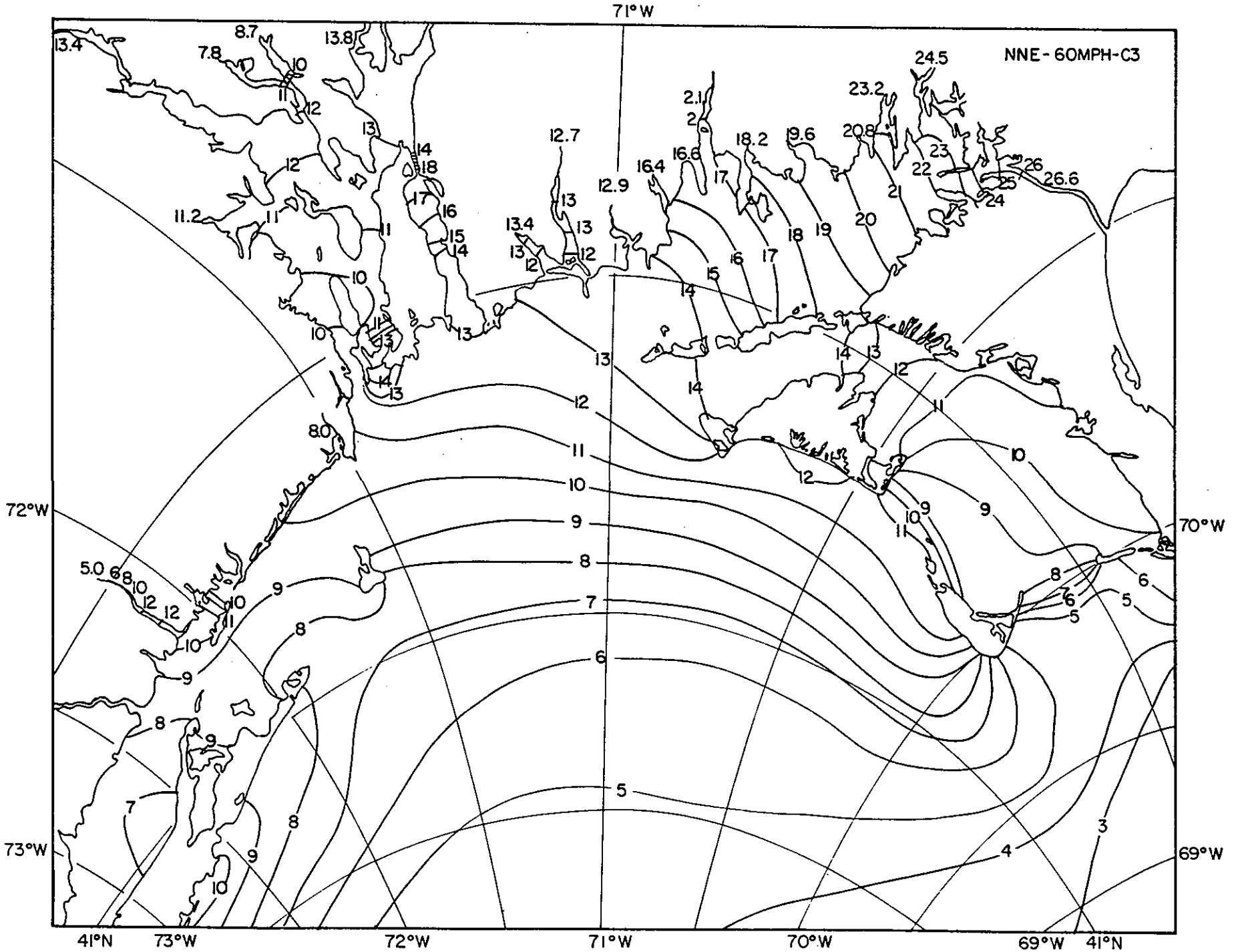
NNE-60MPH-C3
71°W
72°W
73°W
70°W
69°W
41°N

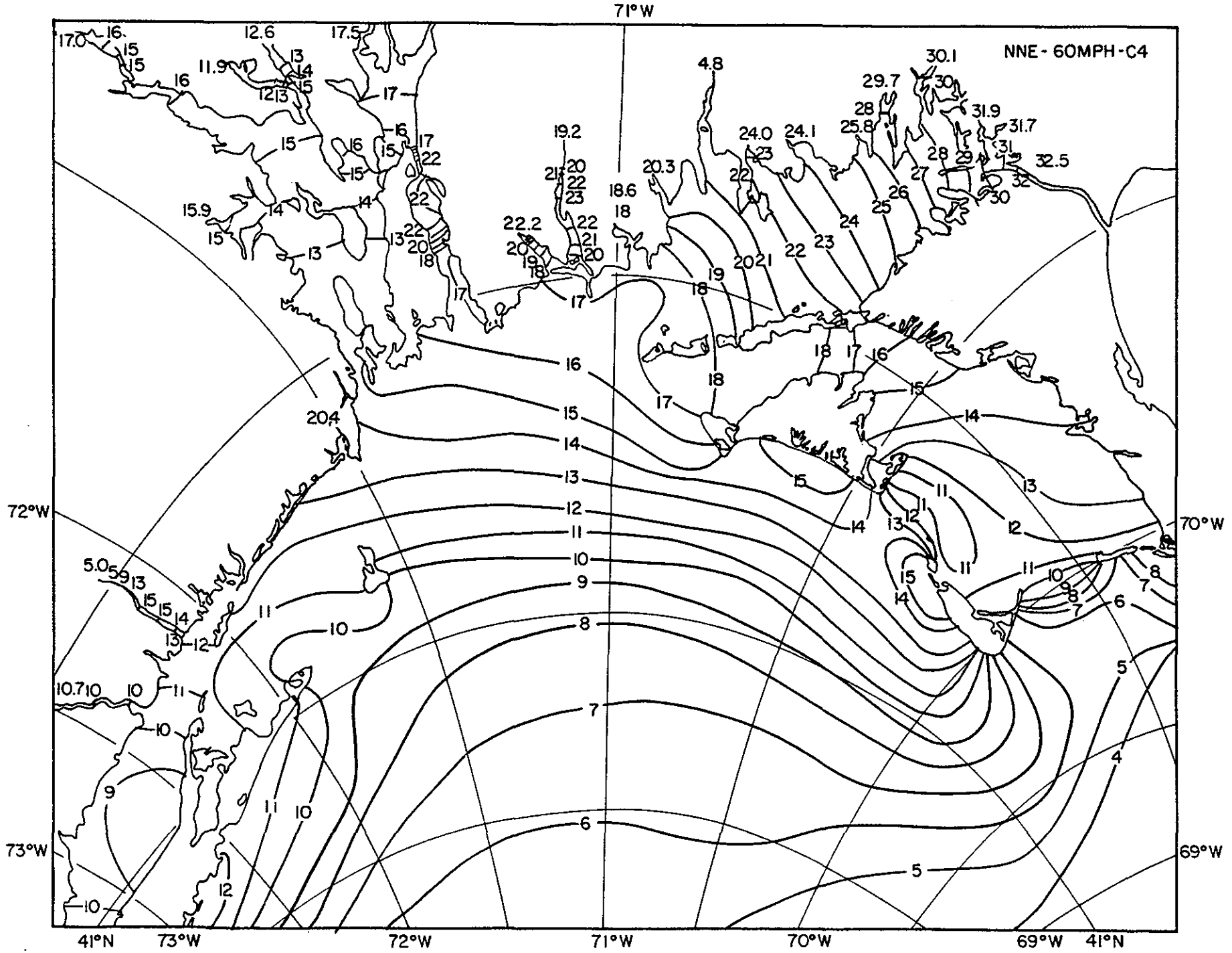
NNE - 60MPH - C4
71°W
72°W
70°W
73°W
69°W
41°N
73°W
72°W
71°W
70°W
69°W
41°N

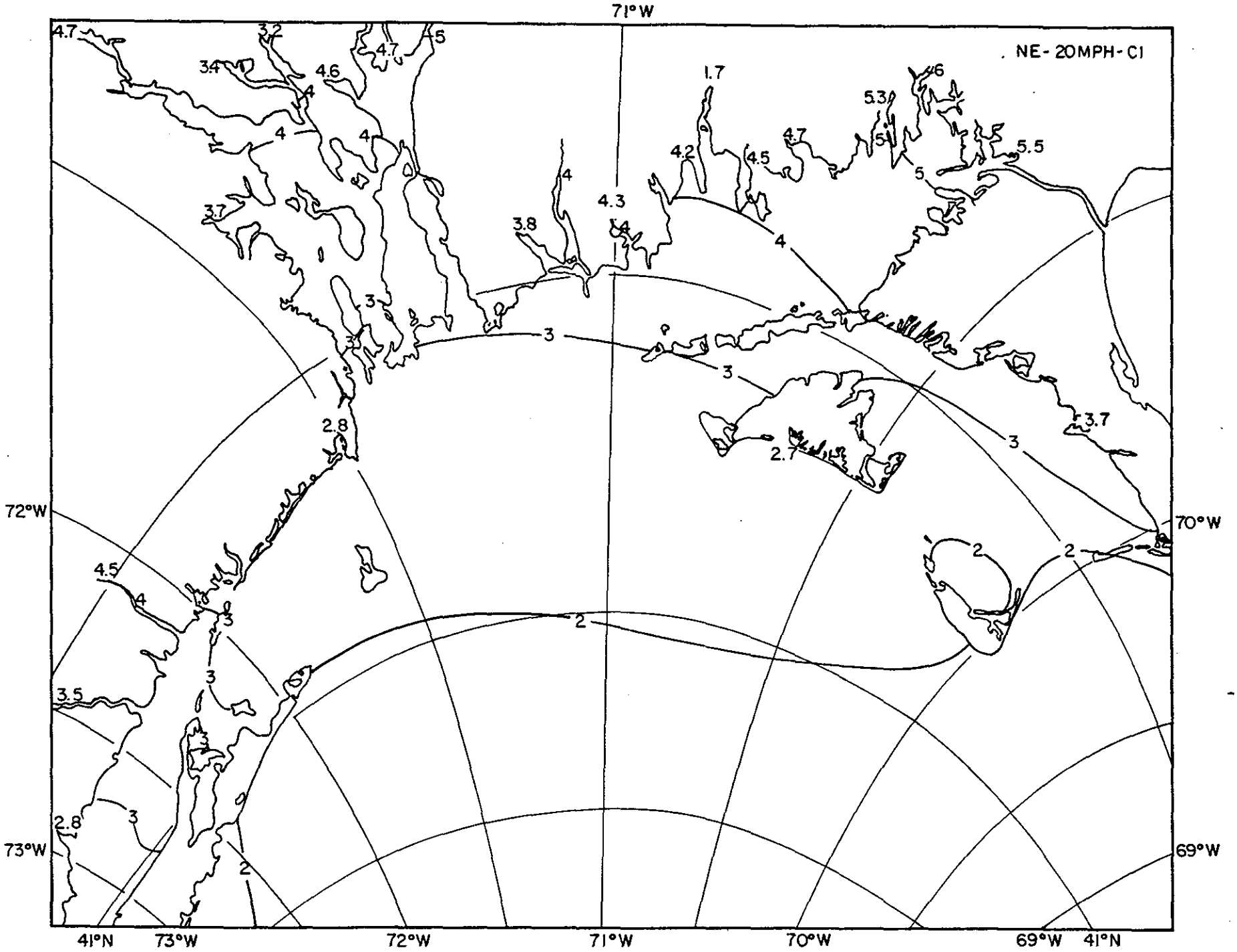
71°W
NE- 20MPH- CI
72°W
70°W
73°W
69°W
41°N
73°W
72°W
71°W
70°W
69°W
41°N

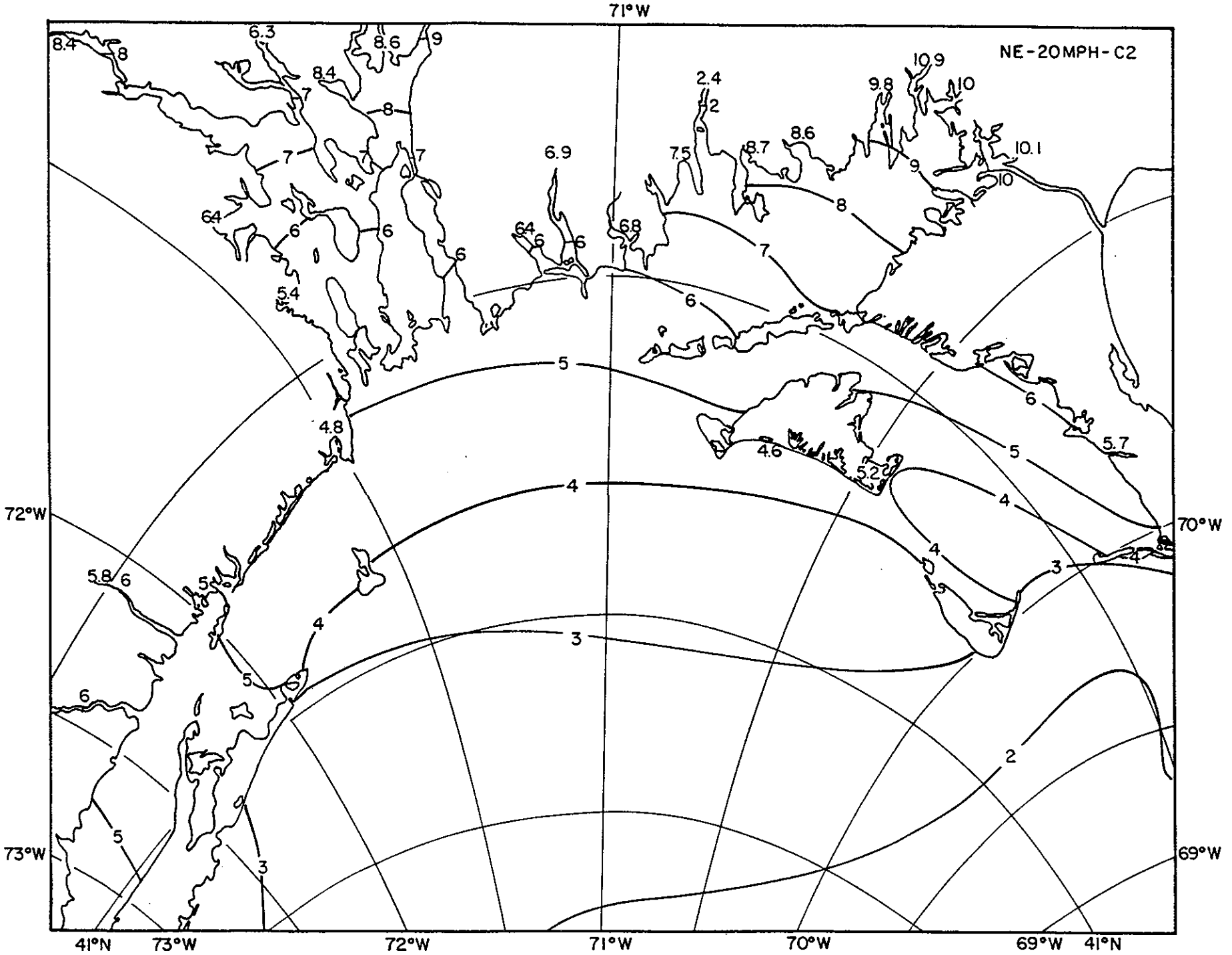
NE-20MPH-C2
71°W
72°W
70°W
73°W
69°W
41°N
73°W
72°W
71°W
70°W
69°W
41°N

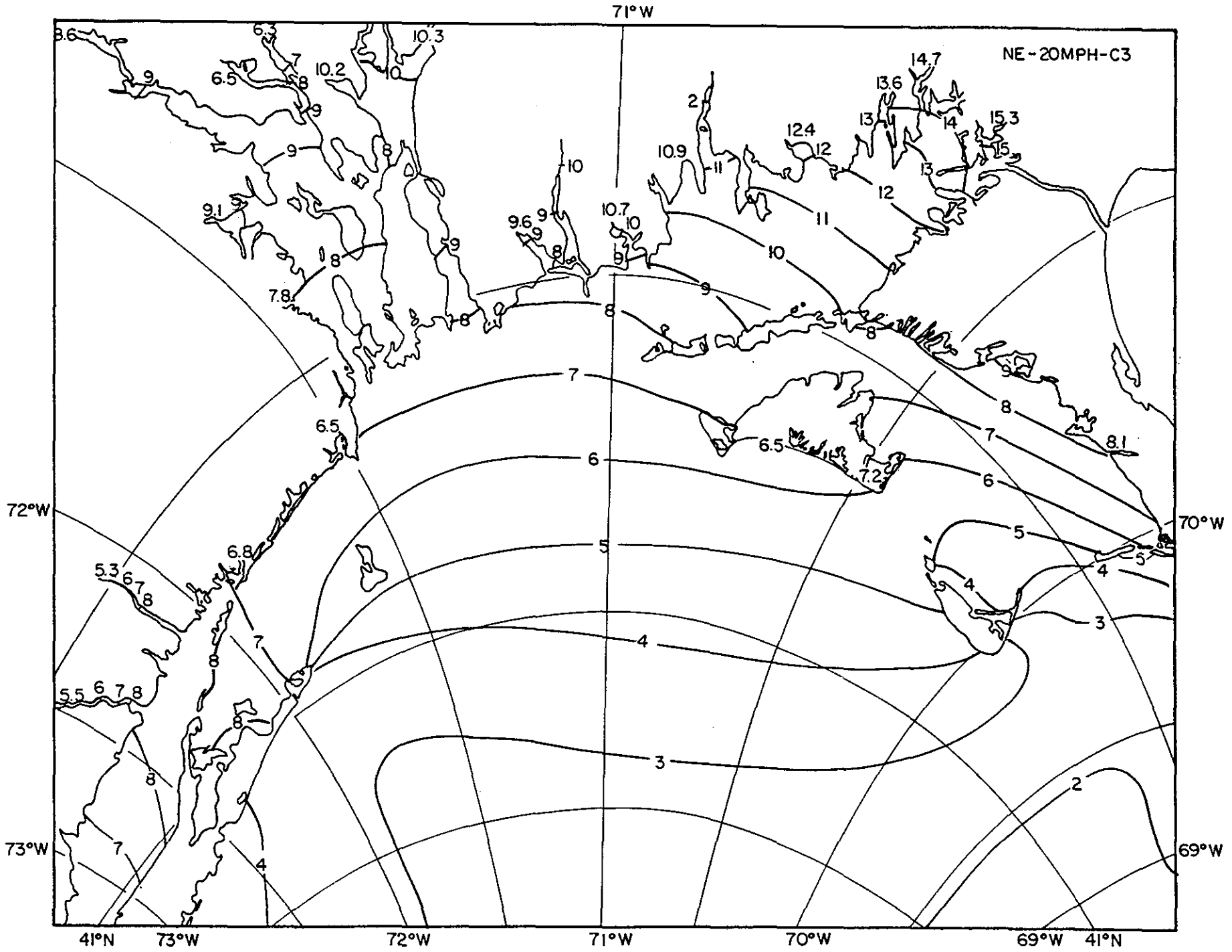
71°W
NE-20MPH-C3
72°W
70°W
73°W
69°W
41°N
73°W
72°W
71°W
70°W
69°W
41°N

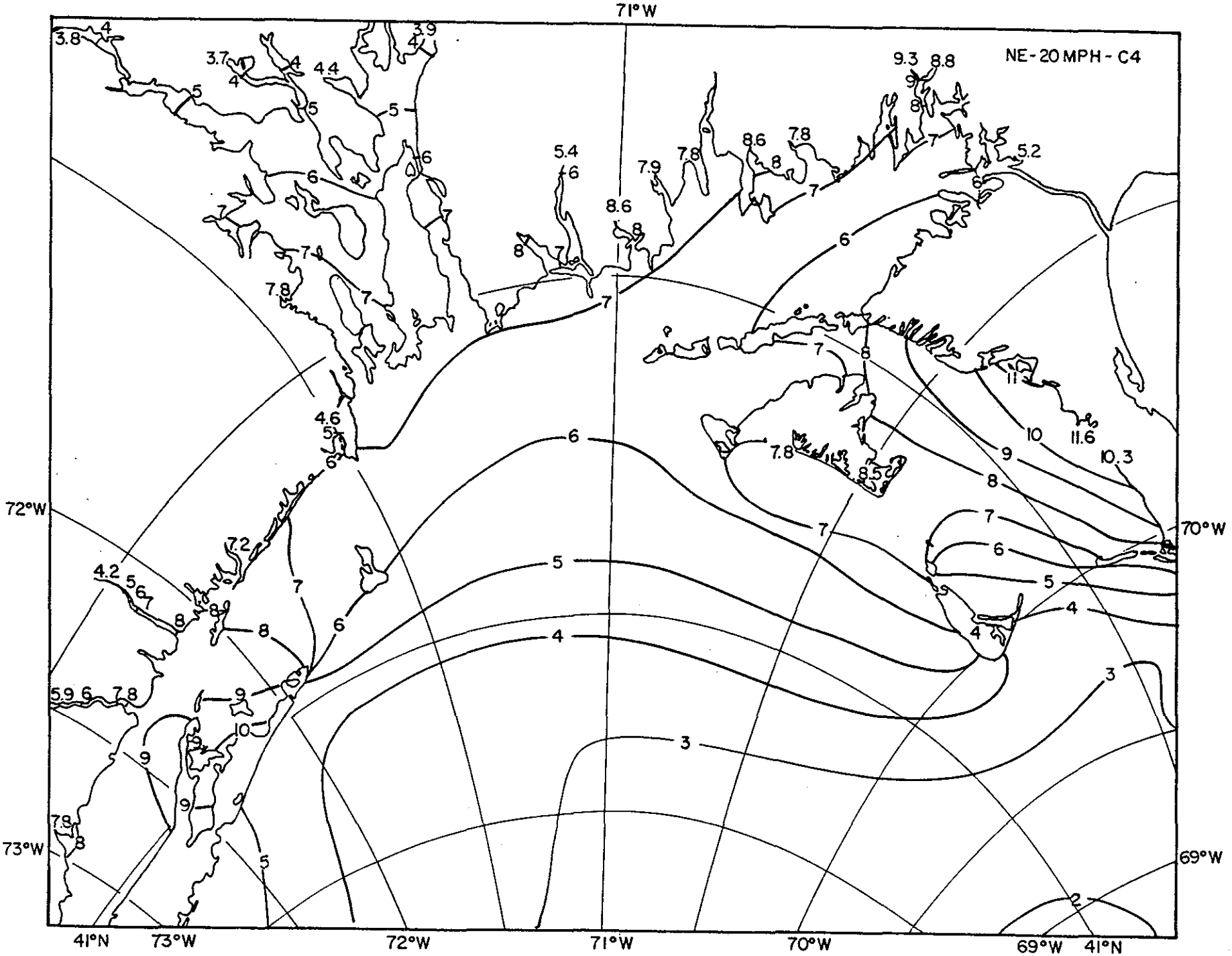
NE-20 MPH - C4
71°W
72°W
73°W
70°W
69°W
41°N

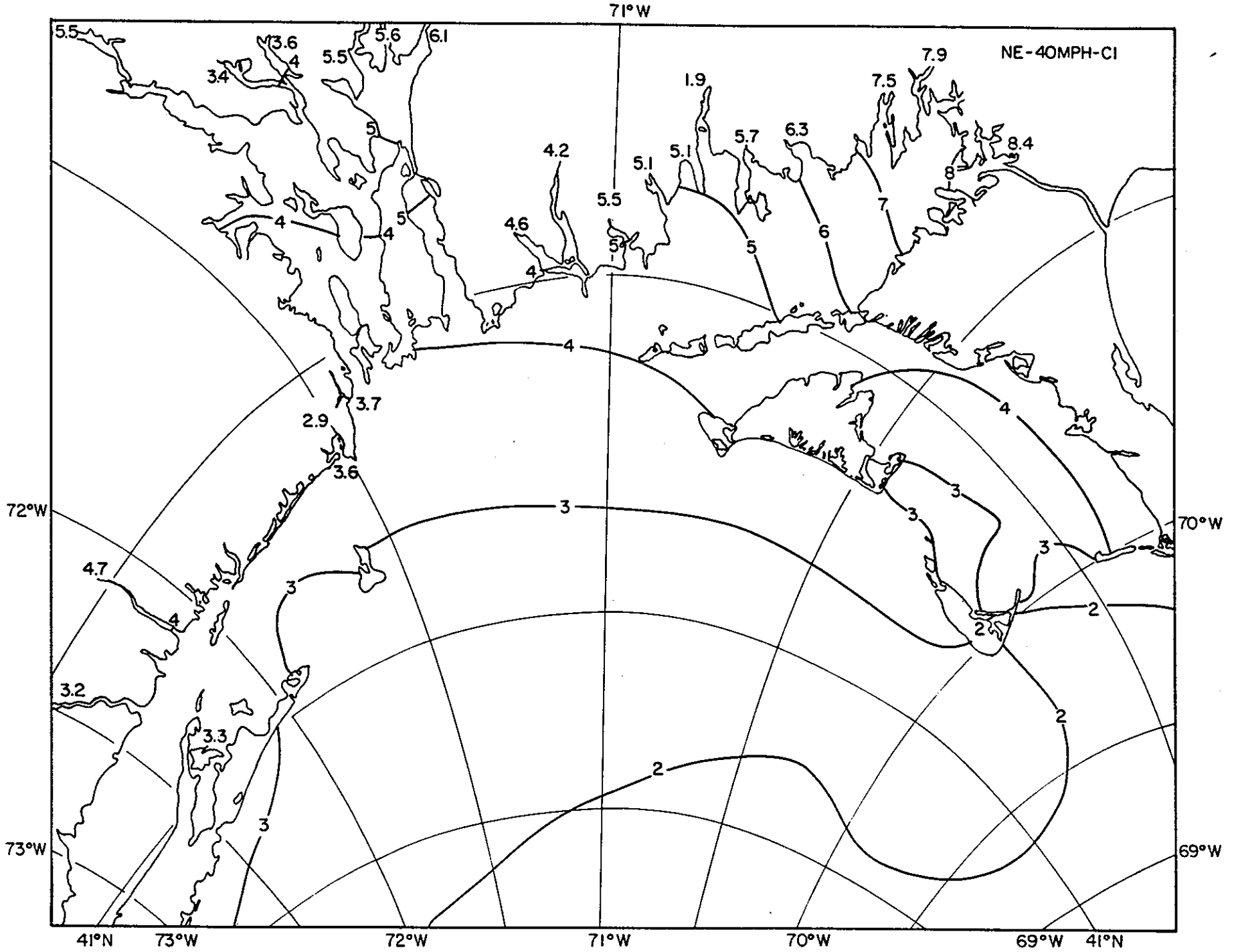
71°W
NE-40MPH-CI
72°W
70°W
73°W
69°W
41°N
73°W
72°W
71°W
70°W
69°W
41°N

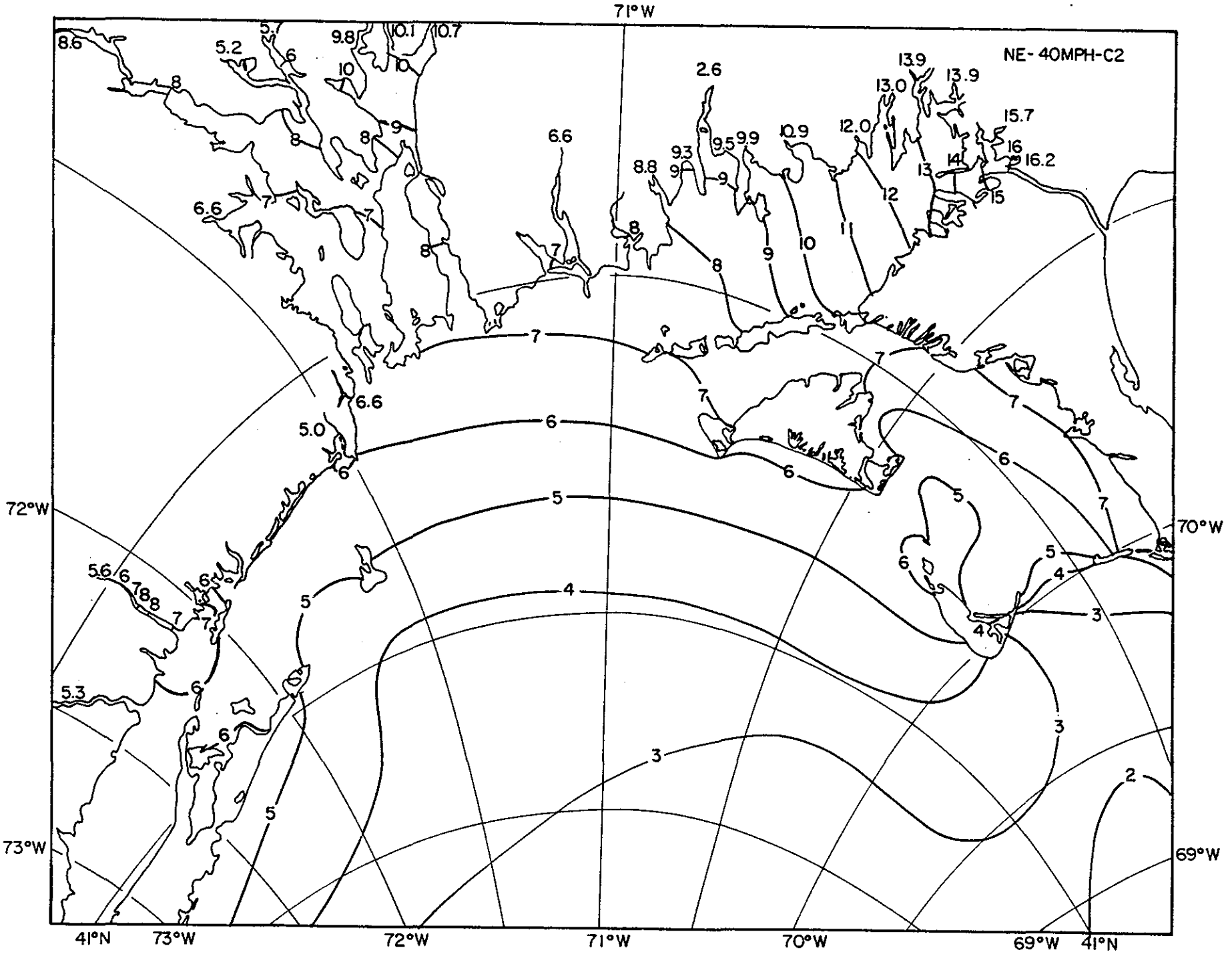
NE-40MPH-C2
71°W
72°W
70°W
73°W
69°W
41°N
73°W
72°W
71°W
70°W
69°W
41°N

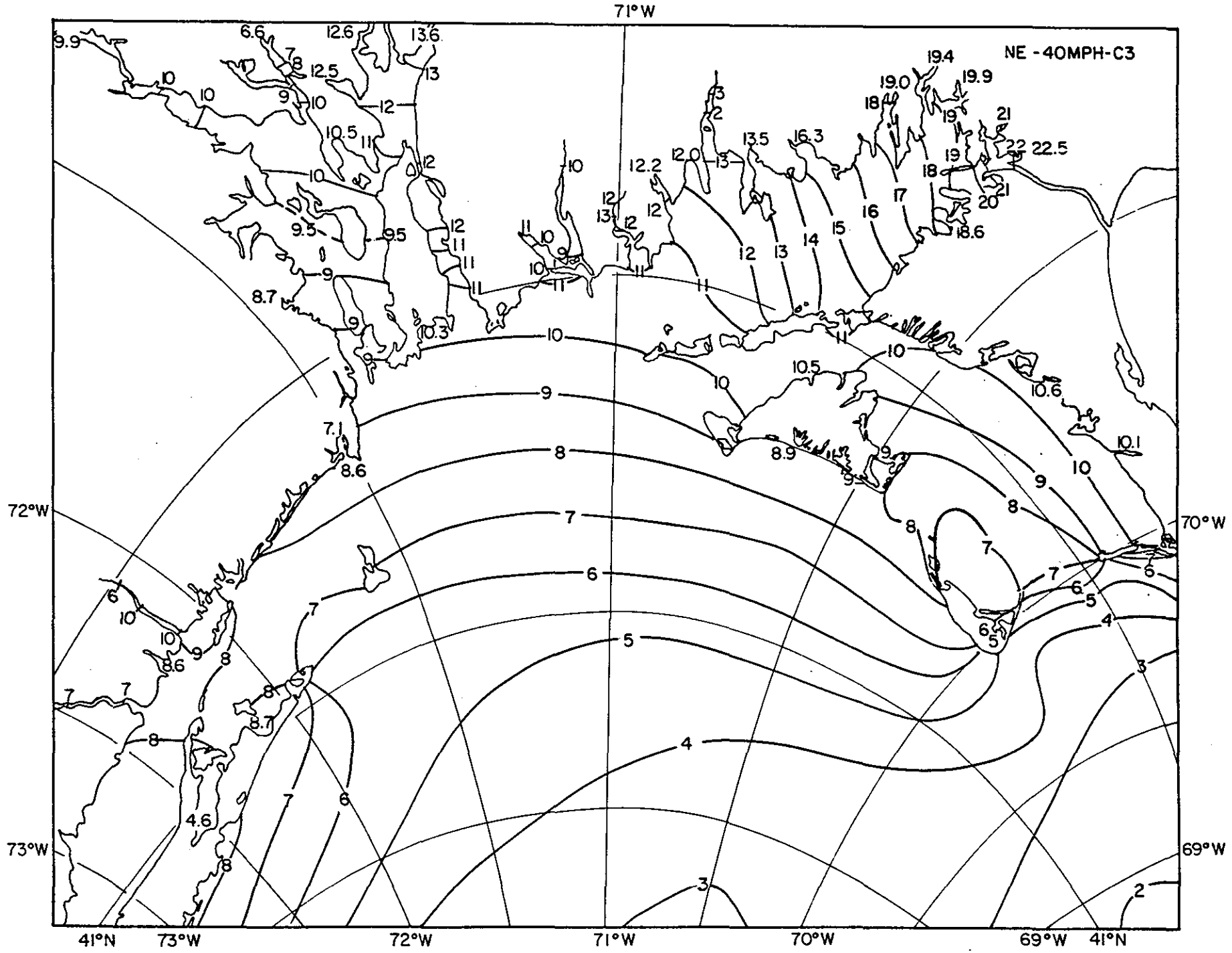
NE - 40MPH-C3
71°W
72°W
70°W
73°W
69°W
41°N
73°W
72°W
71°W
70°W
69°W
41°N

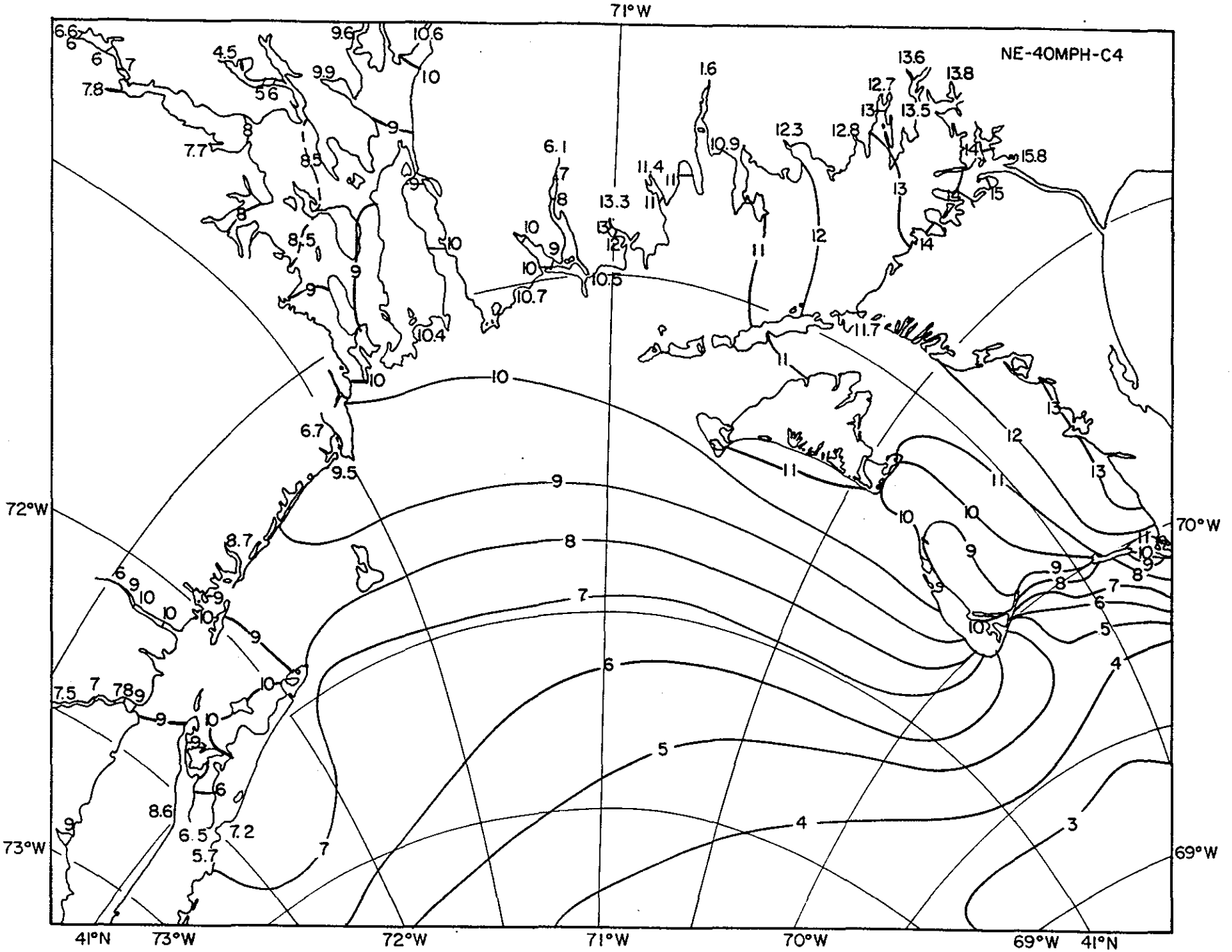
NE-40MPH-C4
71°W
72°W
73°W
70°W
69°W
41°N

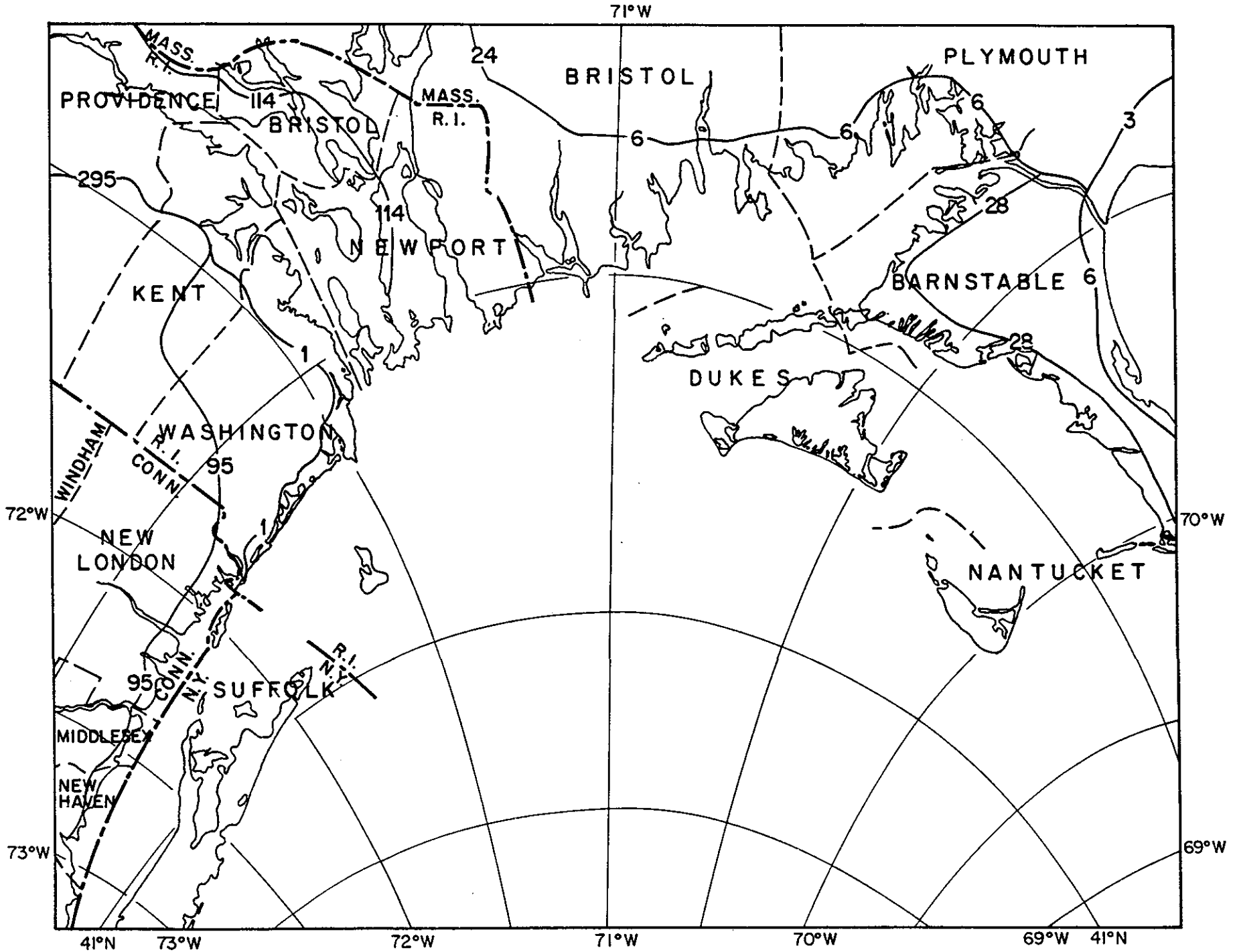
71°W
MASS.
R.I.
PROVIDENCE
114
BRISTOL
MASS.
R.I.
24
BRISTOL
PLYMOUTH
6
6
6
3
295
114
NEWPORT
28
KENT
BARNSTABLE
6
1
28
DUKES
WINDHAM
R.I.
CONN.
WASHINGTON
95
72°W
70°W
NEW
LONDON
NANTUCKET
CONN.
N.Y.
R.I.
N.Y.
95
SUFFOLK
MIDDLESEX
NEW
HAVEN
73°W
69°W
41°N
73°W
72°W
71°W
70°W
69°W
41°N

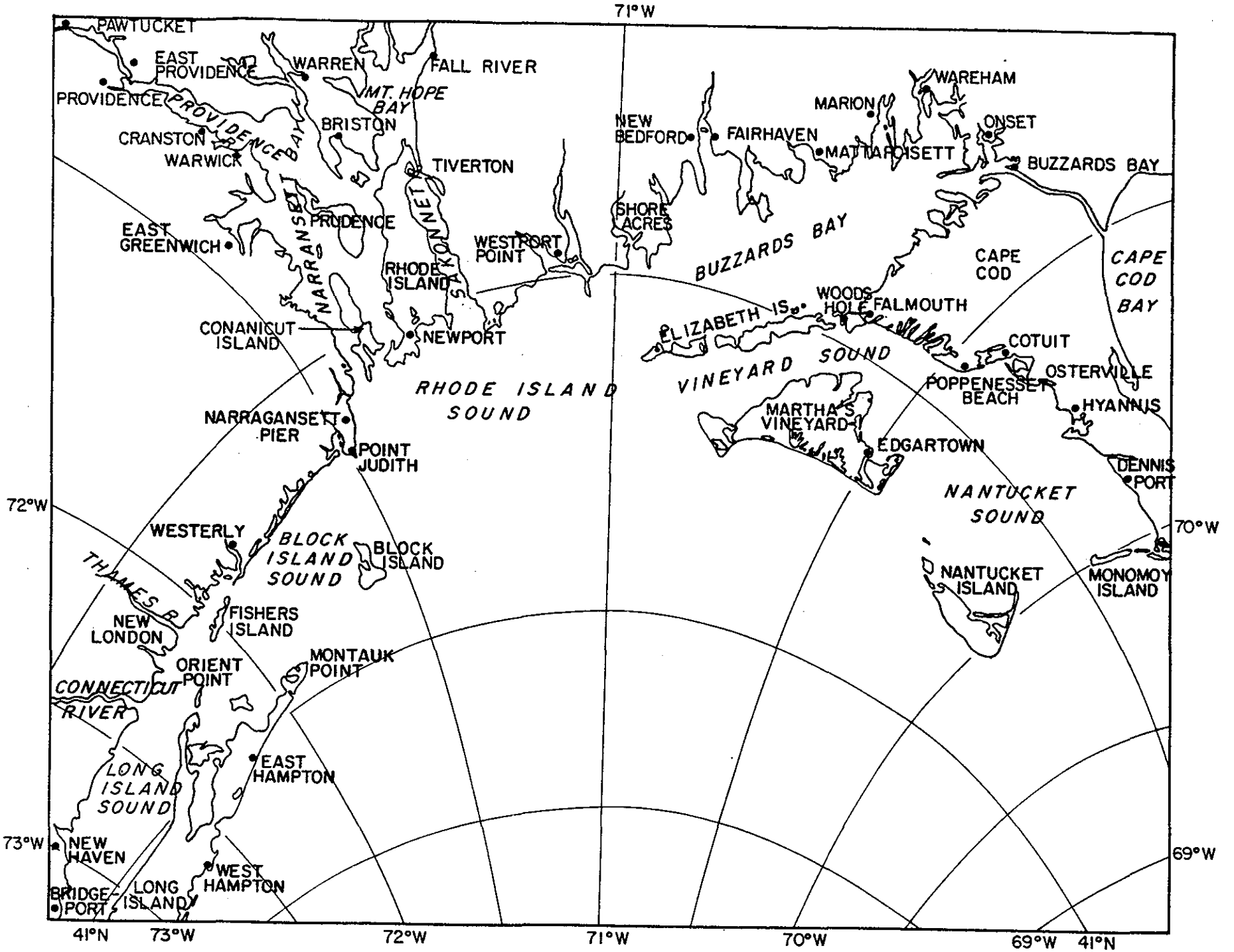
71°W
PAWTUCKET
EAST PROVIDENCE
WARREN
FALL RIVER
PROVIDENCE
MT. HOPE BAY
PROVIDENCE BAY
BRISTON
CRANSTON
WARWICK
TIVERTON
NARRAGANSETT BAY
PRUDENCE
EAST GREENWICH
SAKONNET
WESTPORT POINT
RHODE ISLAND
CONANICUT ISLAND
NEWPORT
RHODE ISLAND SOUND
NARRAGANSETT PIER
POINT JUDITH
72°W
WESTERLY
BLOCK ISLAND SOUND
BLOCK ISLAND
THAMES R.
NEW LONDON
FISHERS ISLAND
ORIENT POINT
MONTAUK POINT
CONNECTICUT RIVER
LONG ISLAND SOUND
EAST HAMPTON
73°W
NEW HAVEN
WEST HAMPTON
BRIDGEPORT
LONG ISLAND
41°N
NEW BEDFORD
FAIRHAVEN
MARION
WAREHAM
ONSET
MATTAPOISETT
BUZZARDS BAY
SHORE ACRES
BUZZARDS BAY
CAPE COD
CAPE COD BAY
WOODS HOLE
FALMOUTH
ELIZABETH IS.
VINEYARD SOUND
COTUIT
OSTERVILLE
POPPENESSET BEACH
HYANNIS
MARTHA'S VINEYARD I.
EDGARTOWN
DENNIS PORT
NANTUCKET SOUND
70°W
NANTUCKET ISLAND
MONOMOY ISLAND
69°W
41°N
73°W
72°W
71°W
70°W
69°W